Seminar at the Michigan Institute for Plasma Science and Engineering (MIPSE)

Plasma diagnostics of sputtering magnetrons from DC to HiPIMS modes

André Anders
Senior Scientist, *Lawrence Berkeley National Laboratory*
Berkeley, California
aanders@lbl.gov
and
Editor-in-Chief, Journal of Applied Physics
American Institute of Physics Publishing
jap-aanders@aip.org

Acknowledgments:
*This presentation includes results of several members of and visitors to the Plasma Applications Group, including **Yuchen Yang, Xue Shoe, Matjaz Panjan, Joakim Andersson, and others**. Work at LBNL is supported by the U.S. Department of Energy under Contract No. DE-AC02-05CH11231.*

Volta, 1800: An Electrical Energy Source

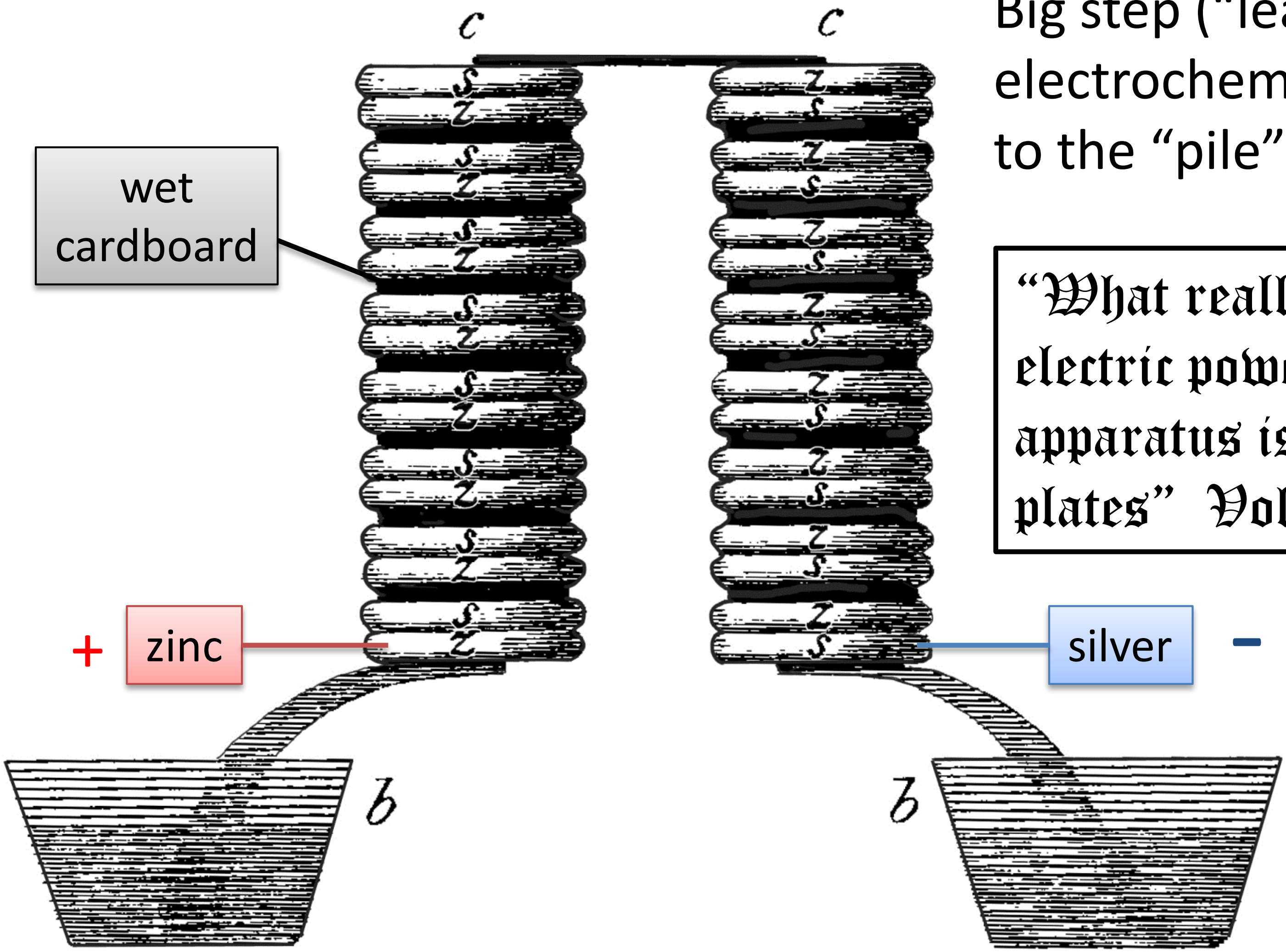

wet cardboard

+ zinc

silver –

Big step ("leap!") from an electrochemical pair (~ 1.5 V) to the "pile" – the battery.

"What really increases the electric power of this apparatus is the number of plates" Volta, 1800

A. Volta, Phil. Mag. VIII (1800) 289.

The Race to More Electrical Energy

- in the 1800s: An institution’s pride was its BATTERY
- (in the 1900s: … its accelerator)
- (in the 2000s: … its fastest computer or highest resolution microscope)

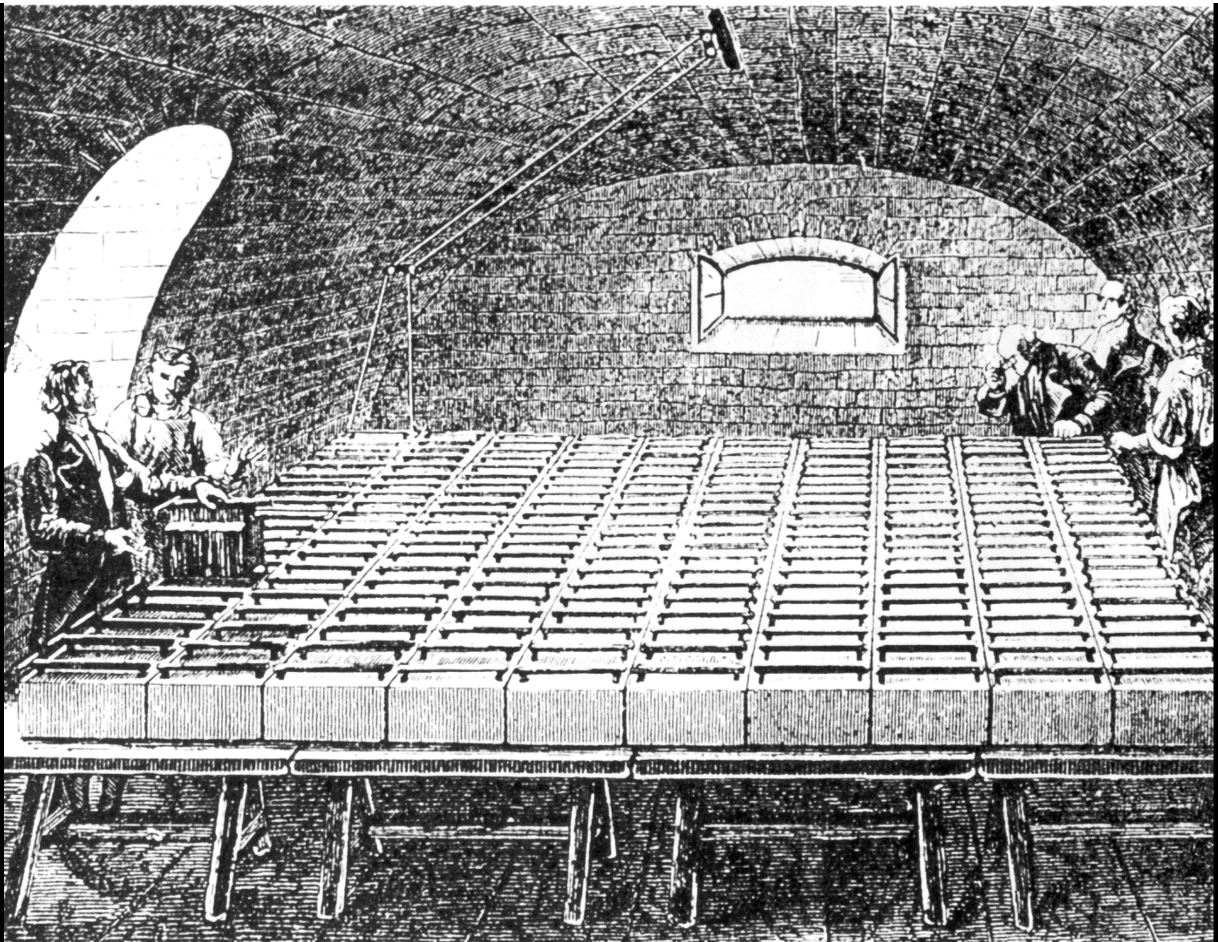

Battery in the basement of the Royal Institution, London, ca. 1815

Higher Voltages Obtained by Induction

- 1830s: Faraday's induction principle → enabled pulsed high voltages in the laboratory
- 1850s: Ruhmkorff developed an induction coil for repetitive pulsed high voltage

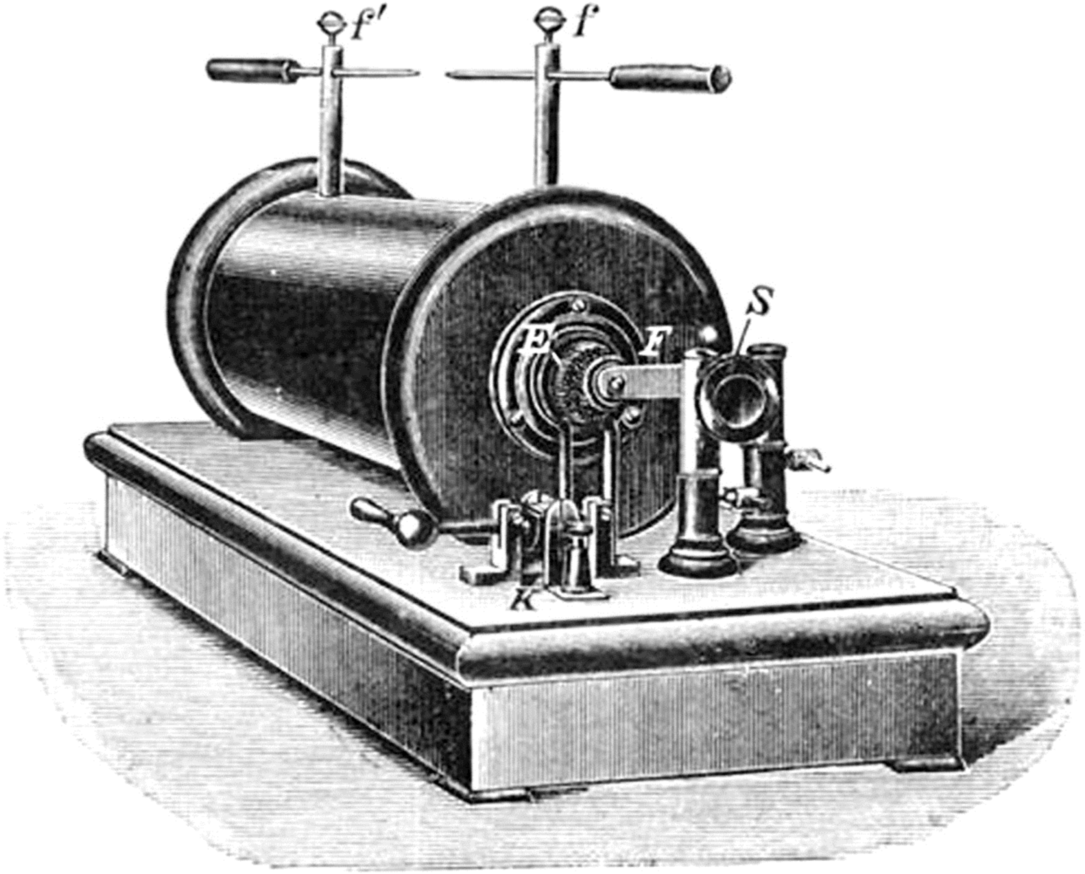

Ruhmkorff's coil was widely used in the second half of the 19th century.

The original source of energy was an electrochemical cell.

Vacuum

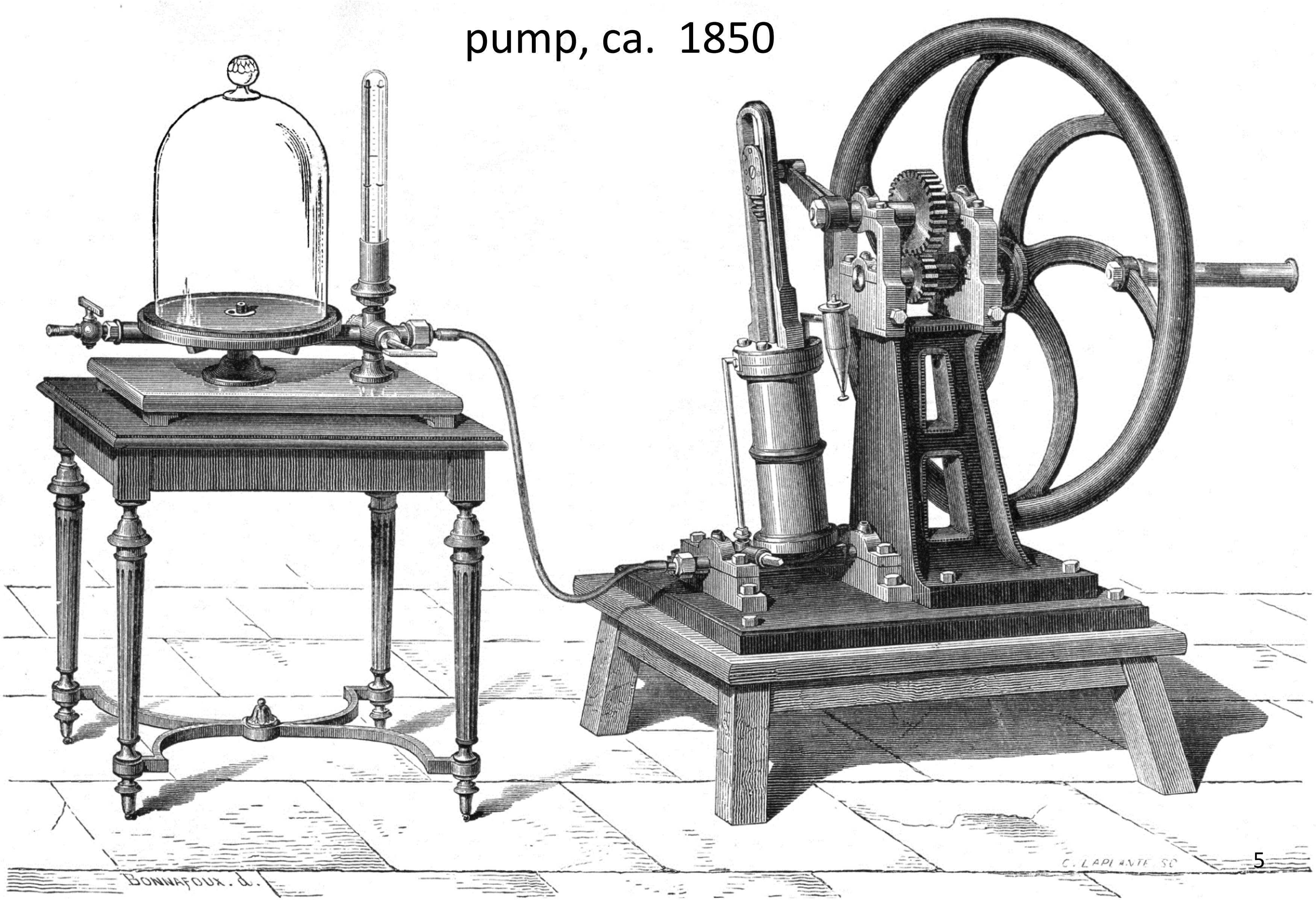

pump, ca. 1850

Grove 1852: Sputtering

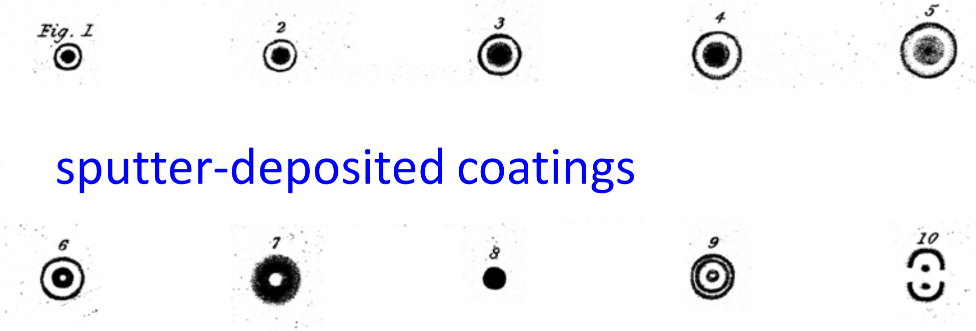

sputter-deposited coatings

First sputtering was ***pulsed*** sputtering!

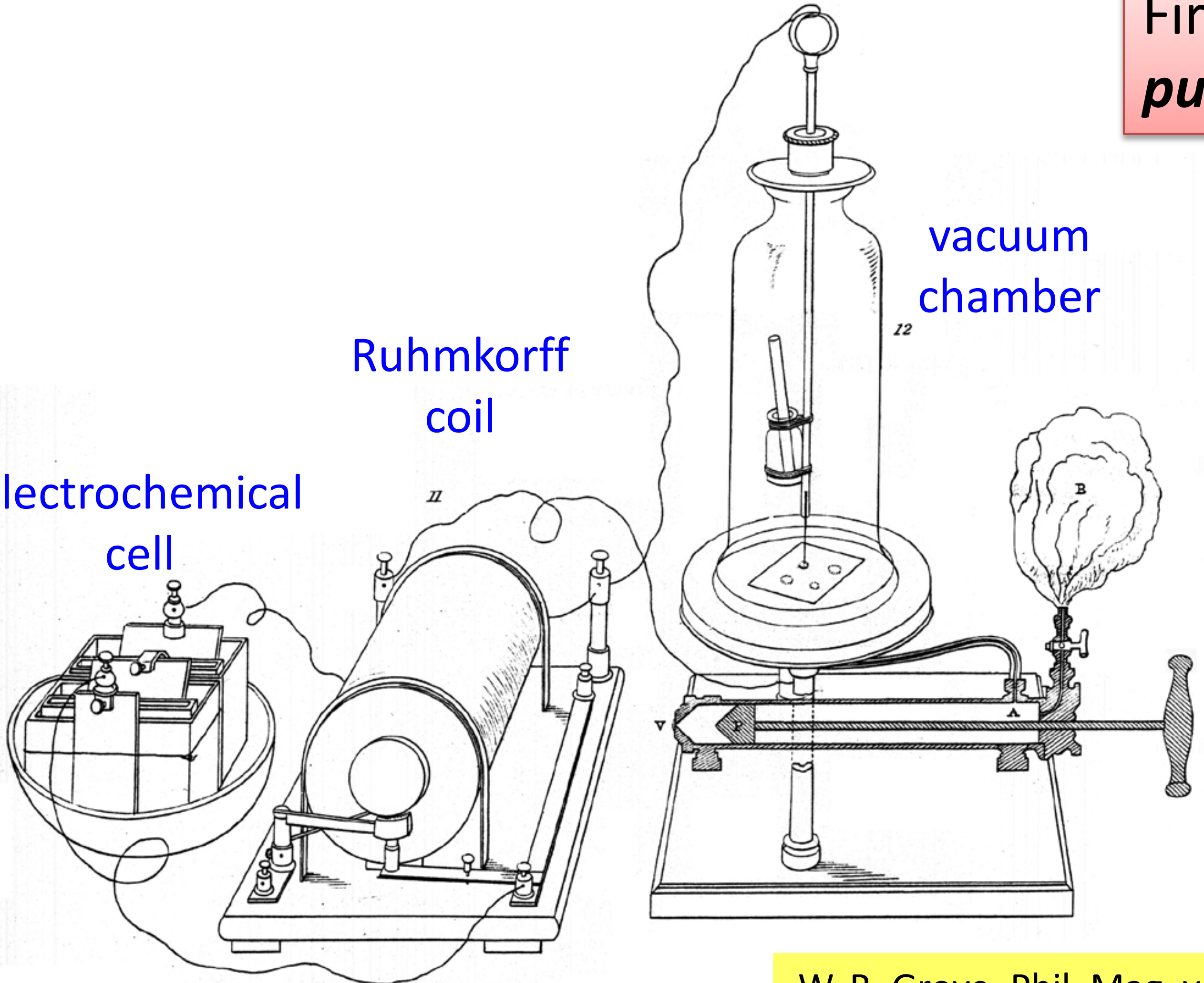

vacuum chamber

Ruhmkorff coil

electrochemical cell

vacuum pump

W. R. Grove, Phil. Mag. vol. **4** Ser. 4 (1852) 498

The Sputtering Process

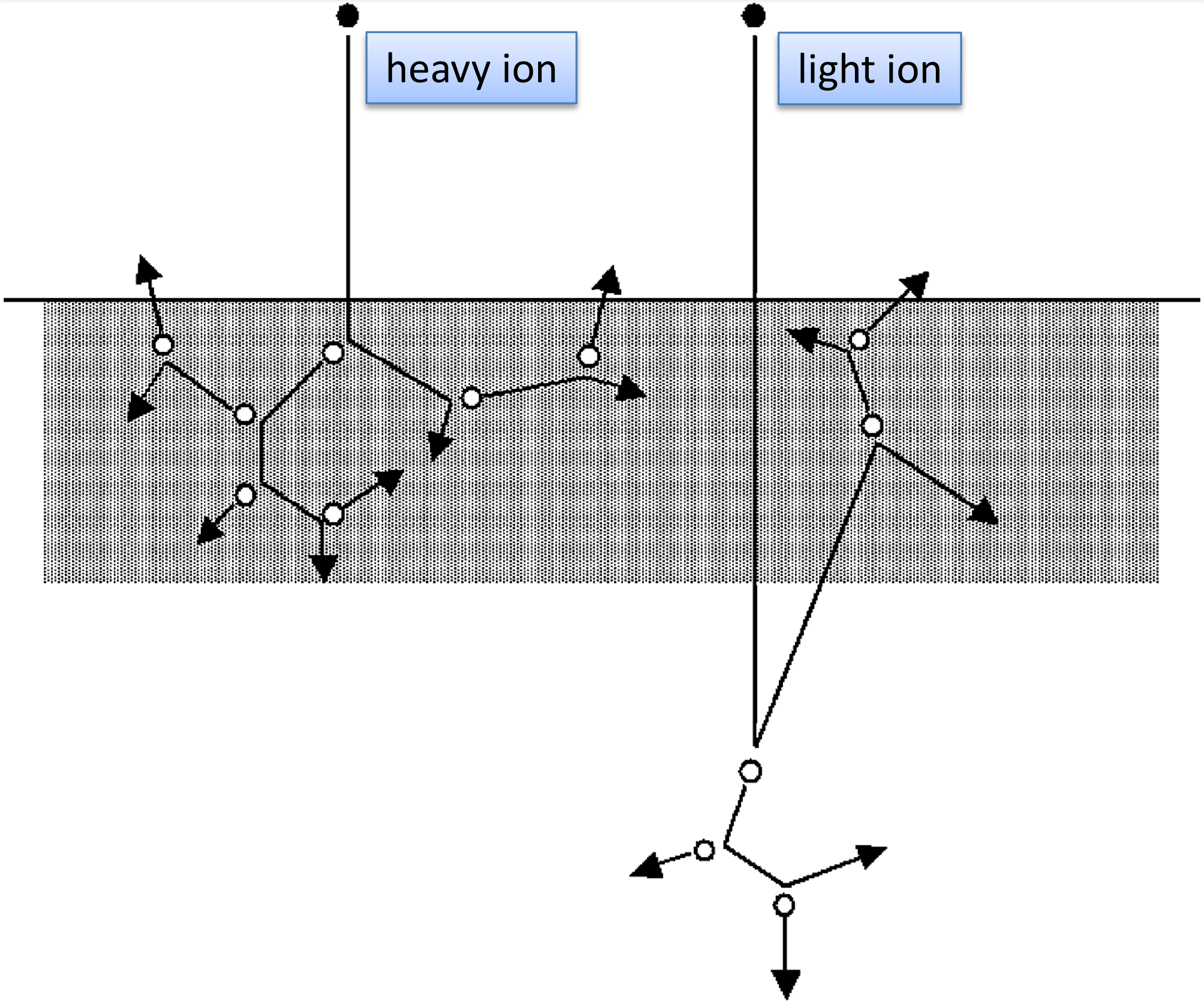

This image, and the following, are from D. Depla, *et al*. (Ed.), Reactive Magnetron Sputtering, Springer, 2008

Early 1970s: Invention of the Planar Magnetron

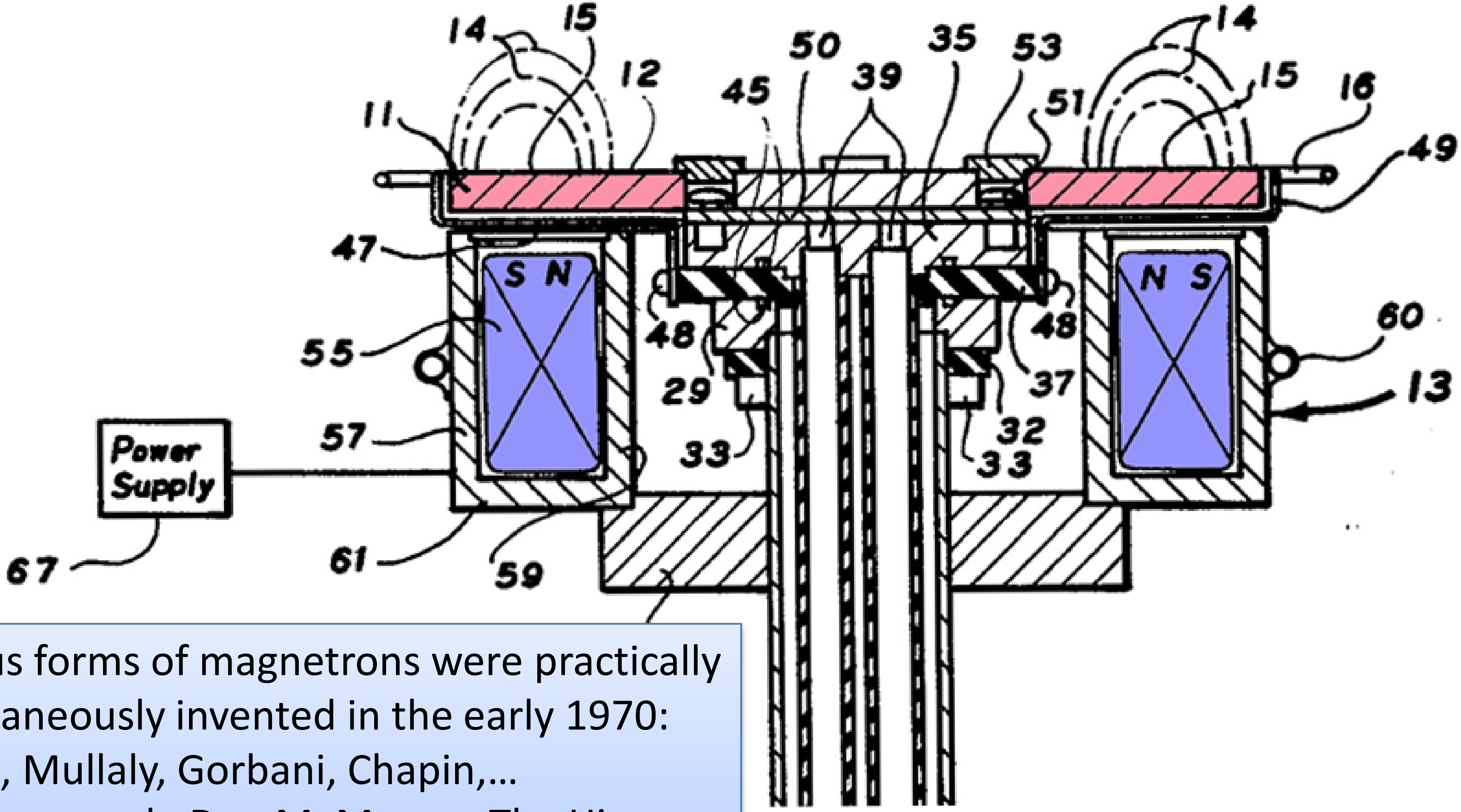

Various forms of magnetrons were practically simultaneously invented in the early 1970: Clarke, Mullaly, Gorbani, Chapin,…
see for example Don M. Mattox, The History of Vacuum Coating Technology, Society of Vacuum Coaters, Albuquerque, 2002.

J. S. Chapin, "Sputtering process and apparatus," US 4,166,018, (filed 1974).

Motion of electrons in a magnetron’s E x B field

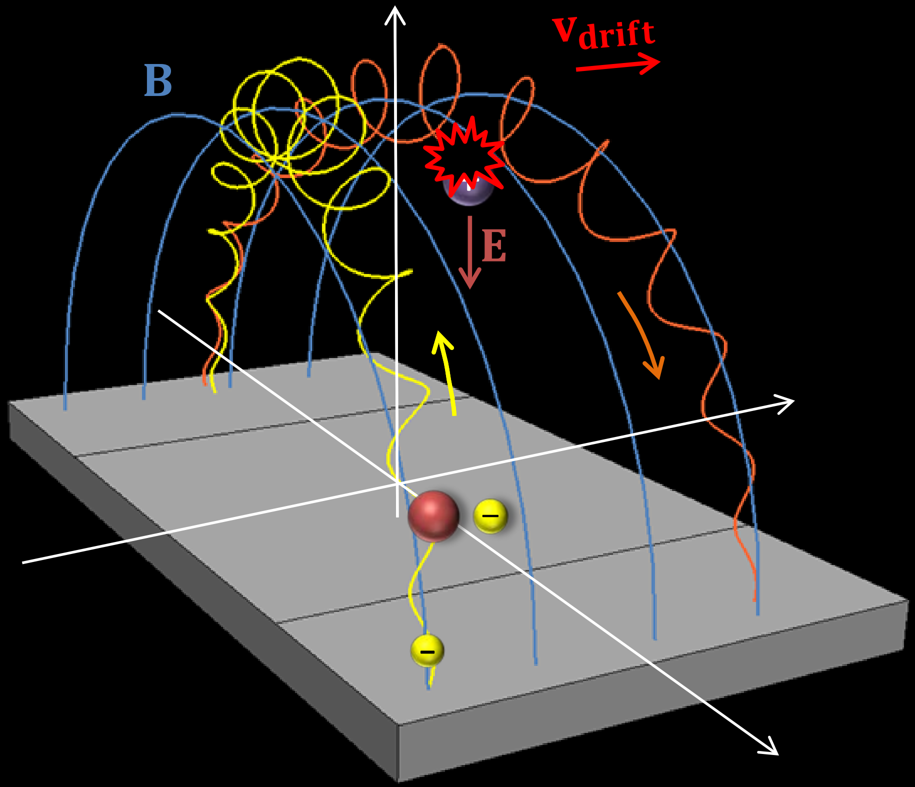

Slide design by Matjaz Panjan.

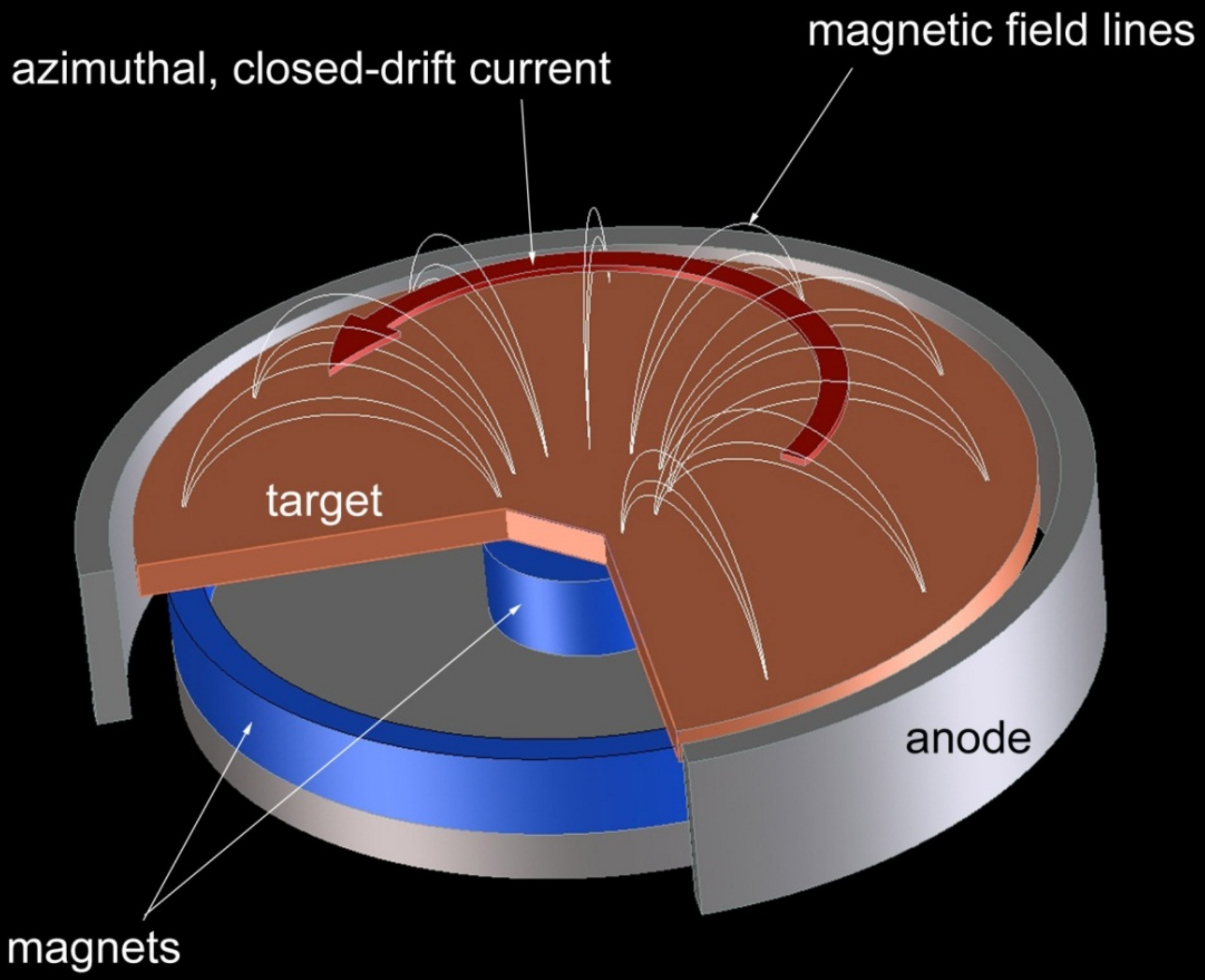

A. Anders, Surf. Coat. Technol. **205** (2011) S1.

Magnetrons

planar, round

dual, cylindrical, rotating

dual, planar, rectangular

examples are from Gencoa.com

Magnetron sputtering enables microprocessor, solid state memory, hard disk, and display fabrication

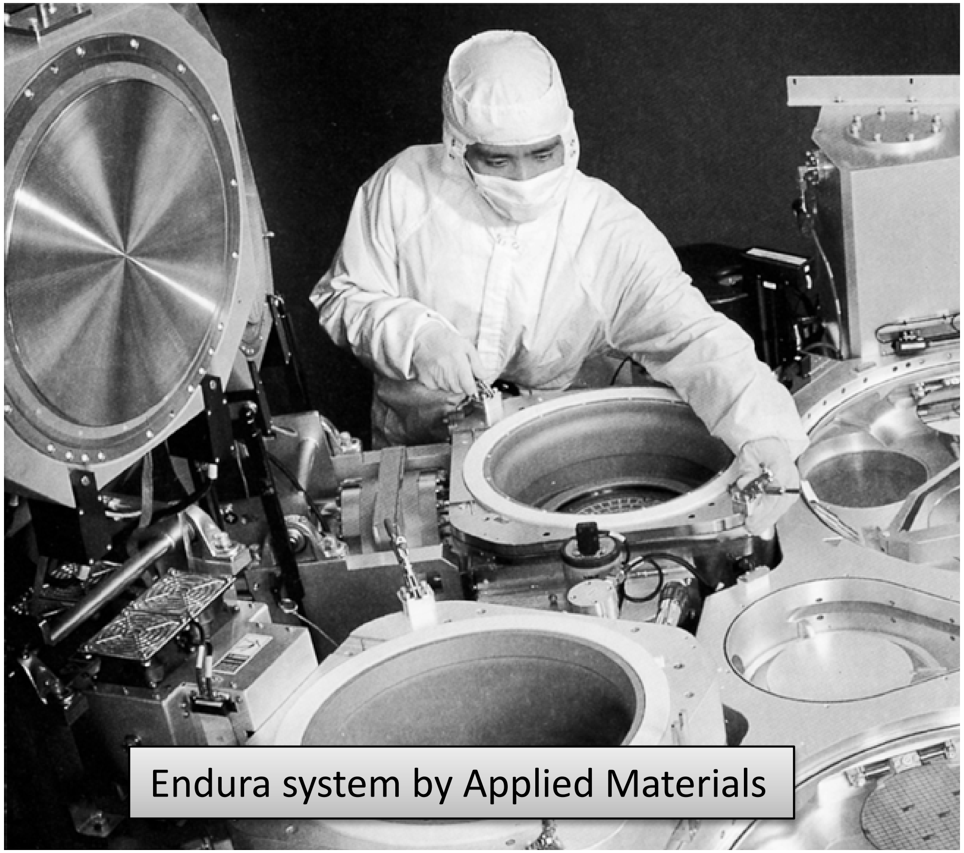

Endura system by Applied Materials

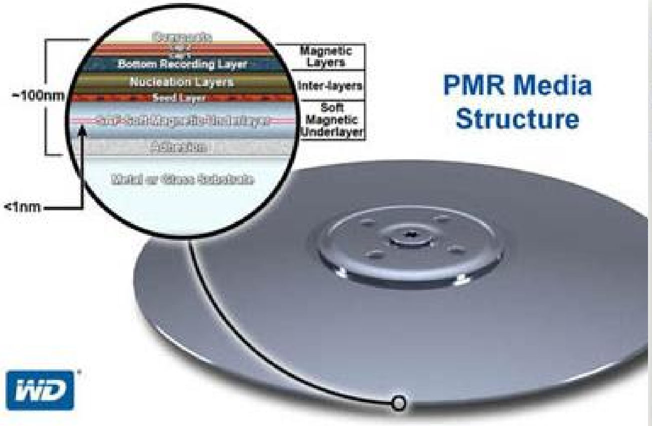

Thorton's Structure Zone Diagram for Sputtering

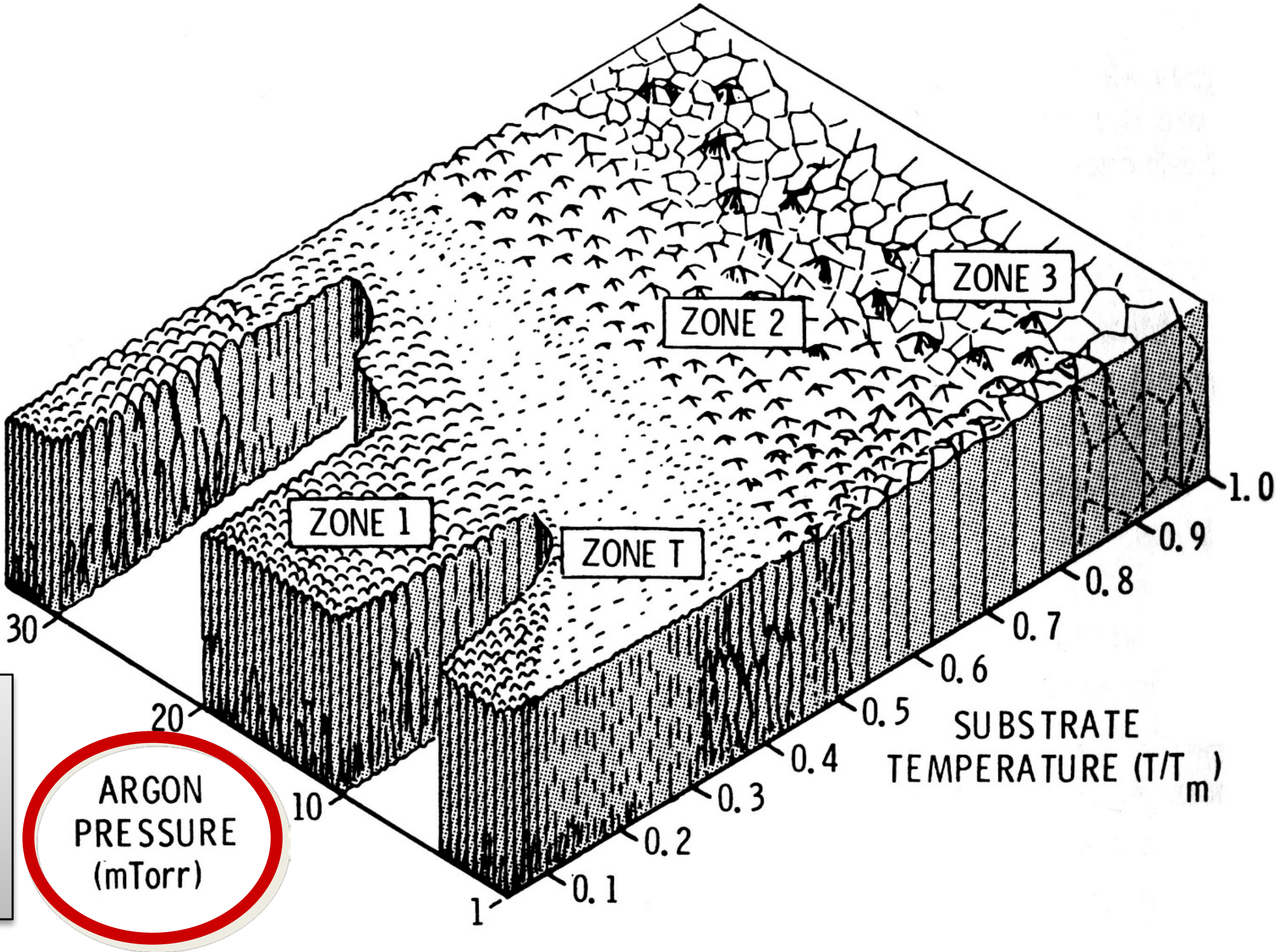

Contains the effects of energetic particle bombardment

J. A. Thornton, *J. Vac. Sci. Technol.* **11** (1974) 666

Energy of Sputtered Atoms: Thompson Distribution: log scale

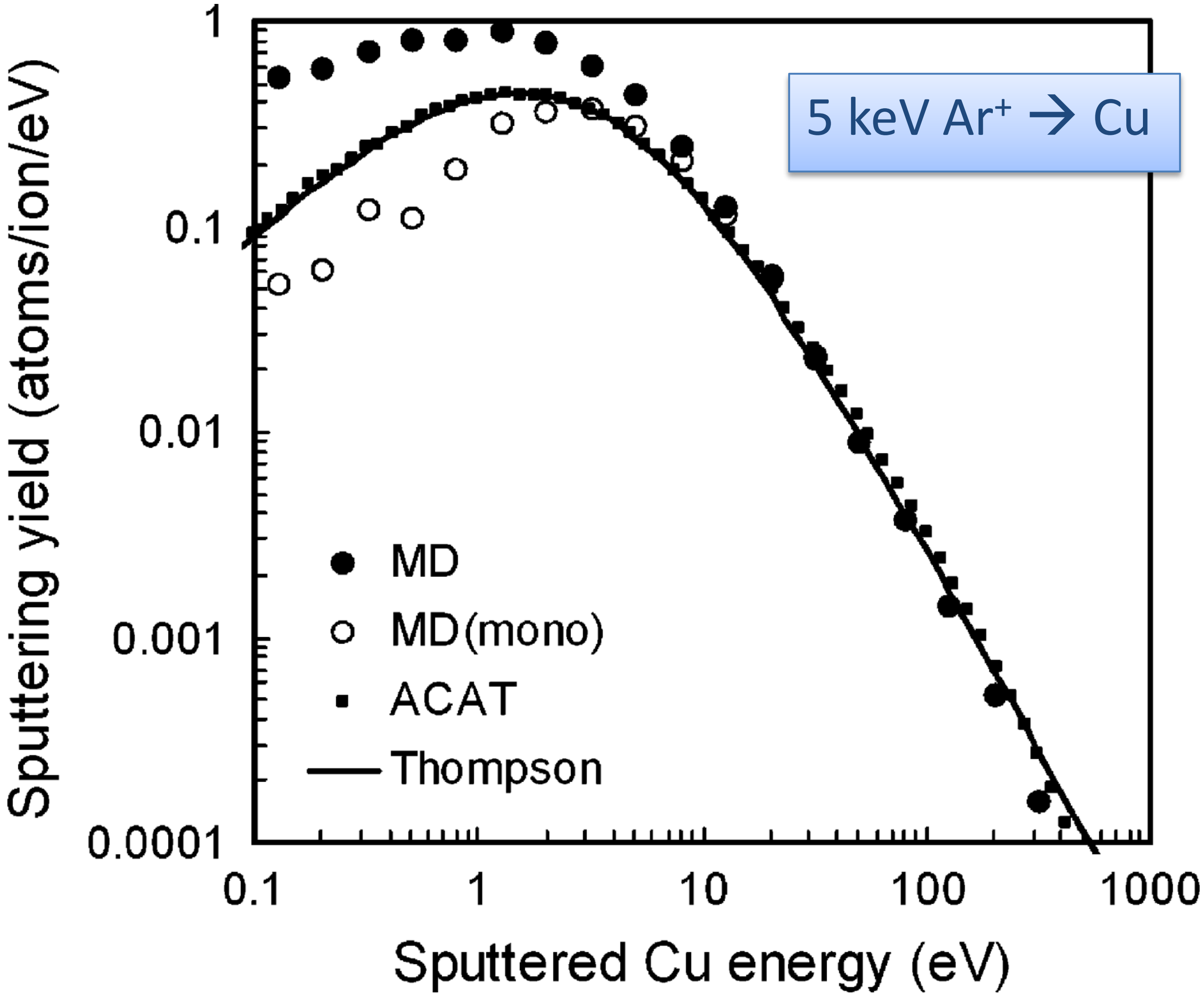

5 keV Ar^+ → Cu

A Generalized Structure Zone Diagram including the Effects of Plasma Assistance to Film Growth

derived from Thornton's diagram, 1974

*T** = normalized temperature and potential energy

*t** = normalized film thickness

*E** = normalized kinetic energy

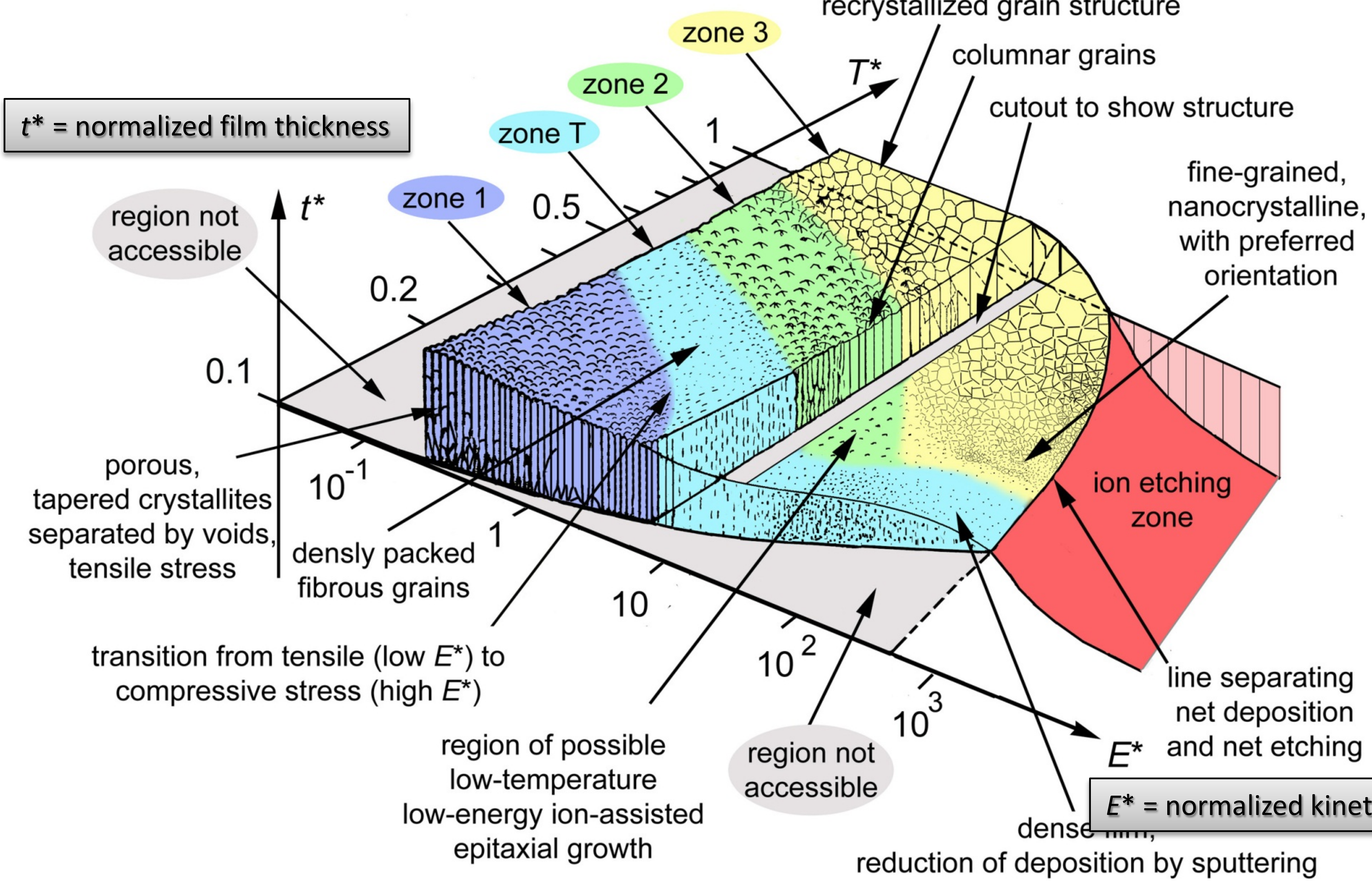

recrystallized grain structure

columnar grains

cutout to show structure

fine-grained, nanocrystalline, with preferred orientation

region not accessible

porous, tapered crystallites separated by voids, tensile stress

densly packed fibrous grains

transition from tensile (low *E**) to compressive stress (high *E**)

region of possible low-temperature low-energy ion-assisted epitaxial growth

region not accessible

ion etching zone

line separating net deposition and net etching

dense film, reduction of deposition by sputtering

A. Anders, Thin Solid Films **518** (2010) 4087

1980s: Unbalanced Magnetron

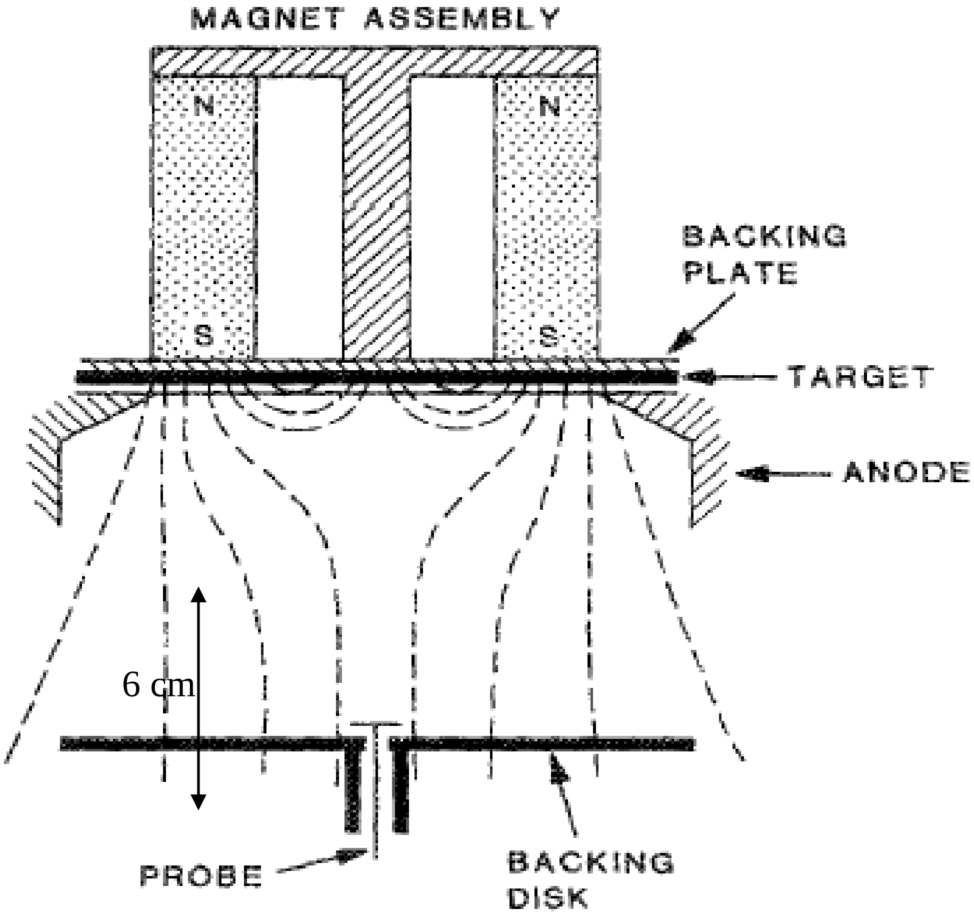

FIG. 1. Magnetron and probe assembly are shown schematically. For the measurements reported here the target to probe distance was maintained at 60 mm.

- Unbalanced magnetic field allows electrons and ions to escape from target, providing a means of ion assistance
- $n_e \sim 10^{12}$, for up to a distance of 10 cm.

B. Windows and N. Savvides, J. Vac. Sci. Technol. A **4** (1986) 453.

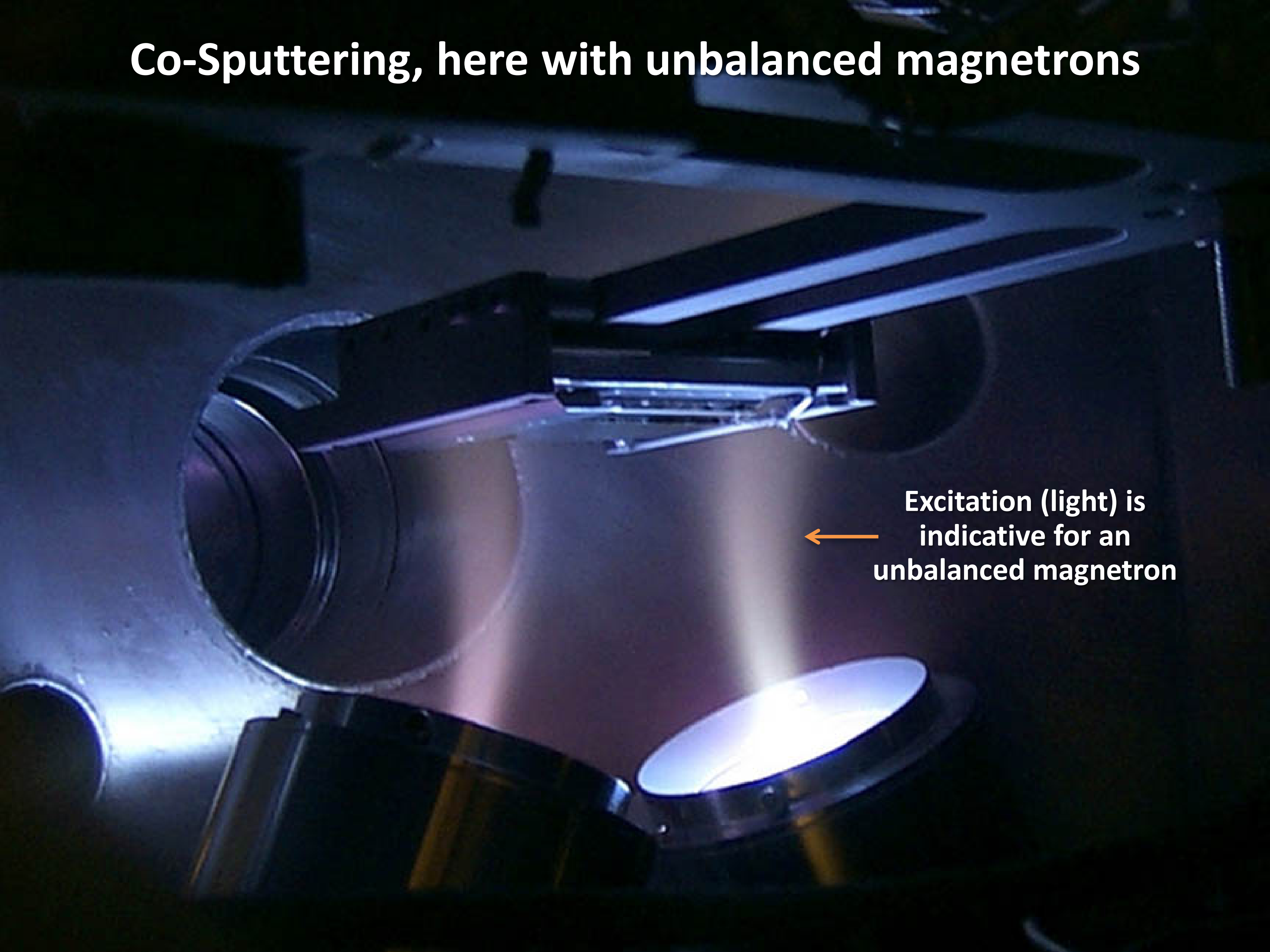

Co-Sputtering, here with unbalanced magnetrons

Excitation (light) is indicative for an unbalanced magnetron

Magnetic Field Structure of an Unbalanced Magnetron

White arrows indicate the DIRECTION of the magnetic field, color indicates the STRENGTH

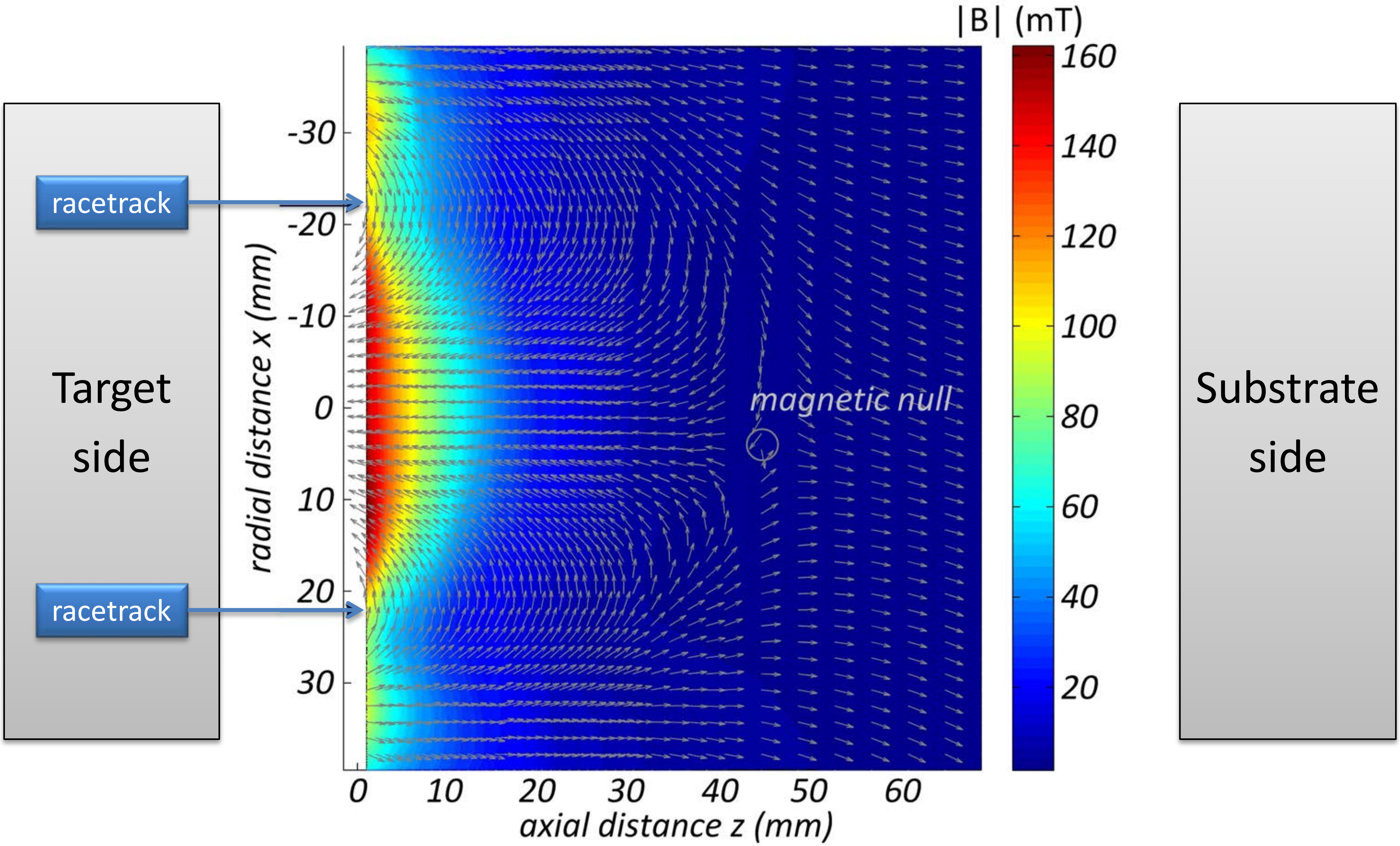

A. Rauch and A. Anders, Vacuum **89** (2013) 53.

Electric Field in Plasma with Magnetic Field

- Plasma potentials can be measured with hot, **emissive probes**
- Here: potential in front of a racetrack of a magnetron (Nb sputtered in Ar)

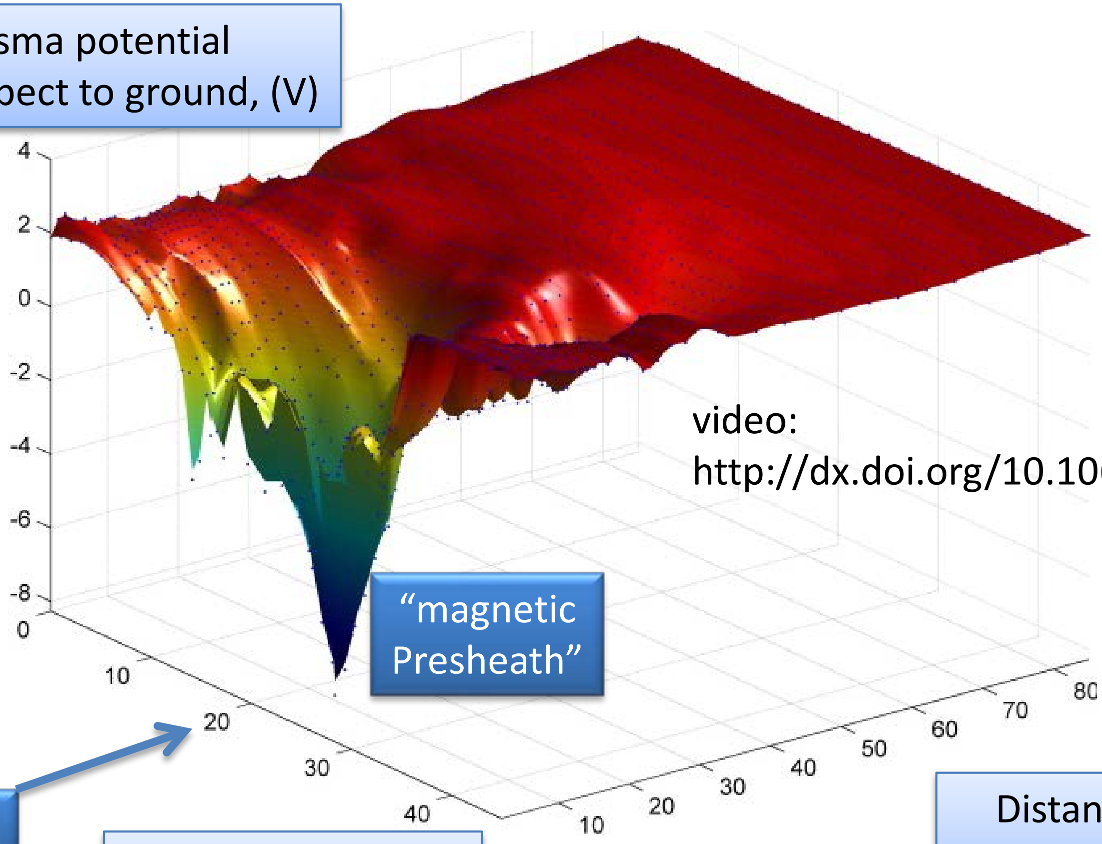

Plasma potential
with respect to ground, (V)

“magnetic
Presheath”

“racetrack”

Distance *r* from
target center, (mm)

Distance *z* from
target surface, (mm)

video:
http://dx.doi.org/10.1063/1.3700242.1

J. Sanders, et al., Rev. Sci. Instrum. **82** (2011) 093505; A. Rauch, et al., J. Appl. Phys. **111** (2012) 083302.

Interesting Consequences of Unbalancing a Magnetron

Not measured

Gyration radius too large to cause electron drift

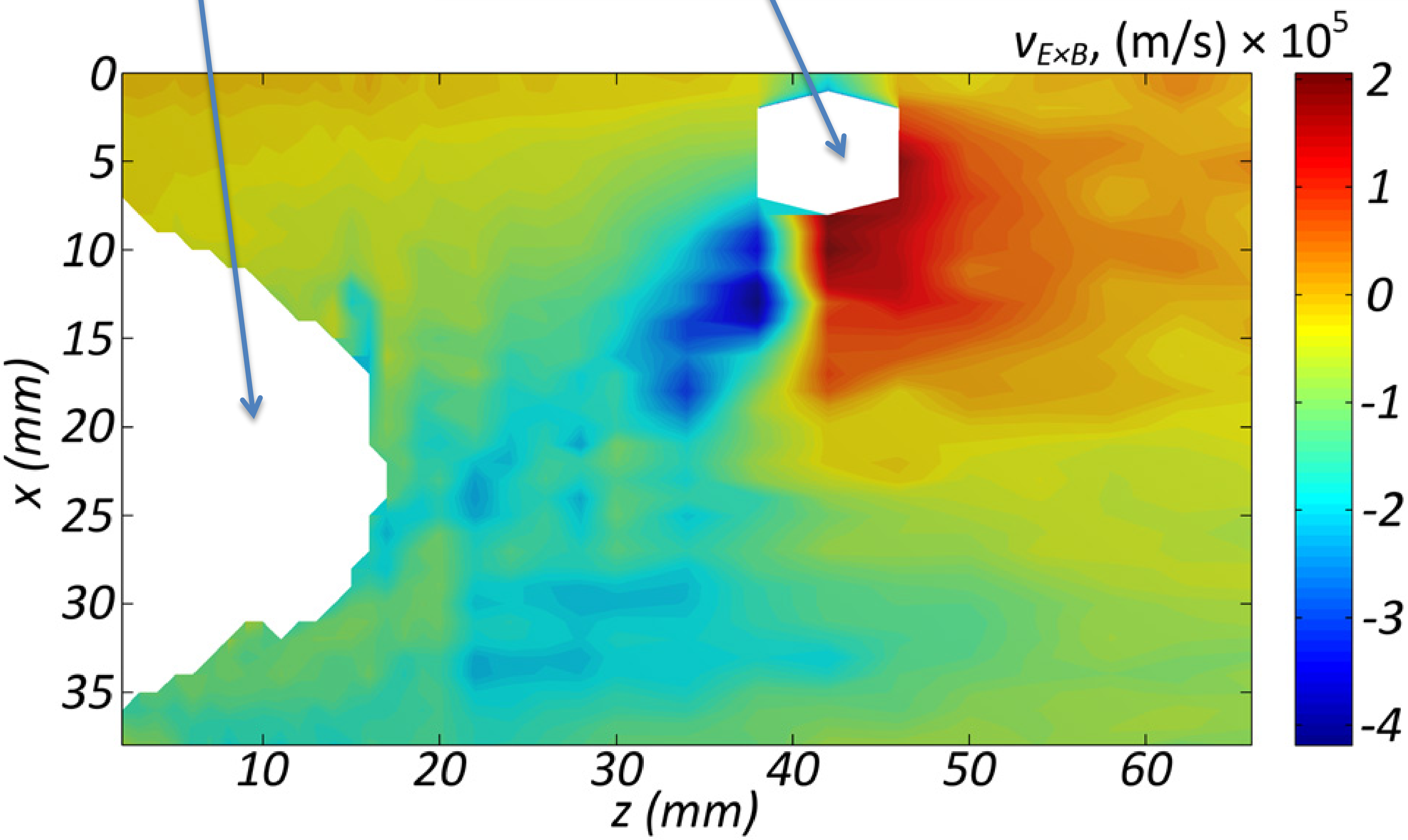

Electron drift velocity can reverse direction as distance to target is increased → one reason for turbulence in magnetron plasma

A. Rauch and A. Anders, Vacuum **89** (2013) 53.

1990s: i-PVD
Magnetron Discharge with Ionization

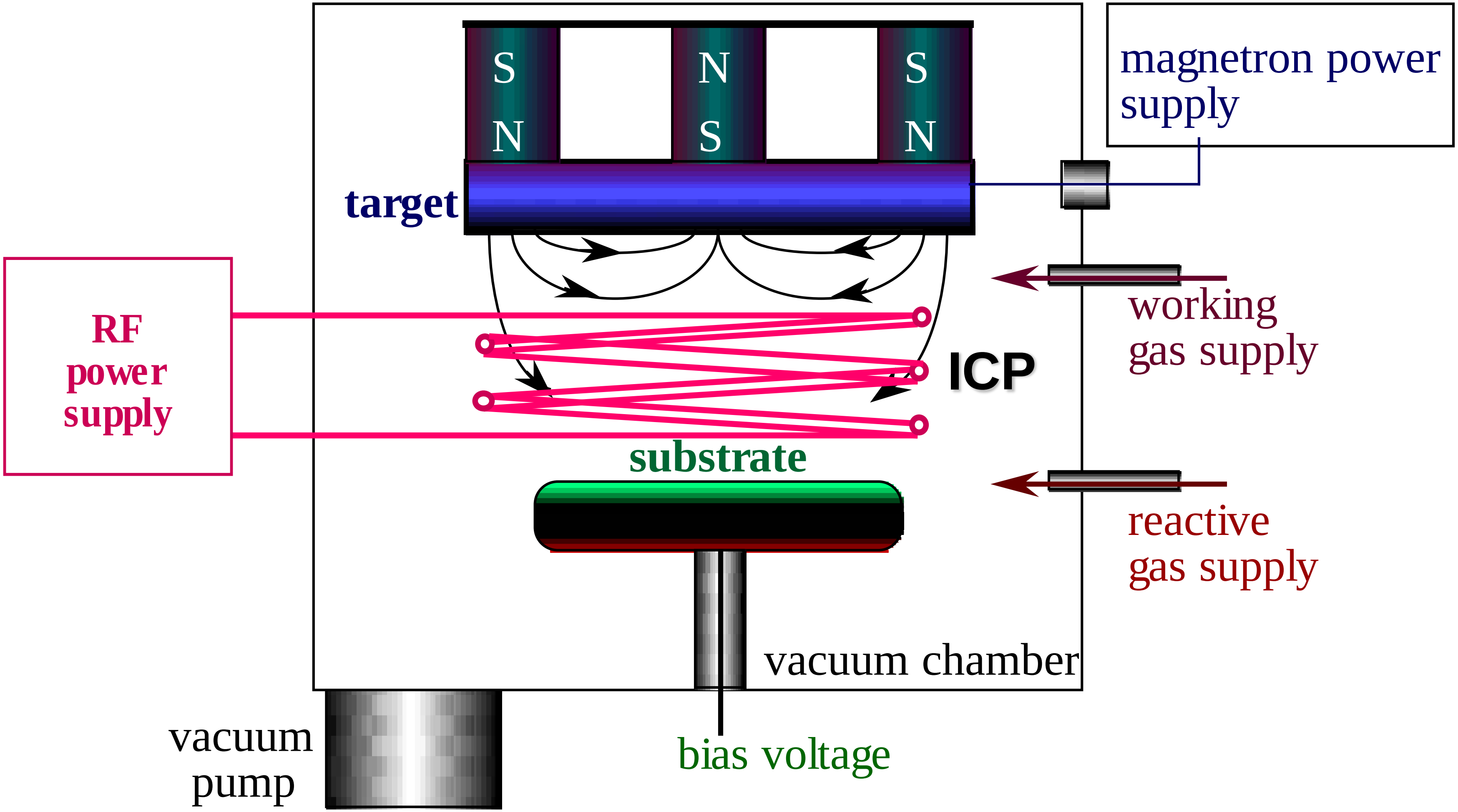

S. M. Rossnagel and J. Hopwood, Appl. Phys. Lett. **63** (1993) 3285-3287

Ionized Physical Vapor Deposition; *Vol.*, edited by J. A. Hopwood (Academic Press, San Diego, CA, 2000).

Turning the Magnetron into a Plasma Source

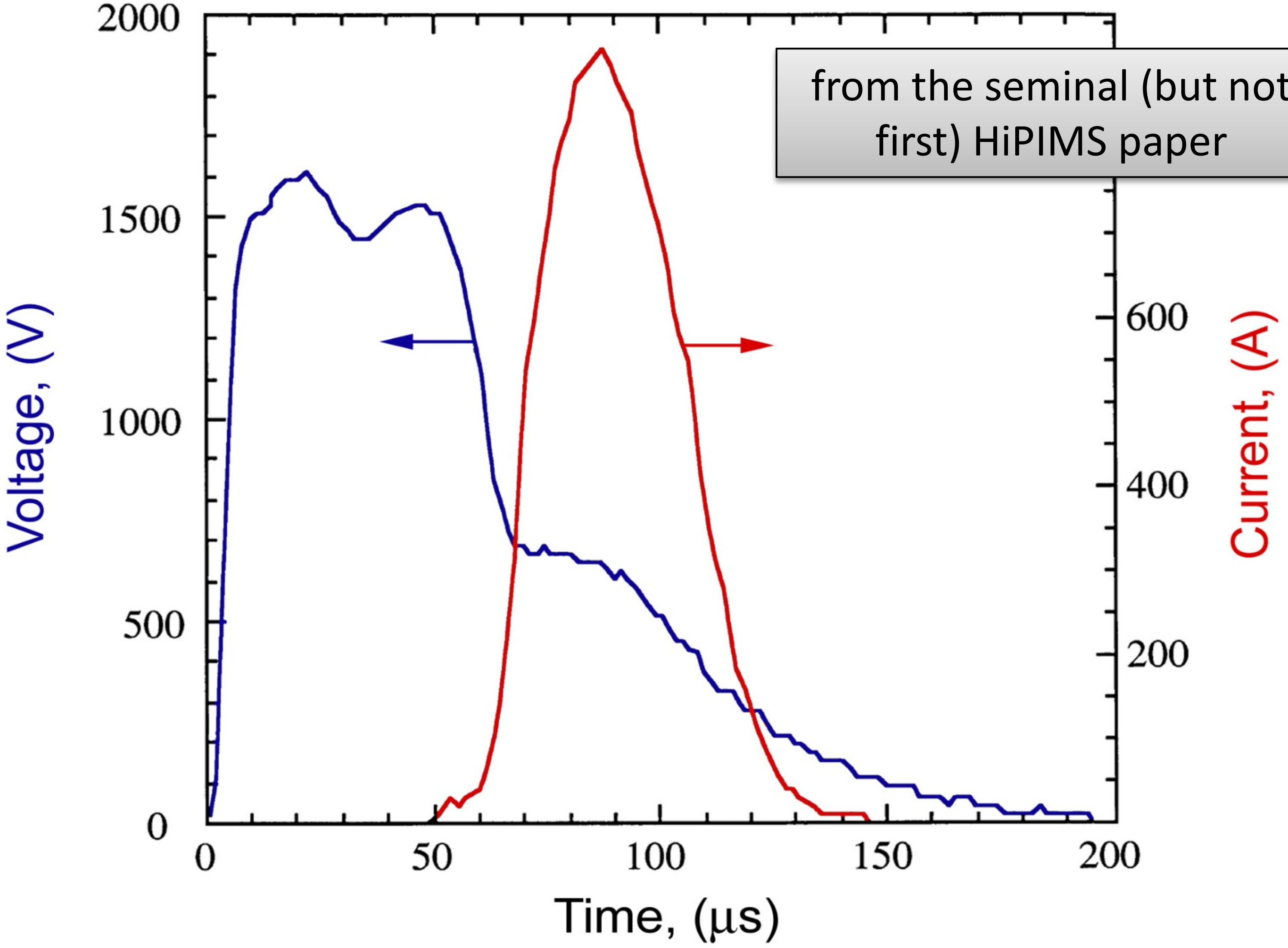

from the seminal (but not first) HiPIMS paper

V. Kouznetsov, *et al.*, Surf. Coat. Technol. **122**, 290-293 (1999)

HiPIMS

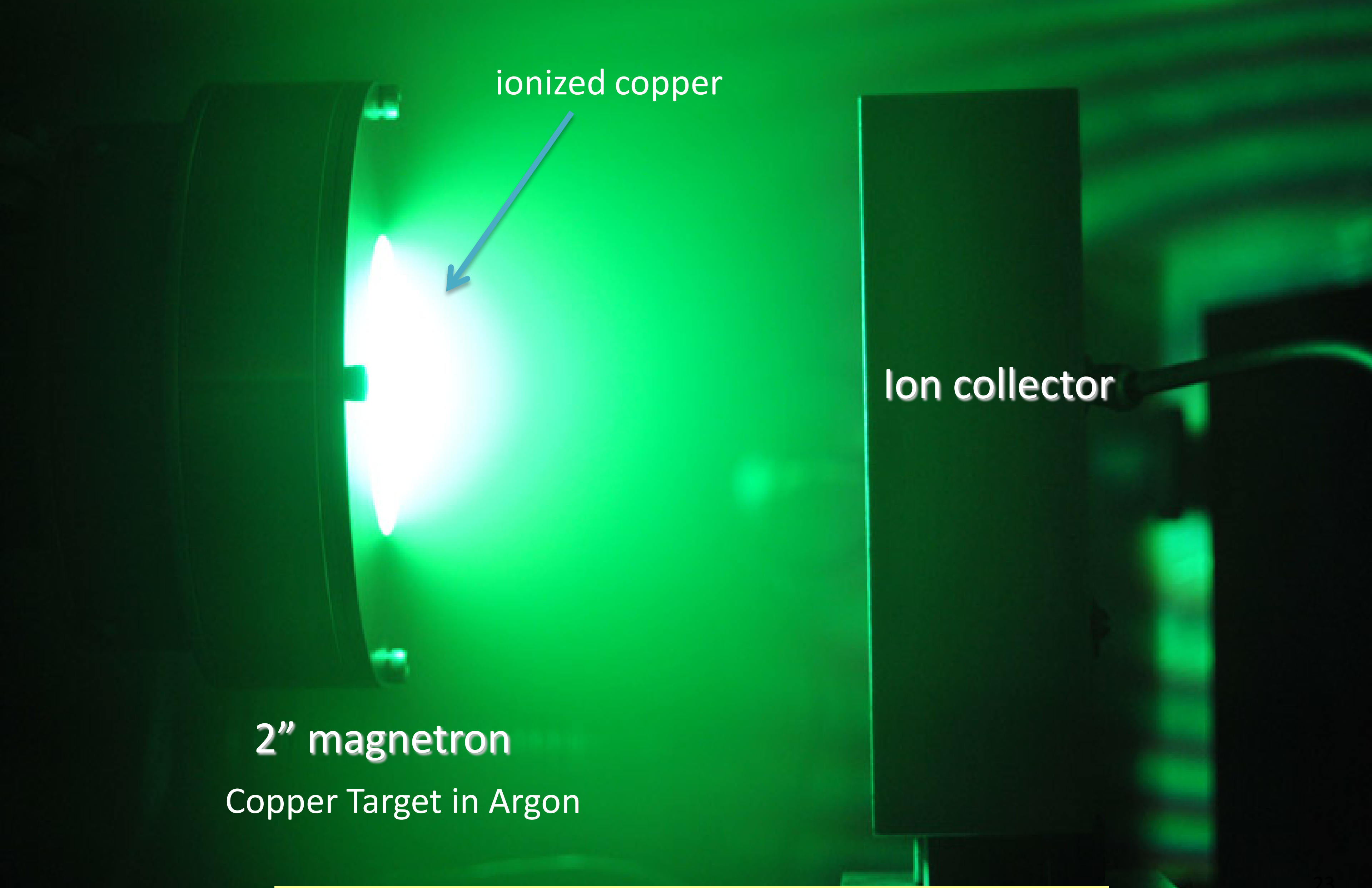

ionized copper

Ion collector

2” magnetron

Copper Target in Argon

J. Andersson and A. Anders, Phys. Rev. Lett. **102** (2009) 045003.

Runaway of Self-Sputtering

Copper target,
2” magnetron

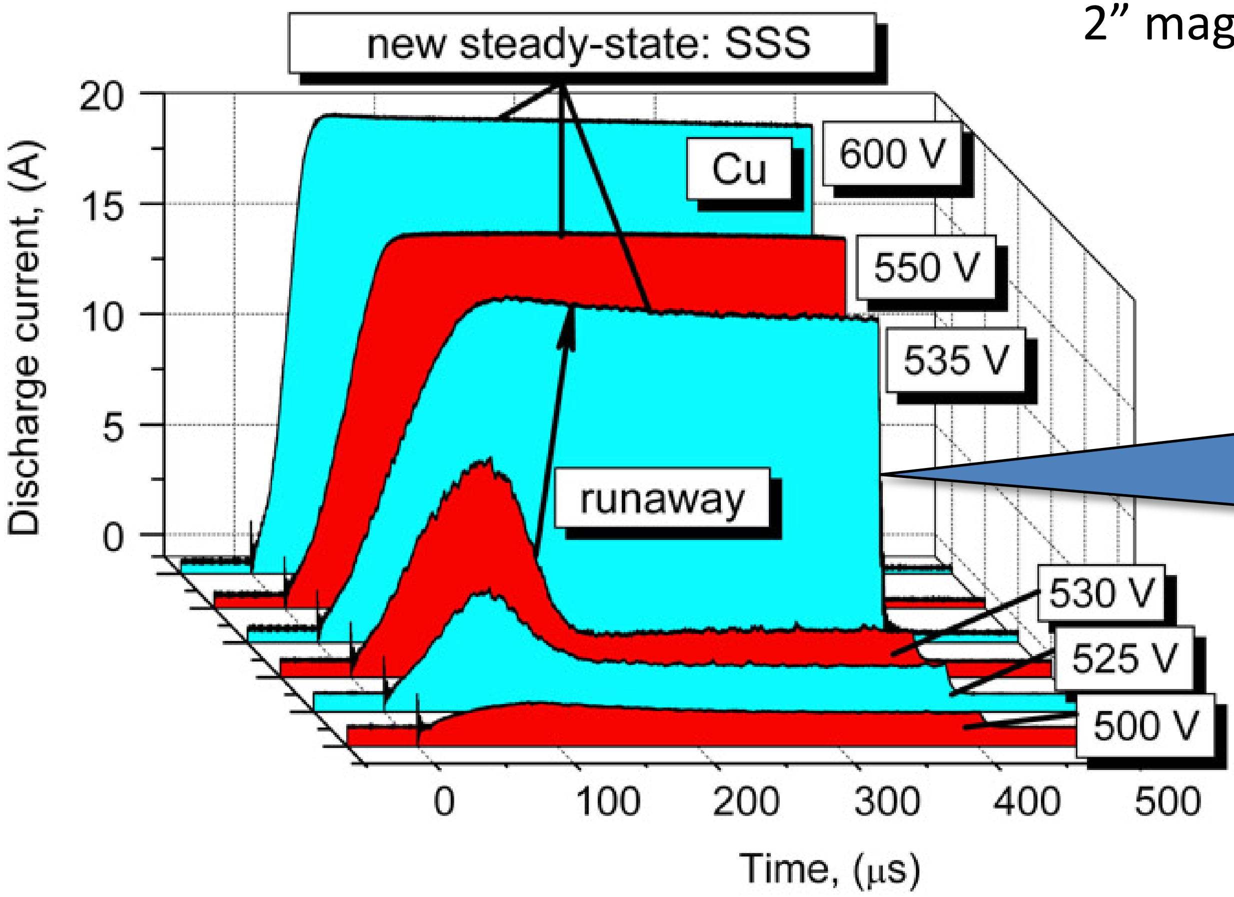

Look for this small change in voltage but huge effect in current!

A. Anders, *et al.*, J. Appl. Phys. **103** (2008) 039901

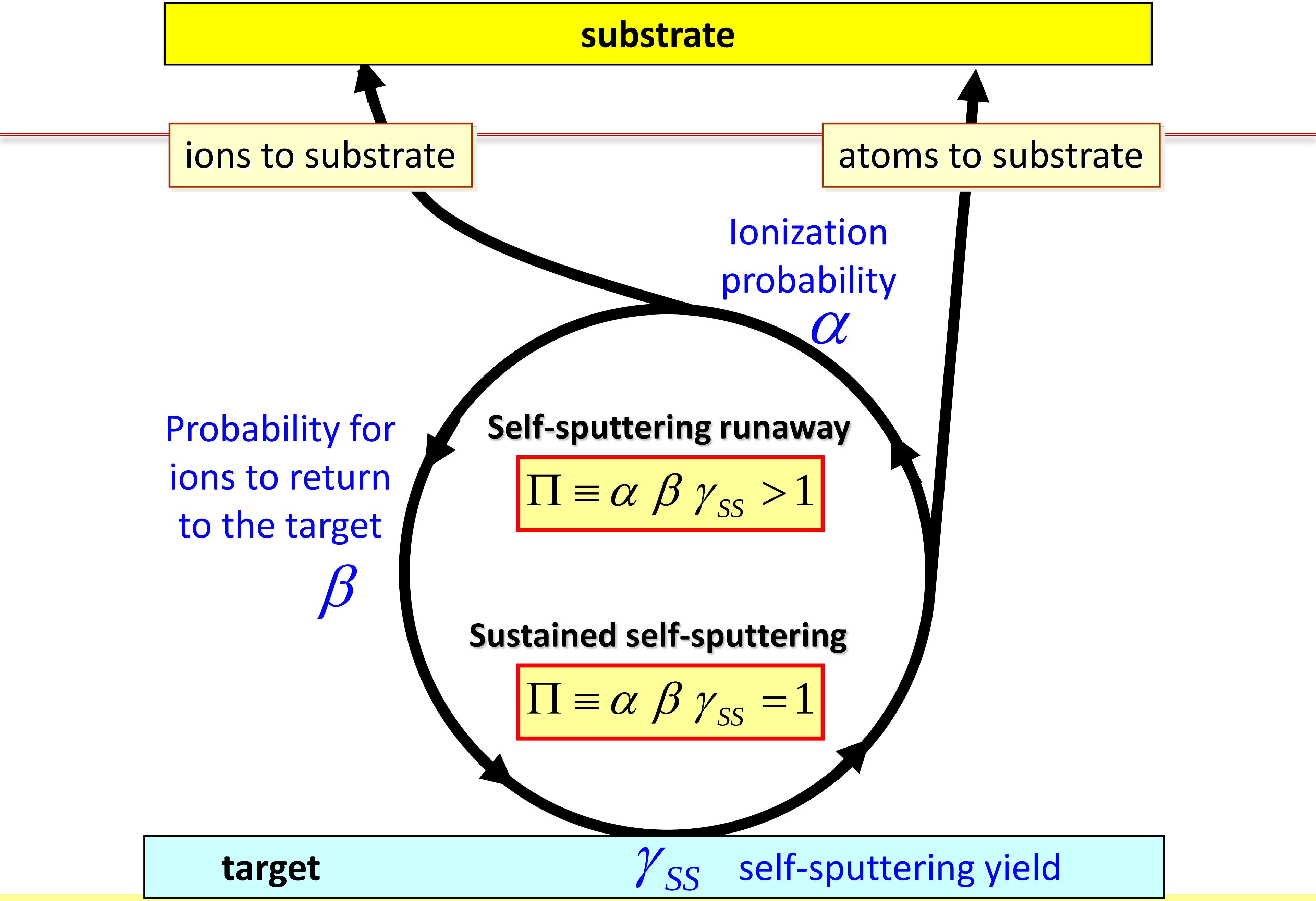

substrate

ions to substrate

atoms to substrate

Ionization probability α

Probability for ions to return to the target β

Self-sputtering runaway

$$\Pi \equiv \alpha \, \beta \, \gamma_{SS} > 1$$

Sustained self-sputtering

$$\Pi \equiv \alpha \, \beta \, \gamma_{SS} = 1$$

target

γ_{SS} self-sputtering yield

N. Hosokawa et al., Proc. 8th Vac. Con., (1980) 11; A. Anders, Appl. Phys. Lett. 92 (2008) 201501
A. Anders, Surf. Coat. Technol. 205 (2011) S1.

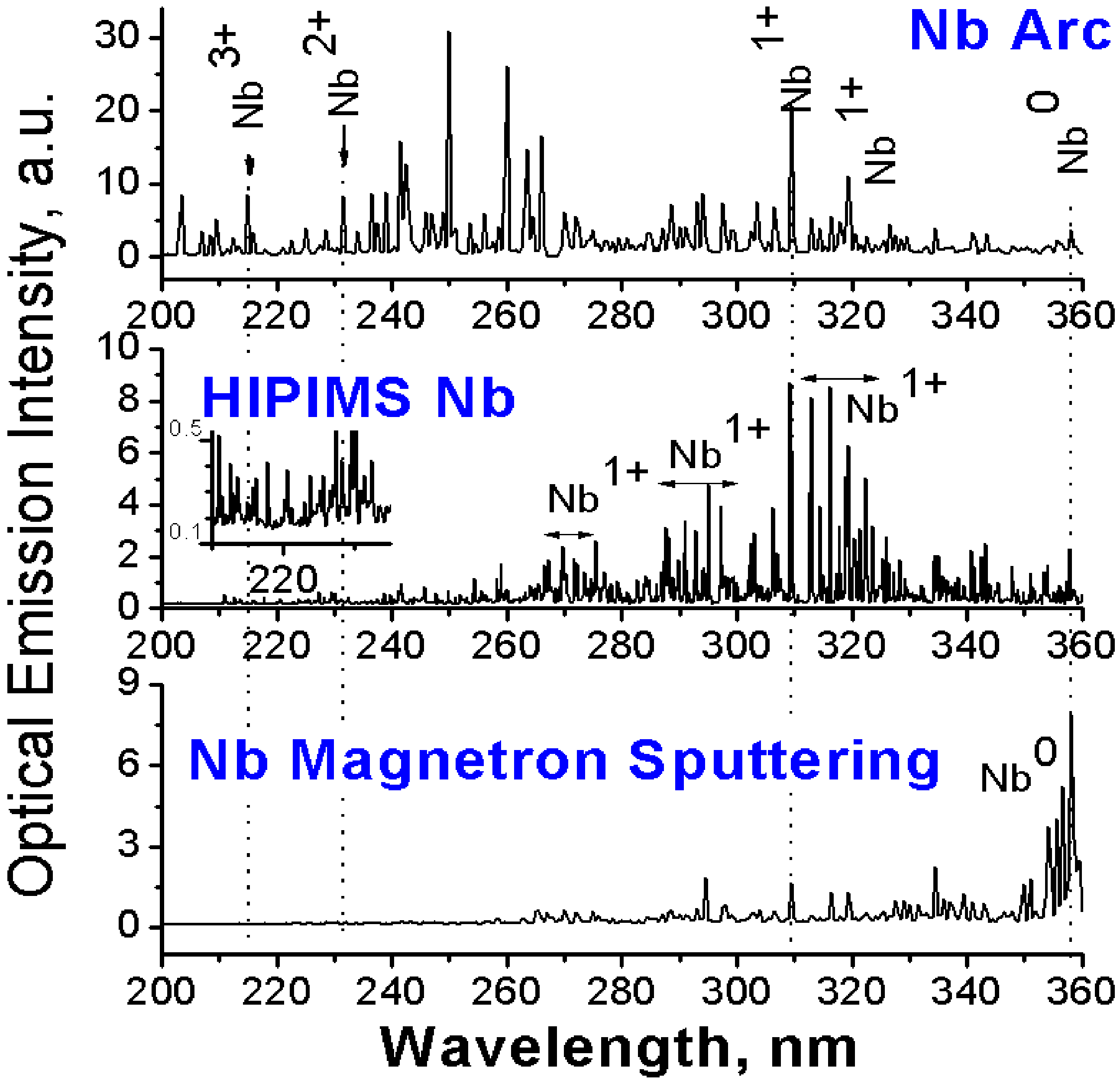

Arc contains multiply charged metal ions

HiPIMS contains mainly singly charged metal ions

Conventional sputtering contains neutral metal atoms

C. Reinhard et al., Thin Solid Films 515 (2007) 3685.

Runaway can be observed for *all* target materials

including those with extremely small self-sputtering yield, which was initially surprising

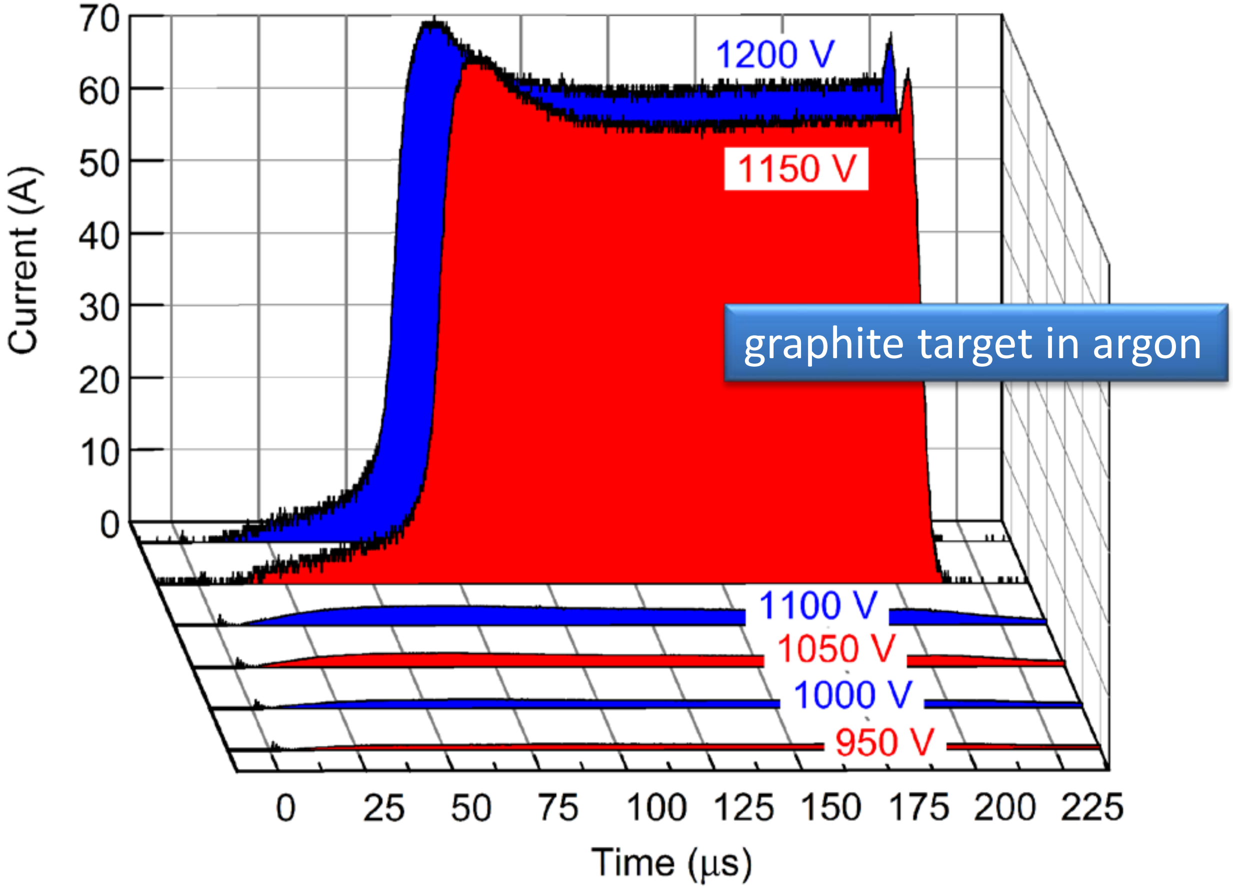

graphite target in argon

A. Anders, *et al*., J. Phys D: Appl. Phys. **45** (2012) 012003.

Generalized Flux Model for HIPIMS

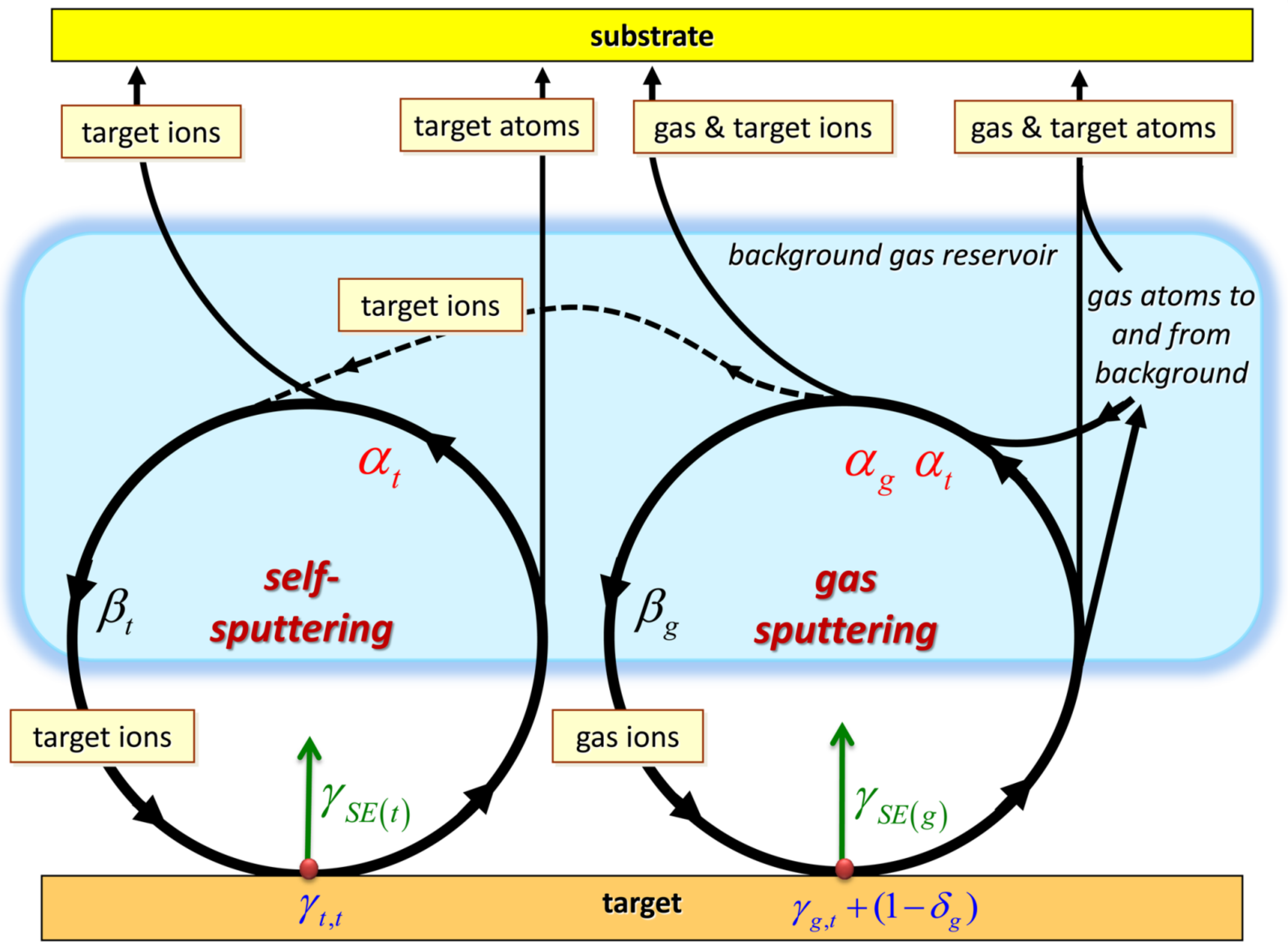

A. Anders, *et al.*, J. Phys D: Appl. Phys. **45** (2012) 012003.

Evidence for Gas-Recycling Model

after runaway to high power, argon emission remains dominant:

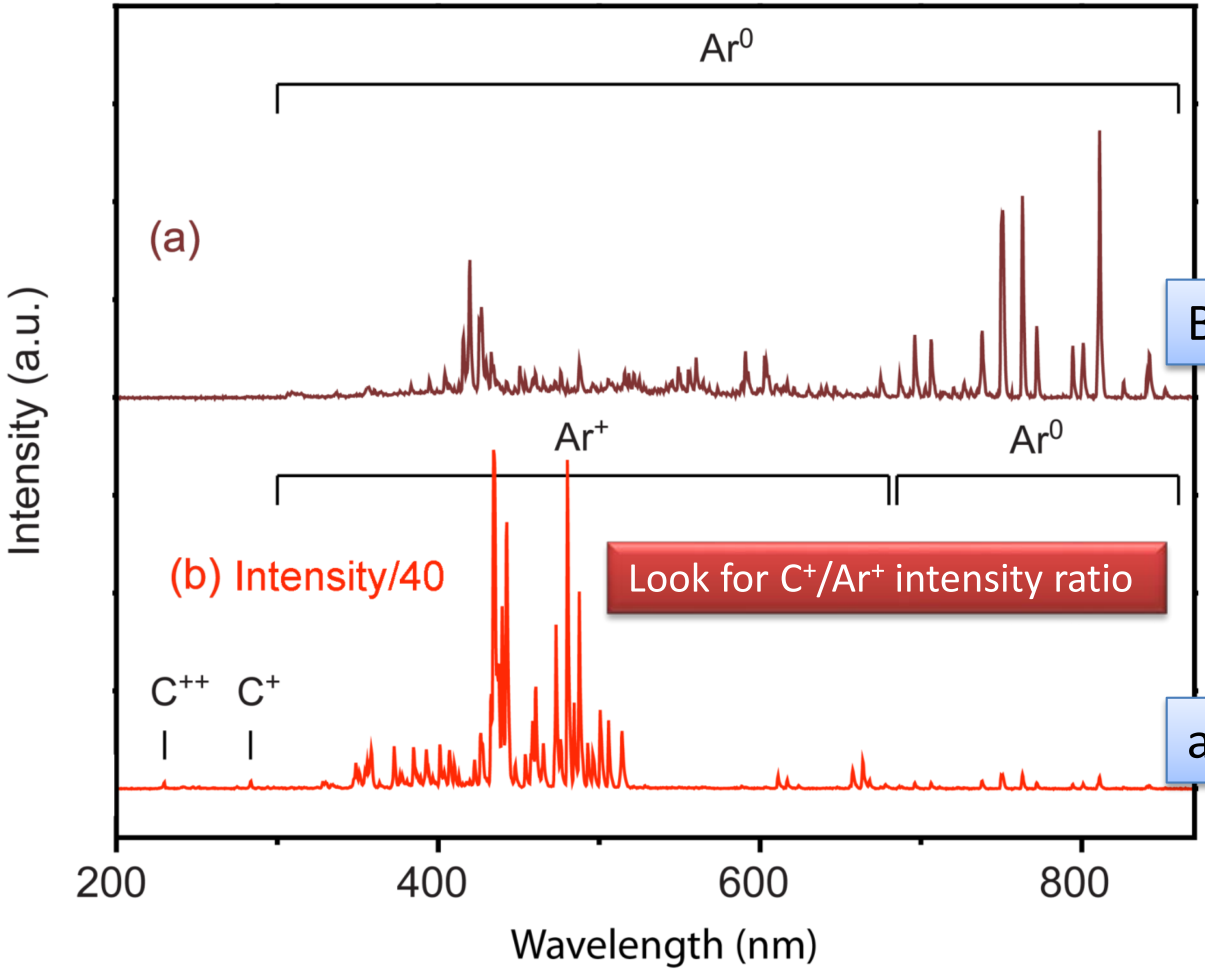

Below runaway, low power

Look for C$^+$/Ar$^+$ intensity ratio

above runaway, high power

A. Anders, *et al.*, J. Phys D: Appl. Phys. **45** (2012) 012003.

Dynamic Gas Rarefaction

Heating of target reduces gas density: may lead to violation of runaway condition

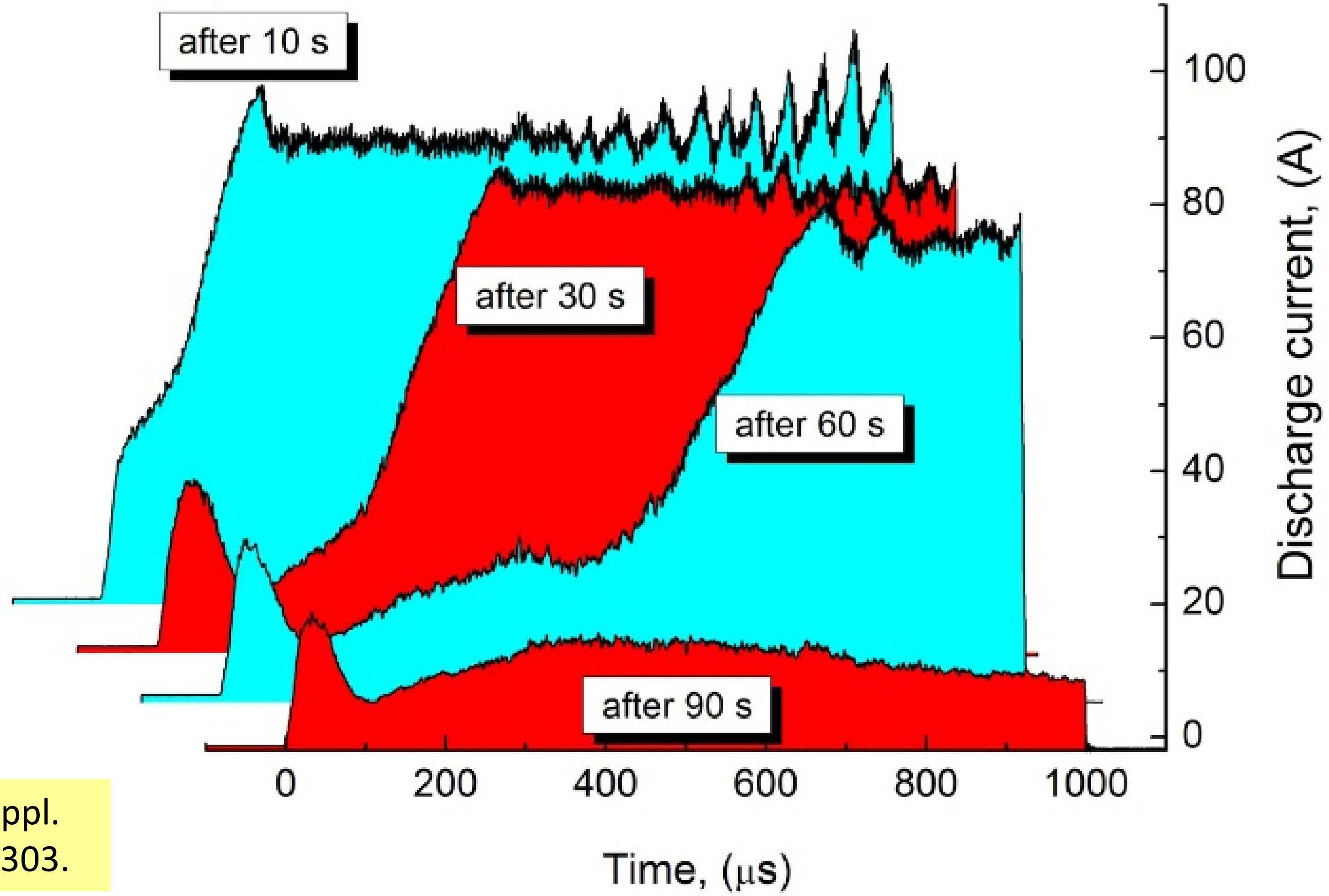

A. Anders, *et al.*, J. Appl. Phys. **102** (2007) 113303.

Ion Energy Distribution Functions

Measured with a differentially pumped M/Q spectrometer

- example: EQP 300 by HIDEN Ltd.
- at Berkeley: sampling orifice is facing the racetrack
- measure ion energy distribution functions for selected mass
- *M/Q* of ion species are selected, for example, the signal of as $^{48}Ti^{4+}$ is at the same location in the “mass spectrum” as $^{12}C^{1+}$

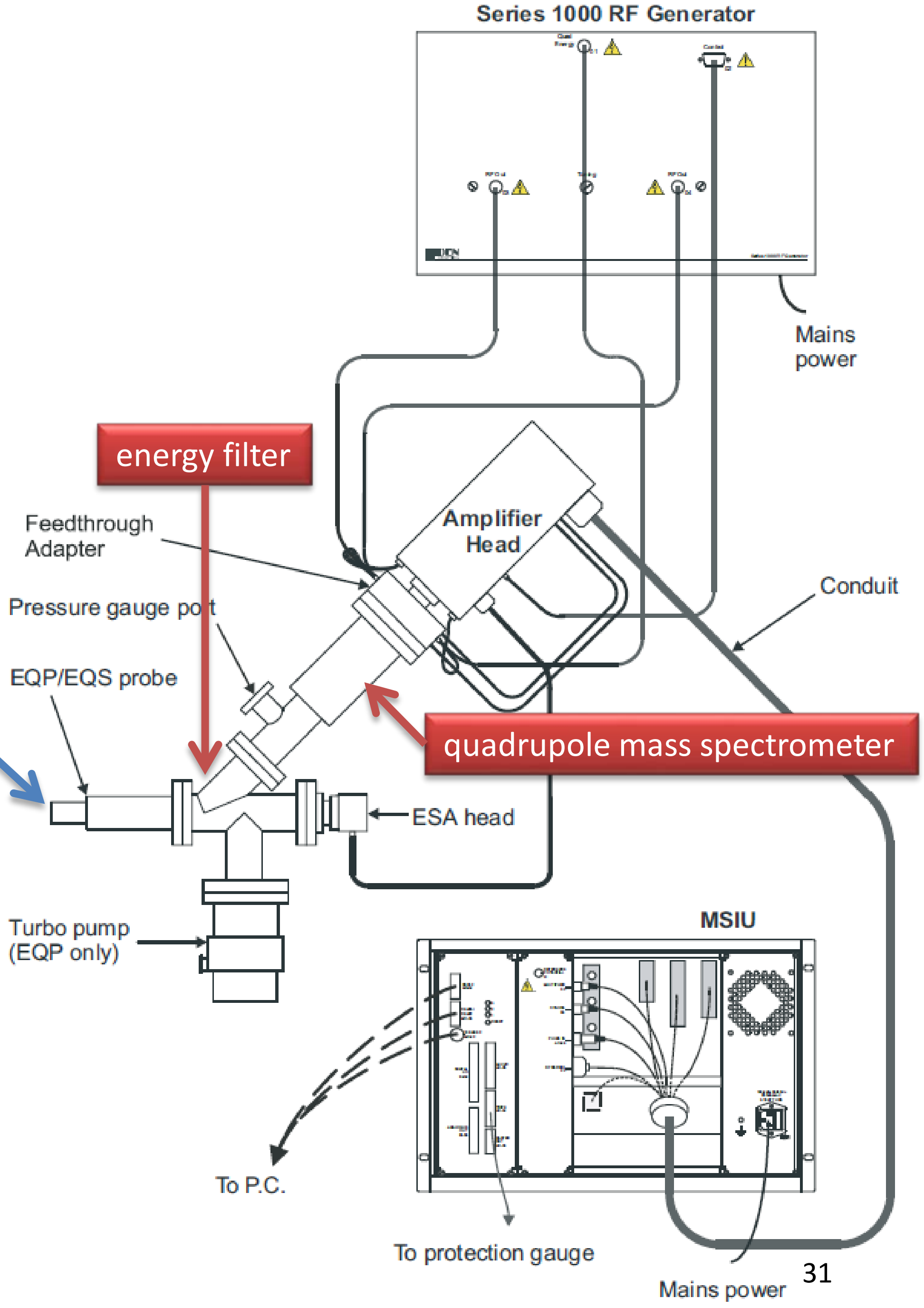

Measurements of Ion Energy Distributions

We use EQP300 by Hiden Ltd.; scan mass up to 300 amu and energies up to 1 keV (neg. and pos. ions)

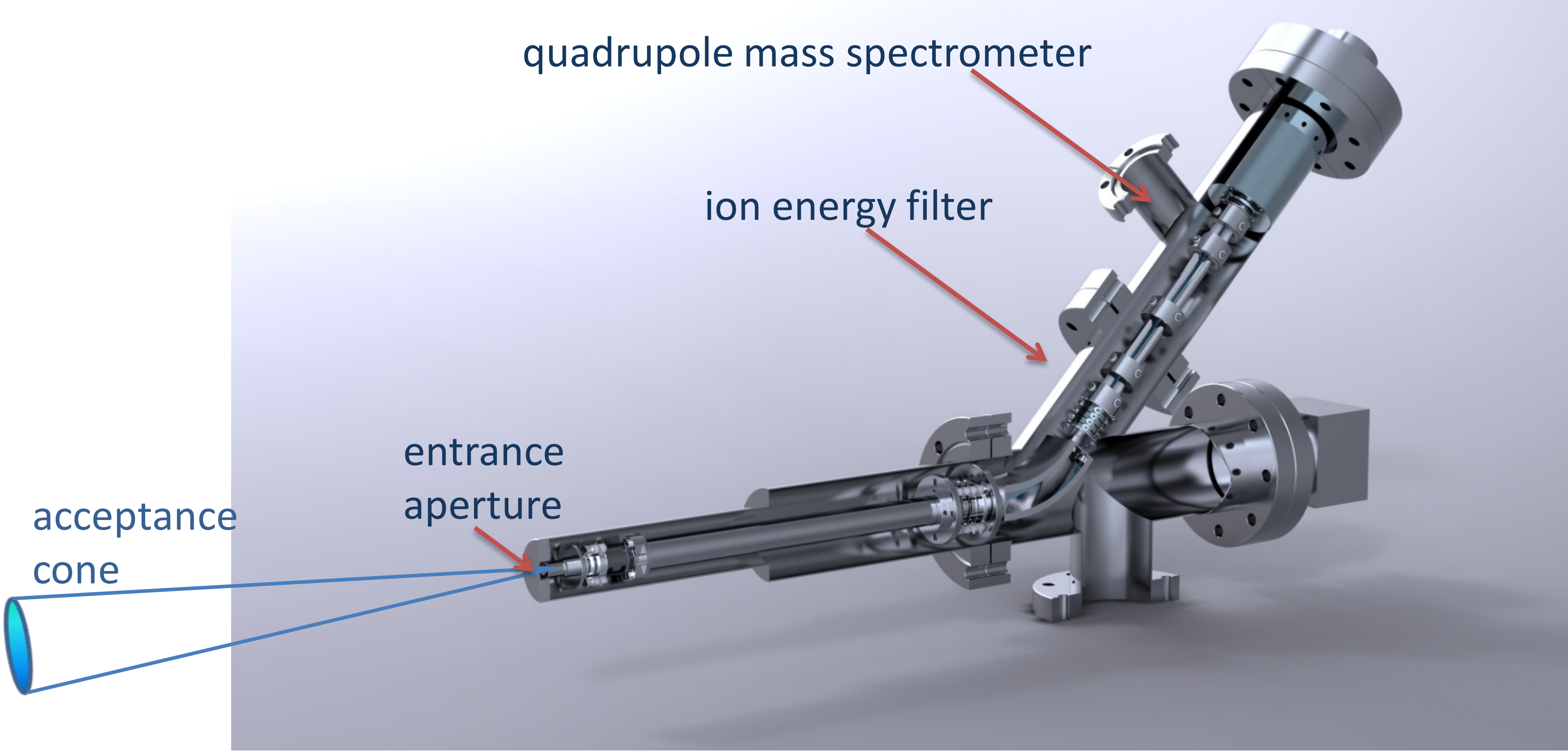

Instrument transmittance function has a greater acceptance cone angle for small (especially < 10 eV) ion energies

Plenty of Evidence for Metal Ionization in HIPIMS

- Example: Ti target, ∅ 5 cm, Ar, 850 V, 60 A after 50 μs
- *M/Q* spectrum sampled for the 100-150 μs window of the 150 μs discharge

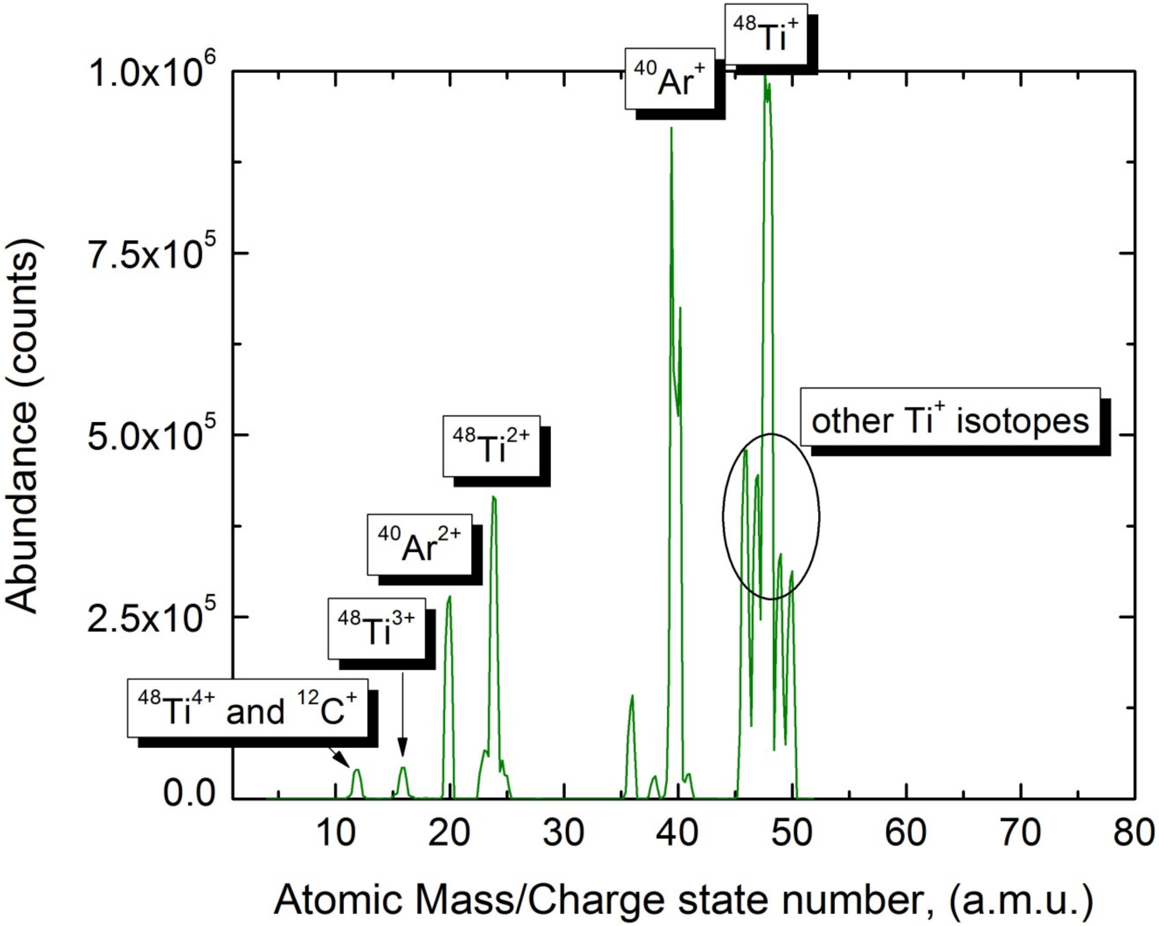

- metal can dominate the plasma
- singly charged ions are most frequent
- even higher charge states are present, up to 4+ detected for extreme power conditions

J. Andersson, *et al.*, Appl. Phys. Lett. **93** (2008) 071504.

Ion Energy Distribution Function – measured azimuthally

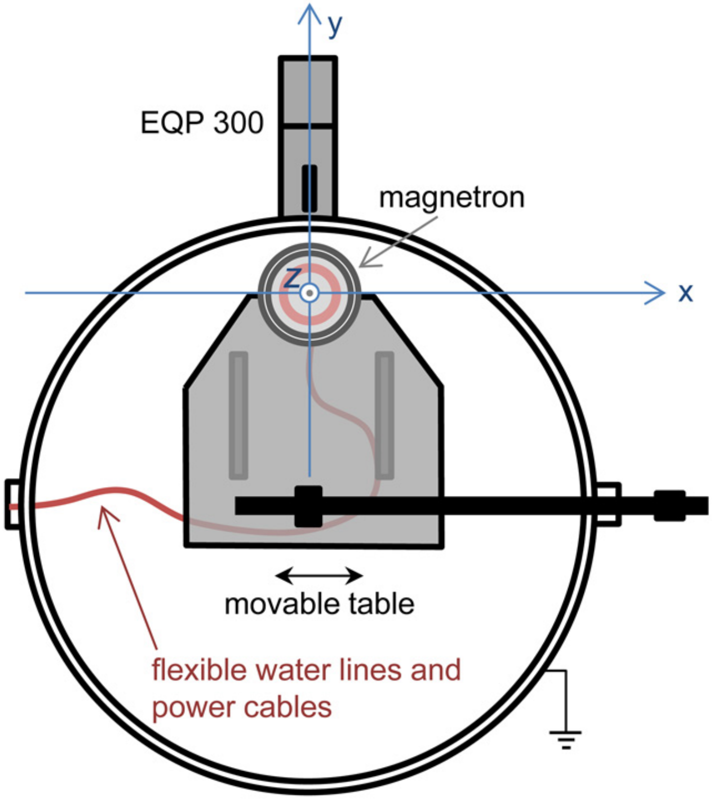

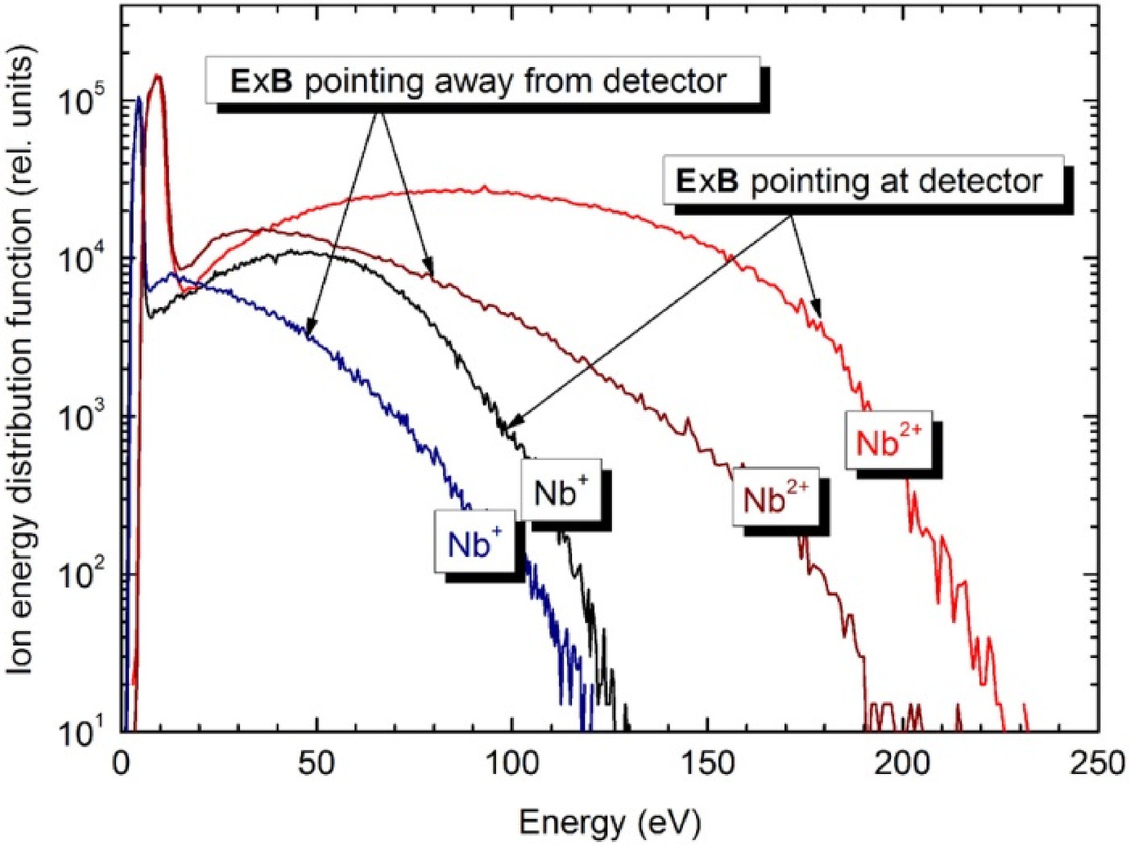

A. Anders, *et al.*, Appl. Phys. Lett. **103** (2013) 144103;
M. Panjan, *et al.*, Plasma Sources Sci. Technol. 23 (2014) 025007.

Recent Research: Ionization Zones are Regions of Elevated Potential → Ions gain extra energy

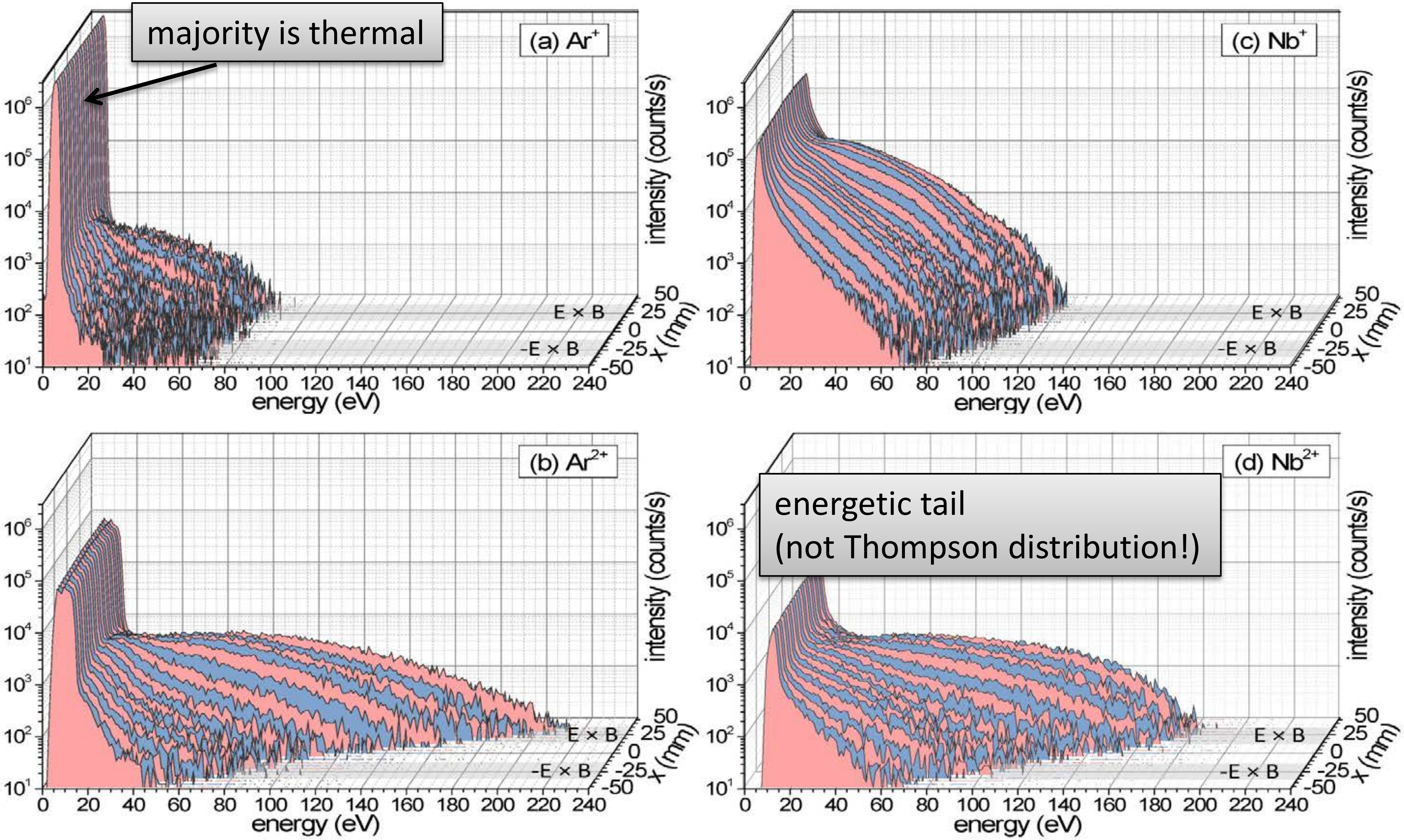

majority is thermal

energetic tail
(not Thompson distribution!)

M. Panjan, *et al*., Plasma Sources Sci. Technol. **23** (2014) 025007.

Thompson-Sigmund Binary Collision Theory

approximation:

$$f_{\text{Thompson}}\left(\varepsilon\right) \propto \frac{\varepsilon}{\left(\varepsilon + \varepsilon_{SB}\right)^{3}}$$

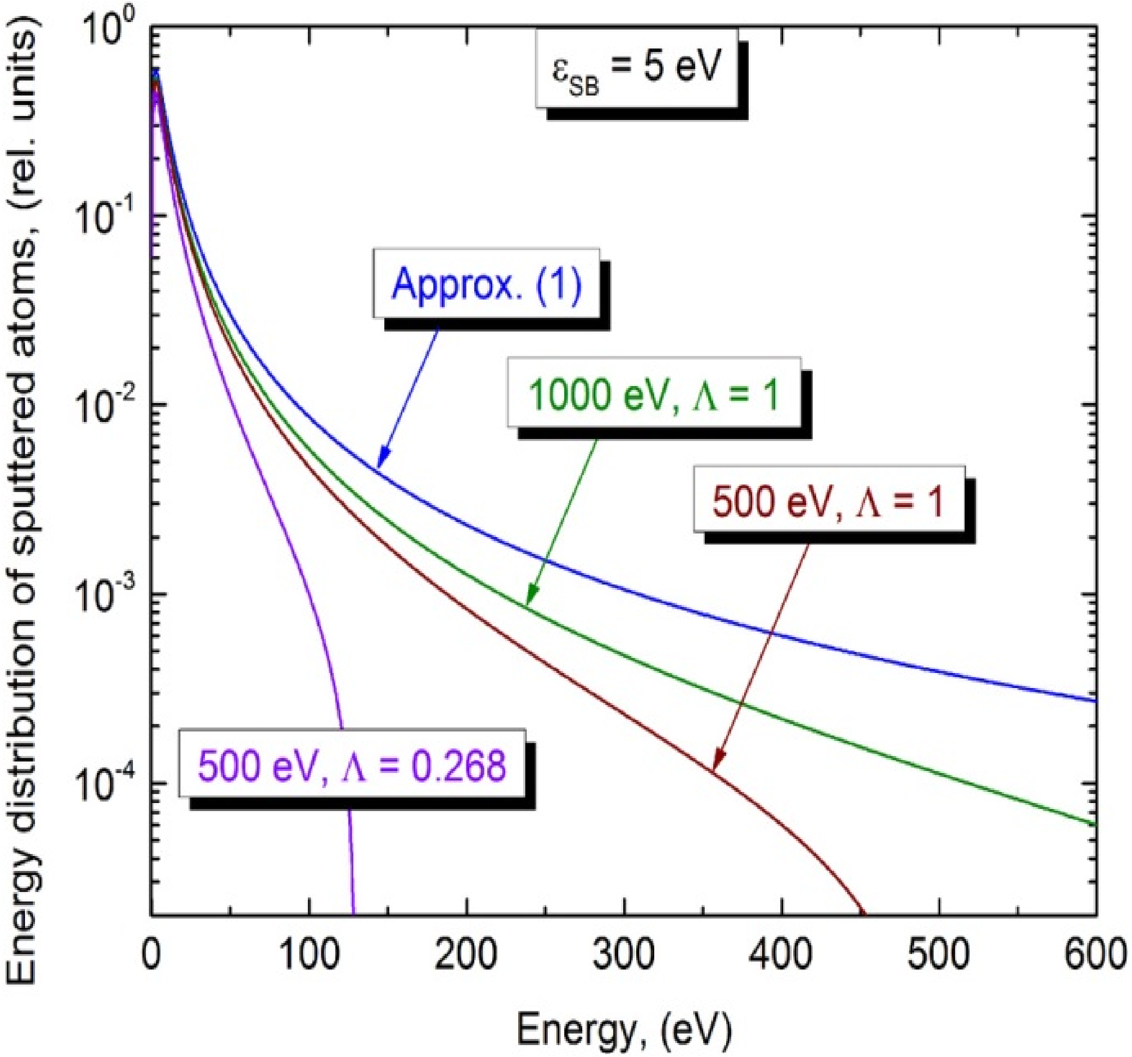

A. Anders, *et al.*, Appl. Phys. Lett. **103** (2013) 144103.

Energizing Electrons in the Sheath Versus in Presheath

- **Thornton paradigm**: $E_{SE} = eV_{sheath}$ and all electron heating results from hot (secondary) electrons
- However, even as the voltage drop in the magnetic presheath is much smaller than in the sheath, the electron current in the presheath is much greater and than in the sheath → *energy dissipation and electron heating in the presheath can be greater than electron heating by secondary electrons*

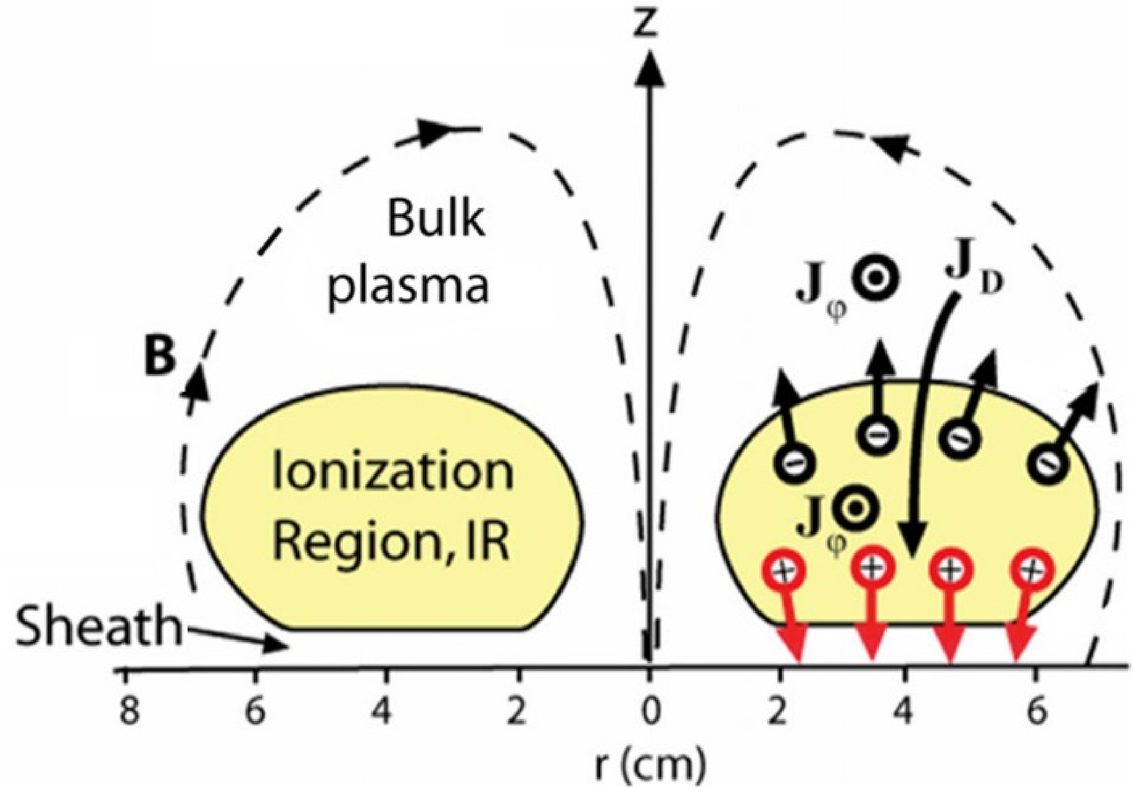

Global ionization model

C. Huo, *et al*., Plasma Sources Sci. Technol. **22** (2013) 045005.

Ionization zones and transport of charged particles

HiPIMS discharge

U = 390 V
I_{av} = 1.25 A
P = 450 W

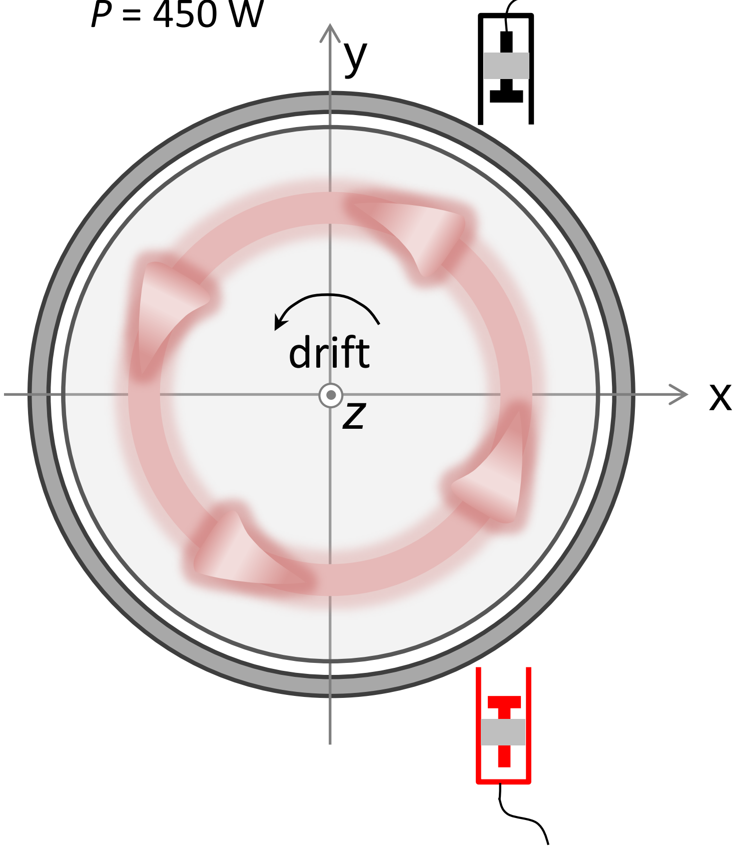

bottom collector

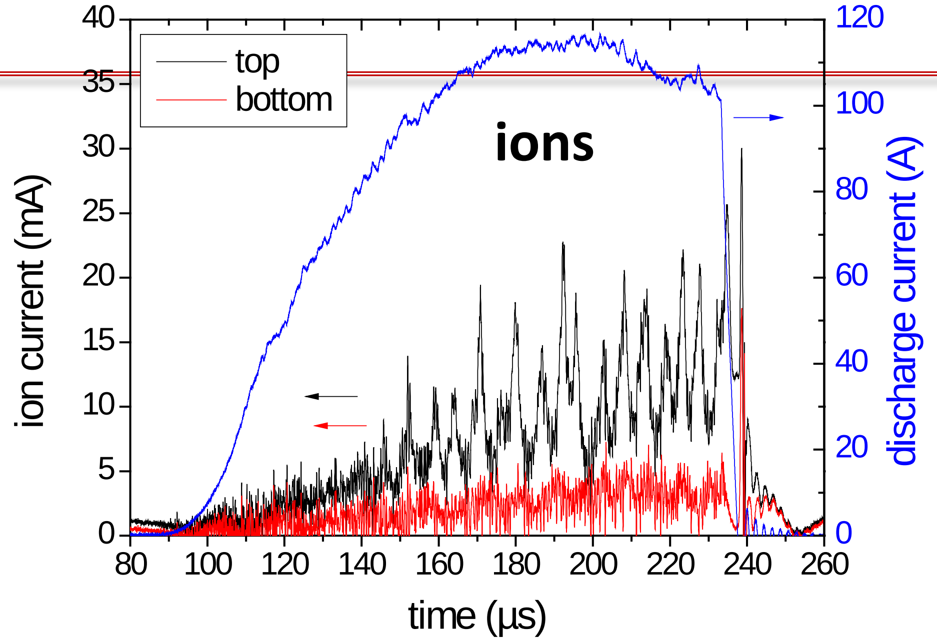

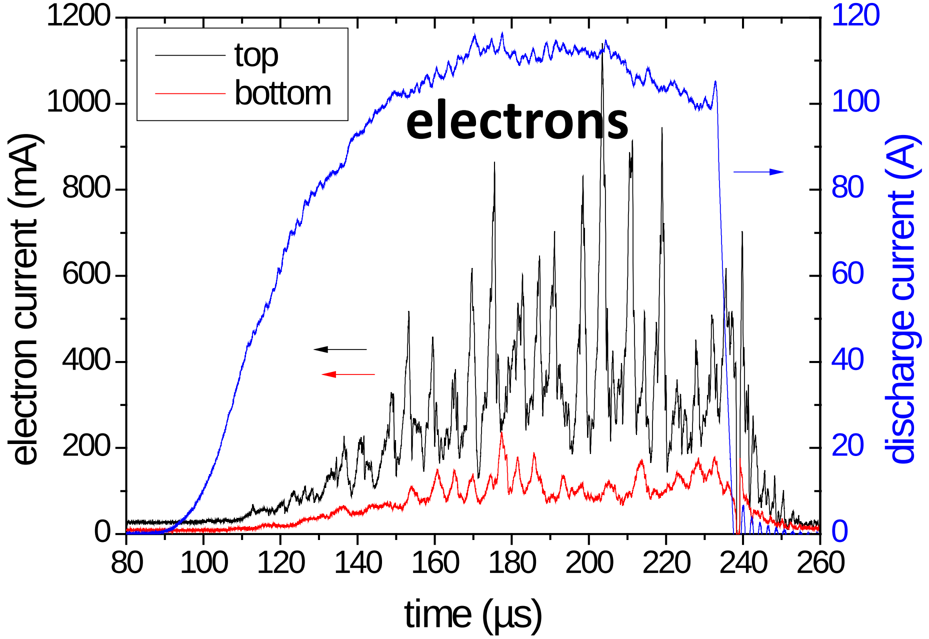

M. Panjan, *et al.*, *Plasma Sources Sci. Technol.*, **23** (2014) 025007.

Biased Probes Indicate Flux Contains Jets, and Suggest Asymmetry Related to ExB Direction

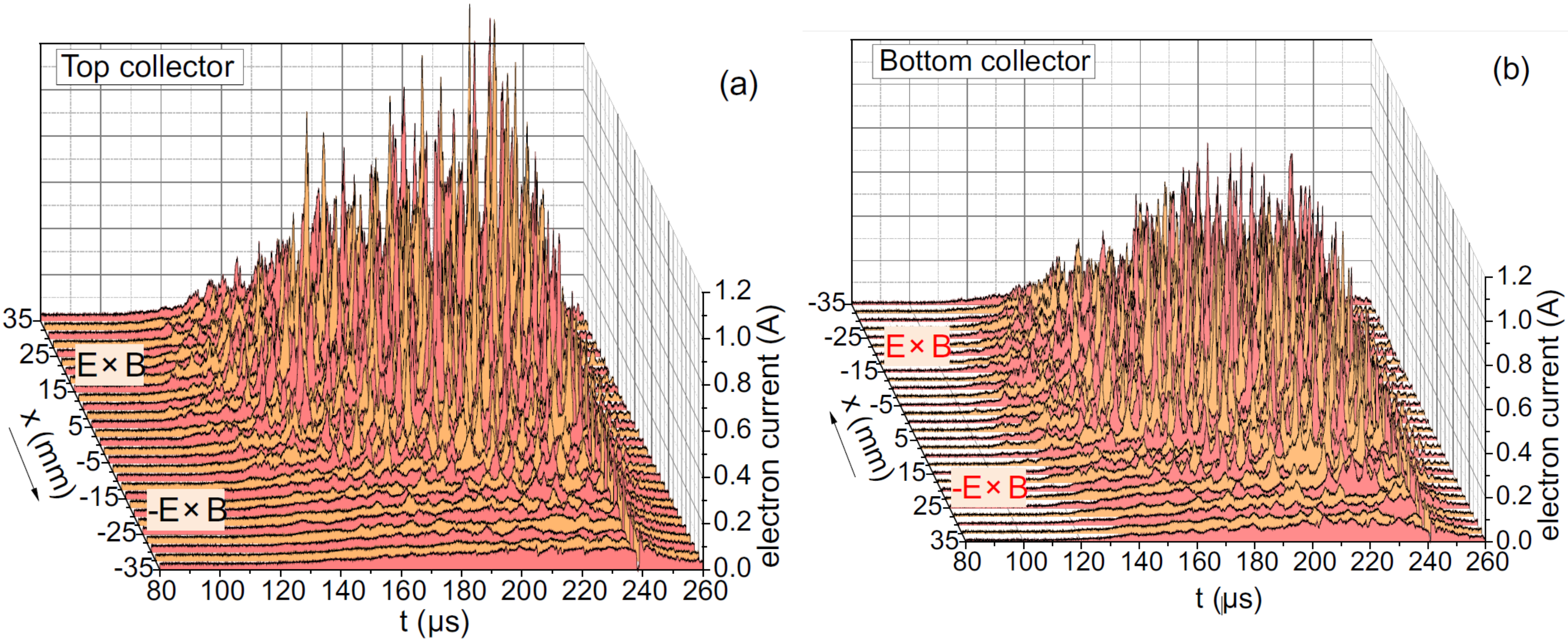

M. Panjan, *et al*., Plasma Sources Sci. Technol. **23** (2014) 025007.

Spectroscopic Diagnostics of HIPIMS

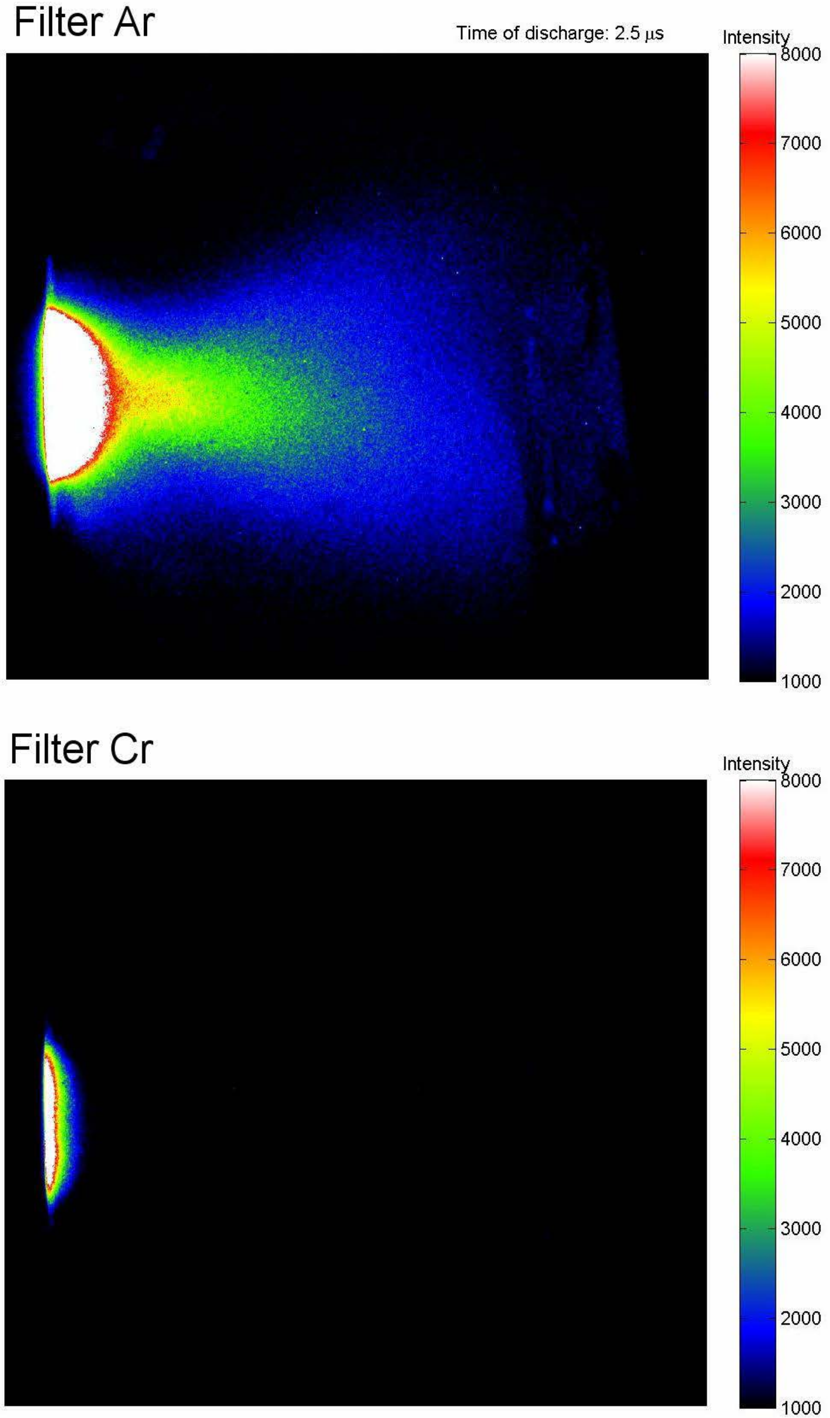

4 Pa, Ar, apply 2000 V

→ Video clip courtesy of Matej Hala.

M. Hála, et al. , IEEE Trans. Plasma Sci. **38** (2010) 3035.

Fast Camera Observations of HIPIMS Discharges

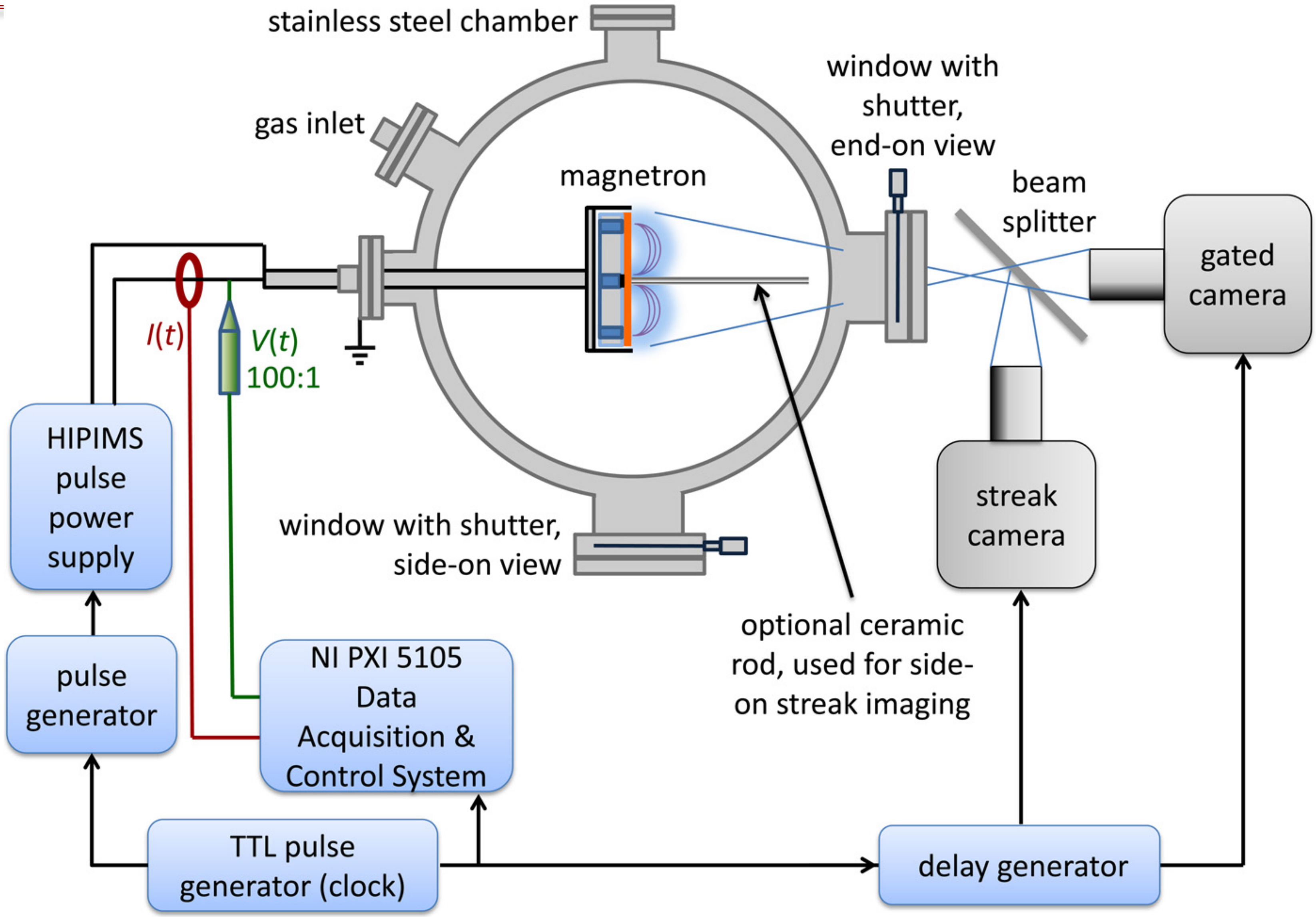

A. Anders, *et al.*, *J. Appl. Phys*. **111** (2012) 053304

Localization of Ionization and Self-Organization

observed by several
groups in the last years

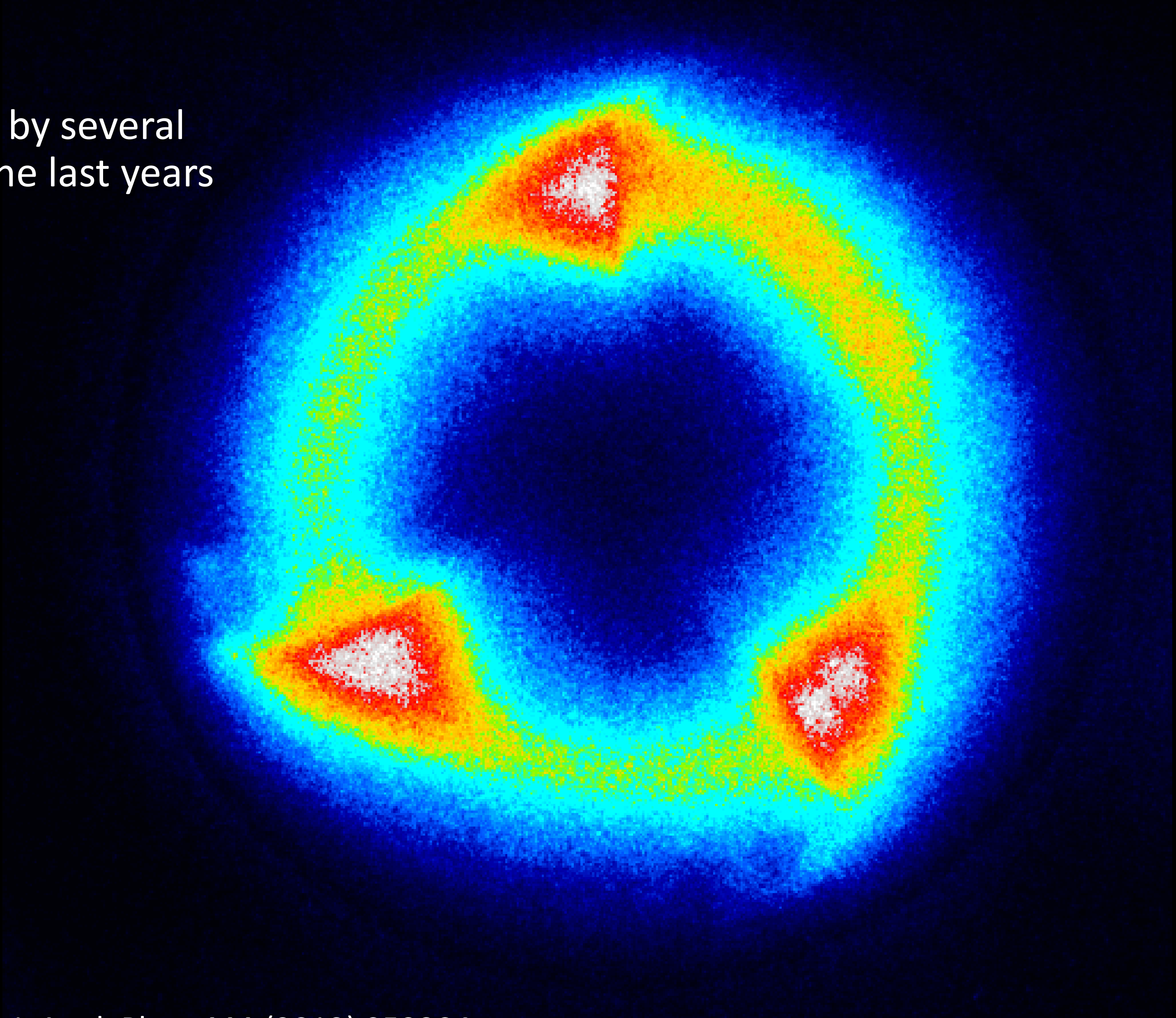

A. Anders, *et al.*, J. Appl. Phys. **111** (2012) 053304

Side-on view frame image

(10 ns snapshot)

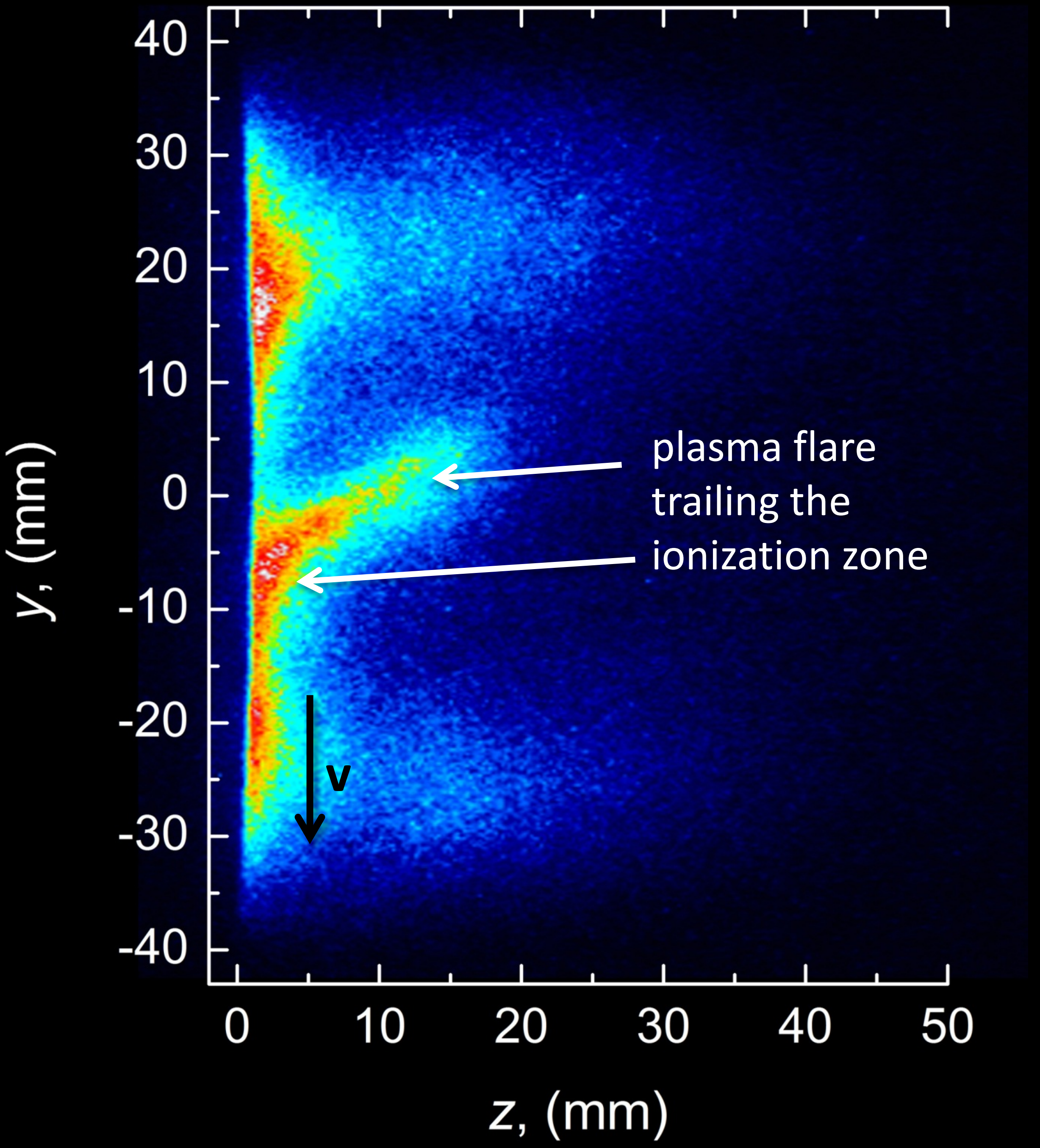

A. Anders, *et al.*, J. Appl. Phys. **111** (2012) 053304

Ionization Zones (Spokes) as Origins of Plasma Flares

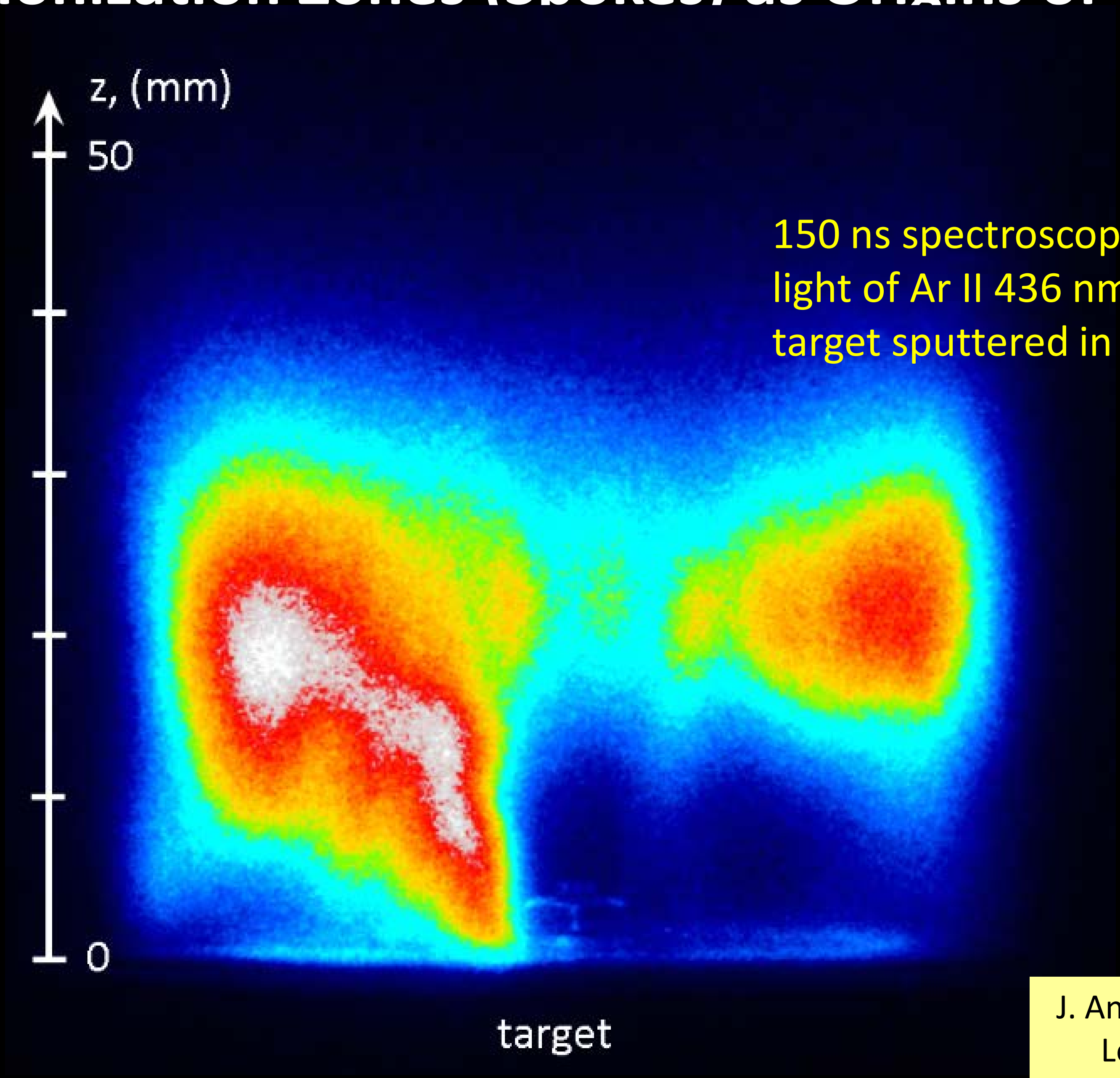

150 ns spectroscopic image in the light of Ar II 436 nm; 7.5 cm Al target sputtered in argon; 100 A

J. Andersson, et al., Appl. Phys. Lett. **103** (2013) 054104.

Streak image sequence, 20 μs sweep time

A. Anders, *et al*., J. Appl. Phys. **111** (2012) 053304

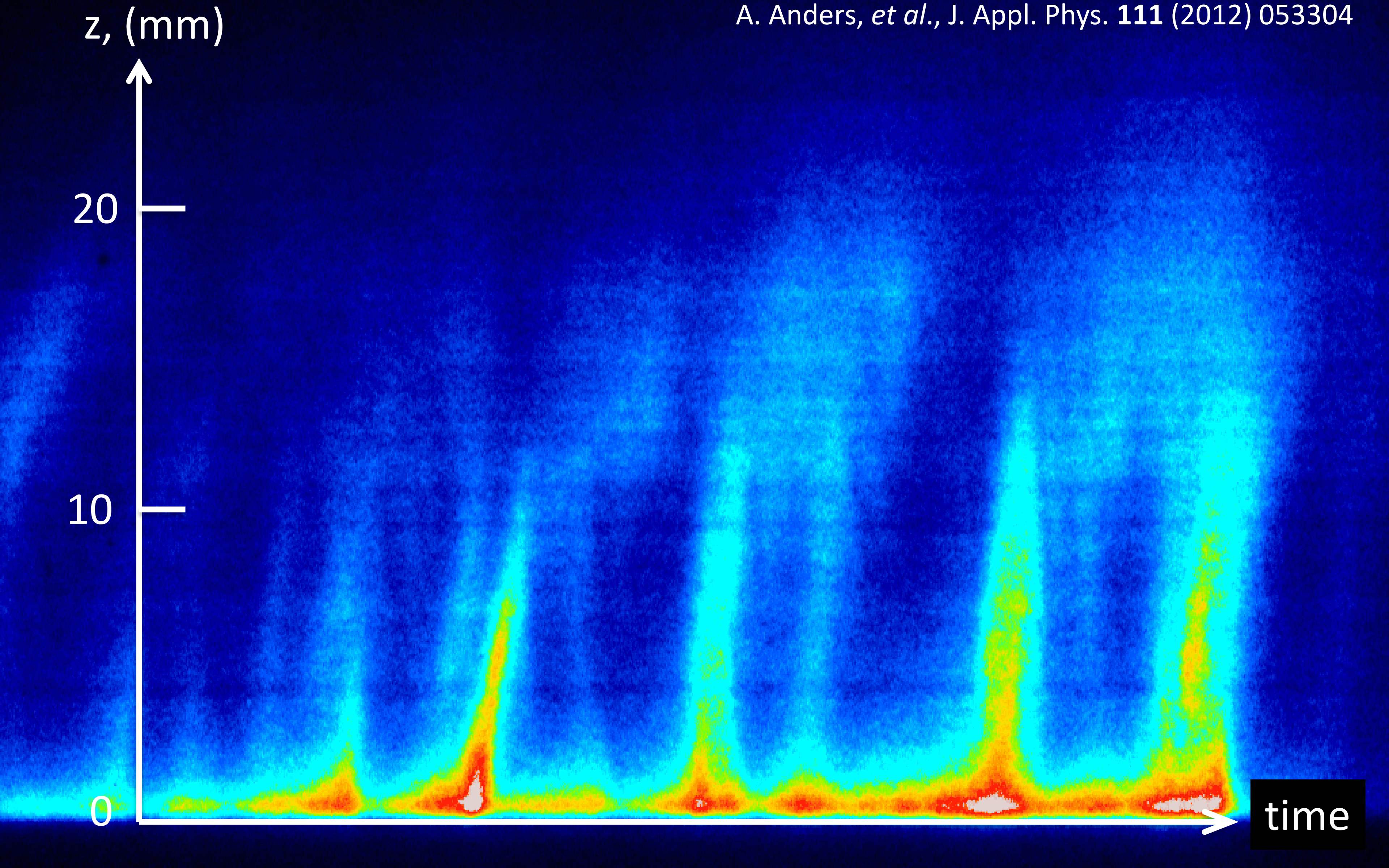

Example of Streak Image, 20 μs sweep time

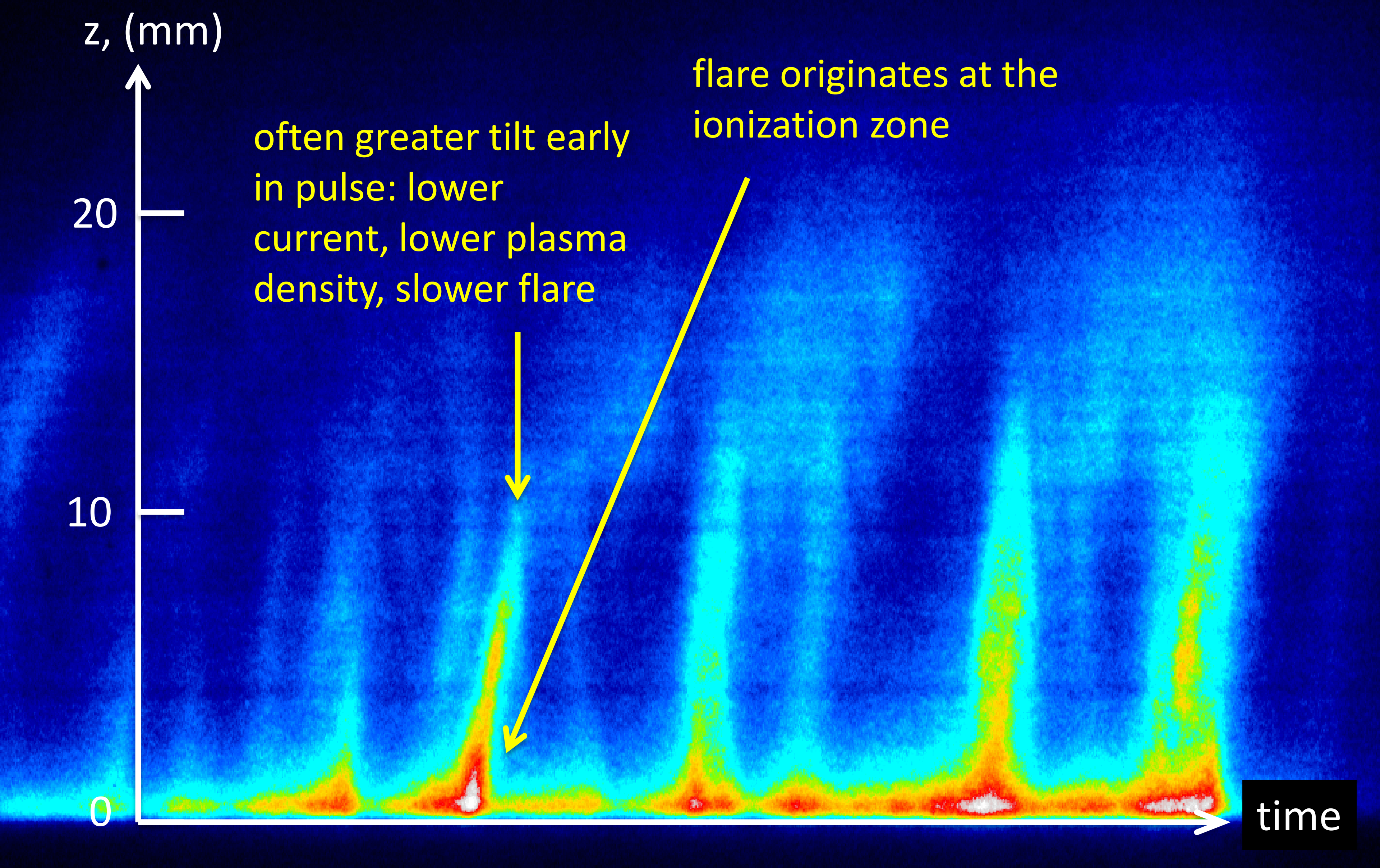

often greater tilt early in pulse: lower current, lower plasma density, slower flare

flare originates at the ionization zone

Evolution of Ionization Zones seen for DC Magnetron Discharges (3” Nb in Ar)

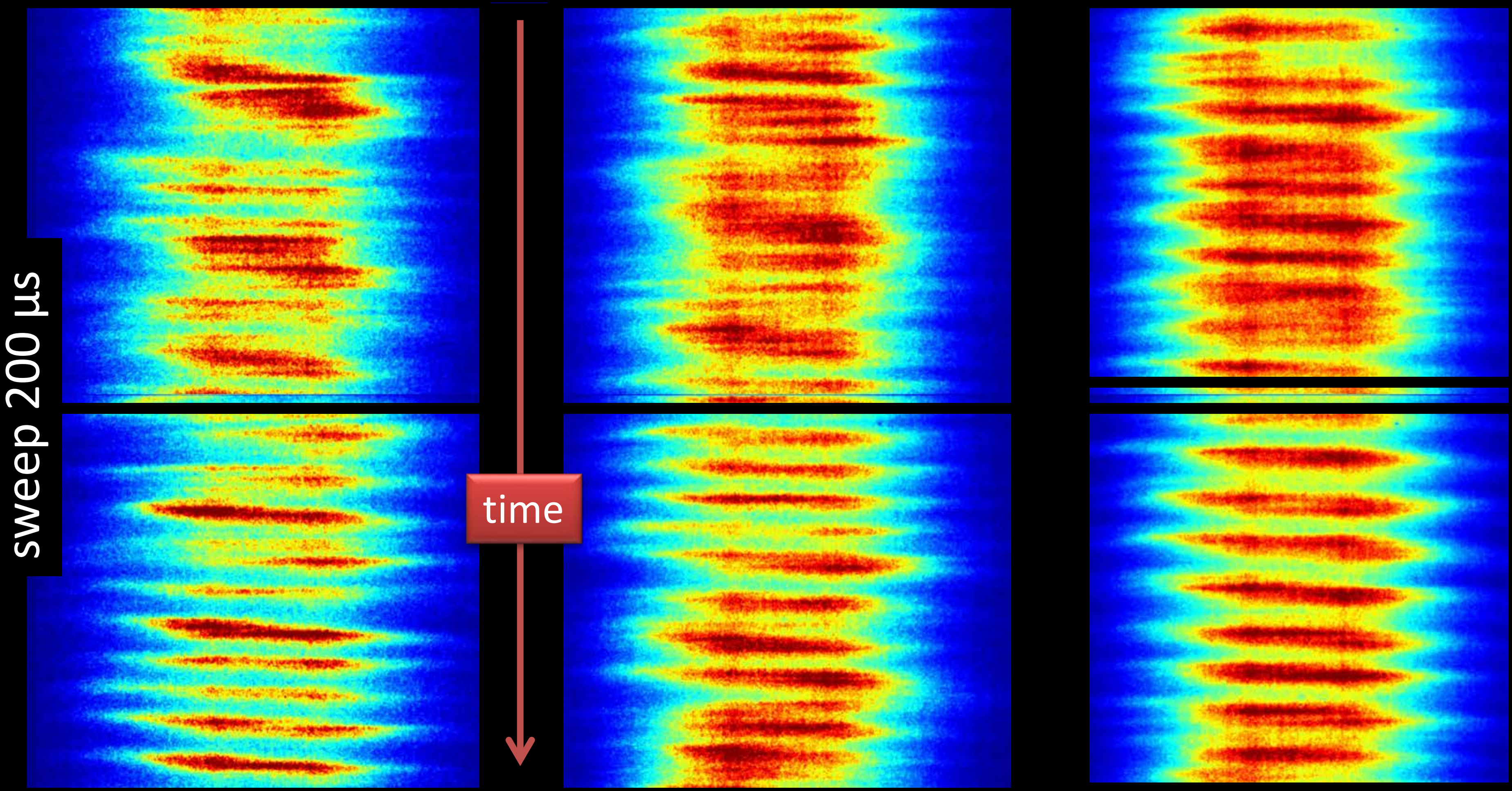

examples of streak camera images, illustrating zone stability vs. change

Y. Yang, *et al.*, Appl. Phys. Lett. **105** (2014) 254101.

More Fast Imaging: Ionization Zones disappear under certain conditions

No distinct zones for copper at high current. Likely cause by high supply of neutrals and cooling of electrons.

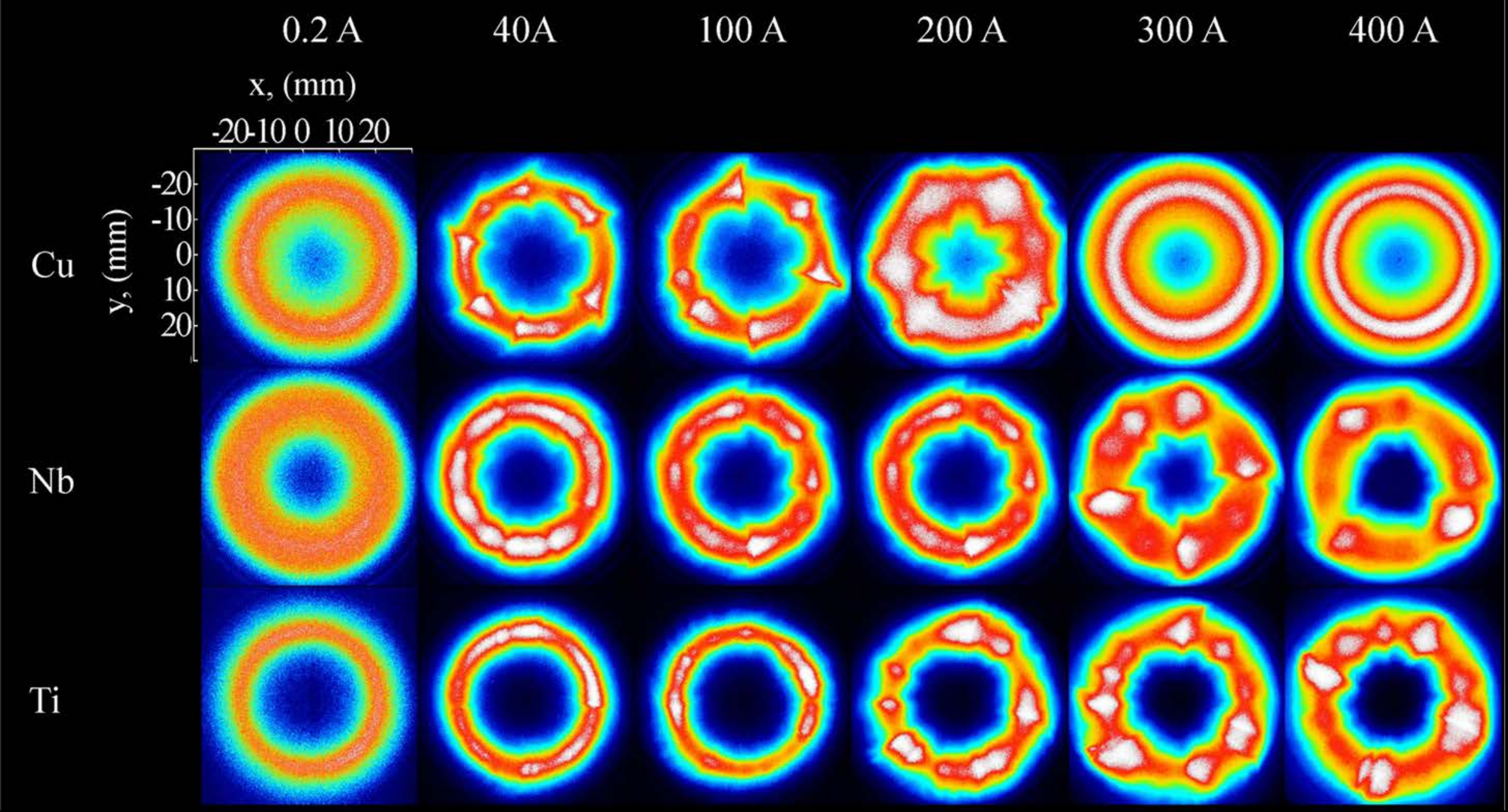

Y. Yang, *et al*., Appl. Phys. Lett. **106** (2015) 124102.

Spectroscopic Imaging:
End-on view through Spectral Filter.
→ Evidence for Concentration of Ionization.

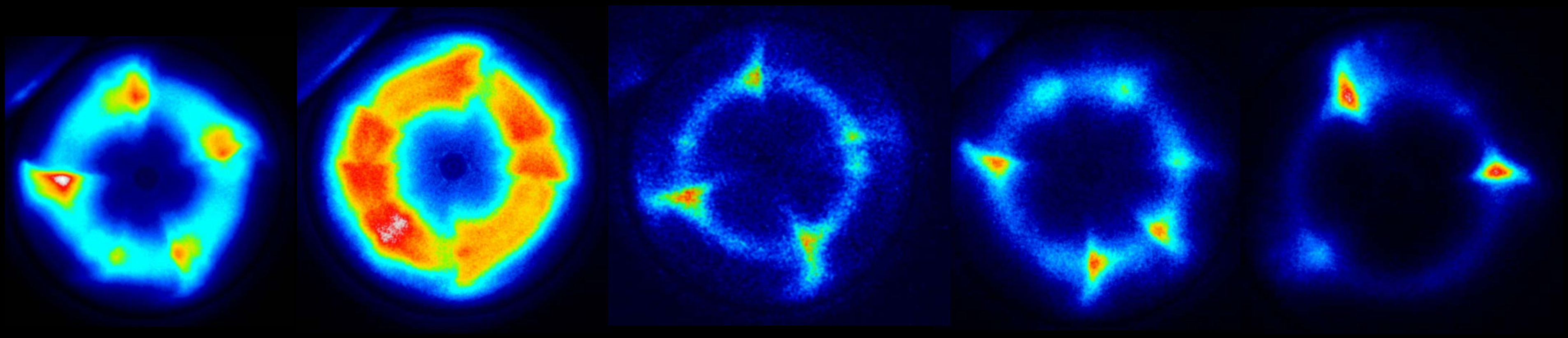

300-800 nm

Al I,
from 3.14 eV

Ar I
from 13.3 eV

Al II,
from 15.06 eV

Ar II,
from 19.22 eV

Al, 0.25 Pa Ar, 100 A, 150 ns snapshots

- → ionization occurs primarily in the ionization zones, little elsewhere
- → the higher the upper excitation level the more focussed appears the plasma

A. Andersson, *et al*., Appl. Phys. Lett. **103** (2013) 054104.

Light can be seen as strongly related to the potential hump structure

side-on view

end–on view

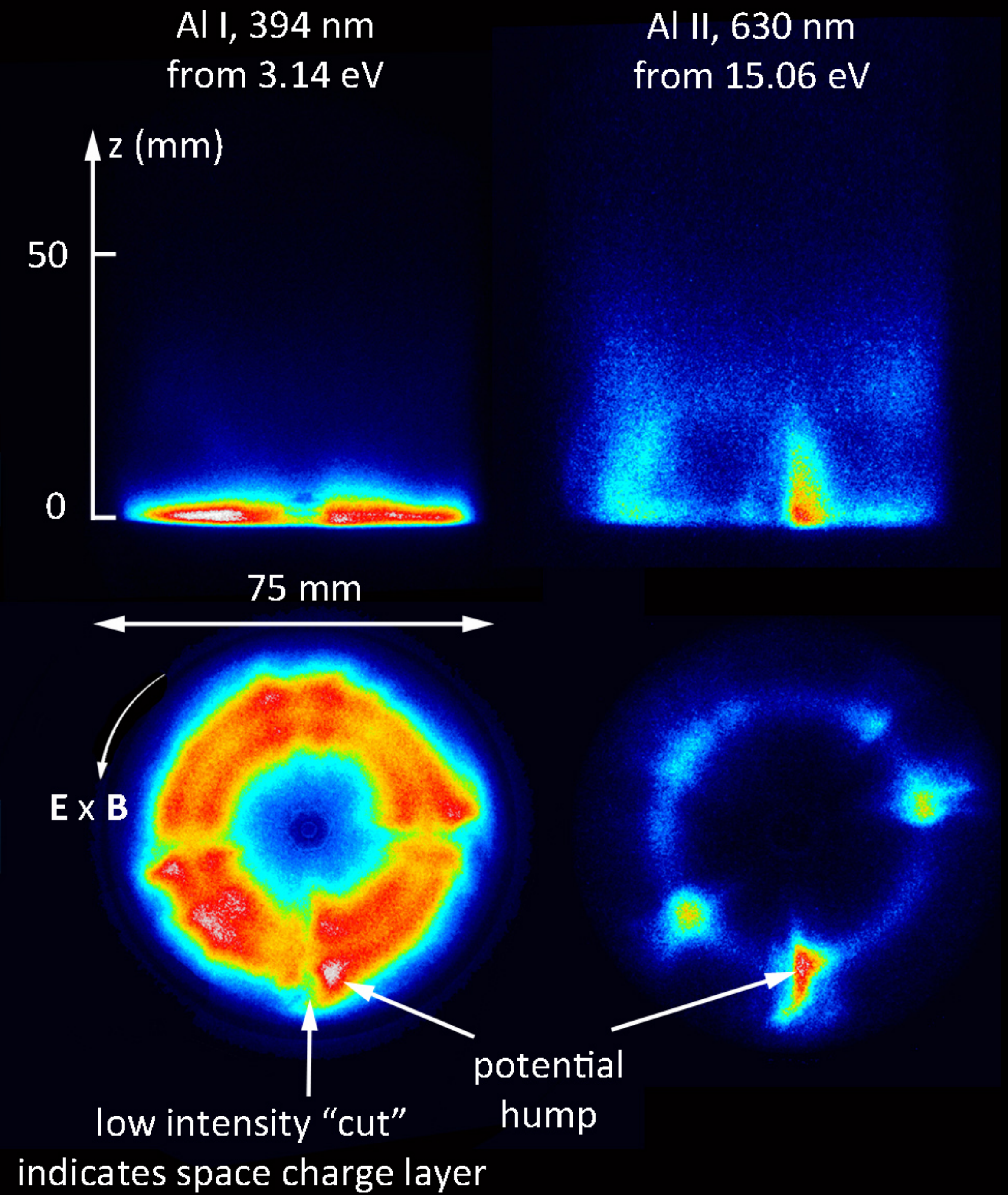

potential hump

low intensity “cut” indicates space charge layer

A. Anders, Appl. Phys. Lett. **105** (2014) 244104.

Cu target, gasless

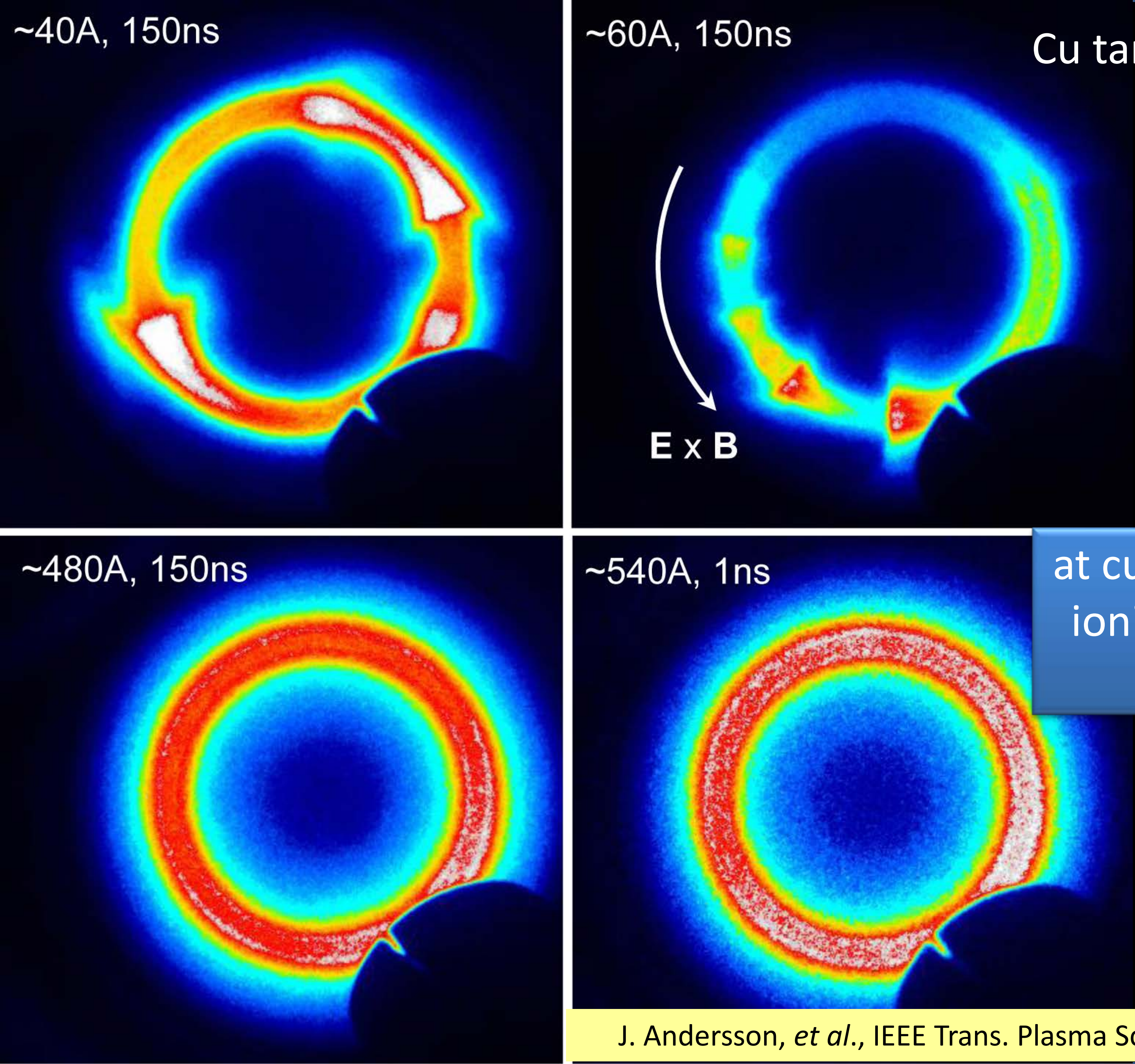

at current > 300 A ionization zones are lost!

J. Andersson, *et al*., IEEE Trans. Plasma Sci. **42** (2014) 2856.

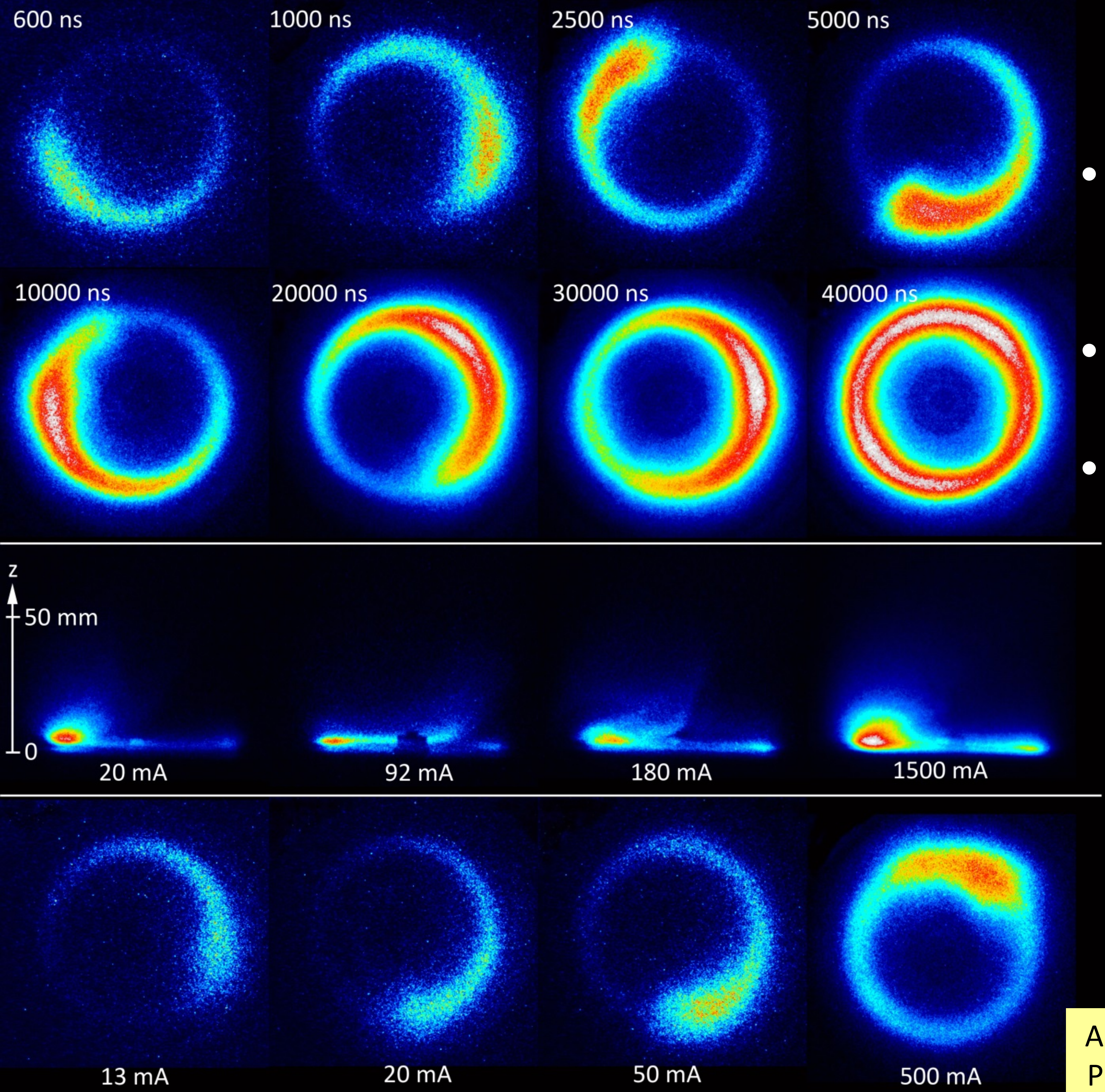

Ionization zones exist:

- even DC at low current, all the way to 4 mA!
- also in reactive systems
- with much slower motion than HiPIMS

Nb in Ar

A. Anders, *et al.*, IEEE Trans. Plasma Sci. **42** (2014) 2578.

Pulsed dc:
Transition Region

Reversal of direction!

From E x B to - E x B
at about 6 A.

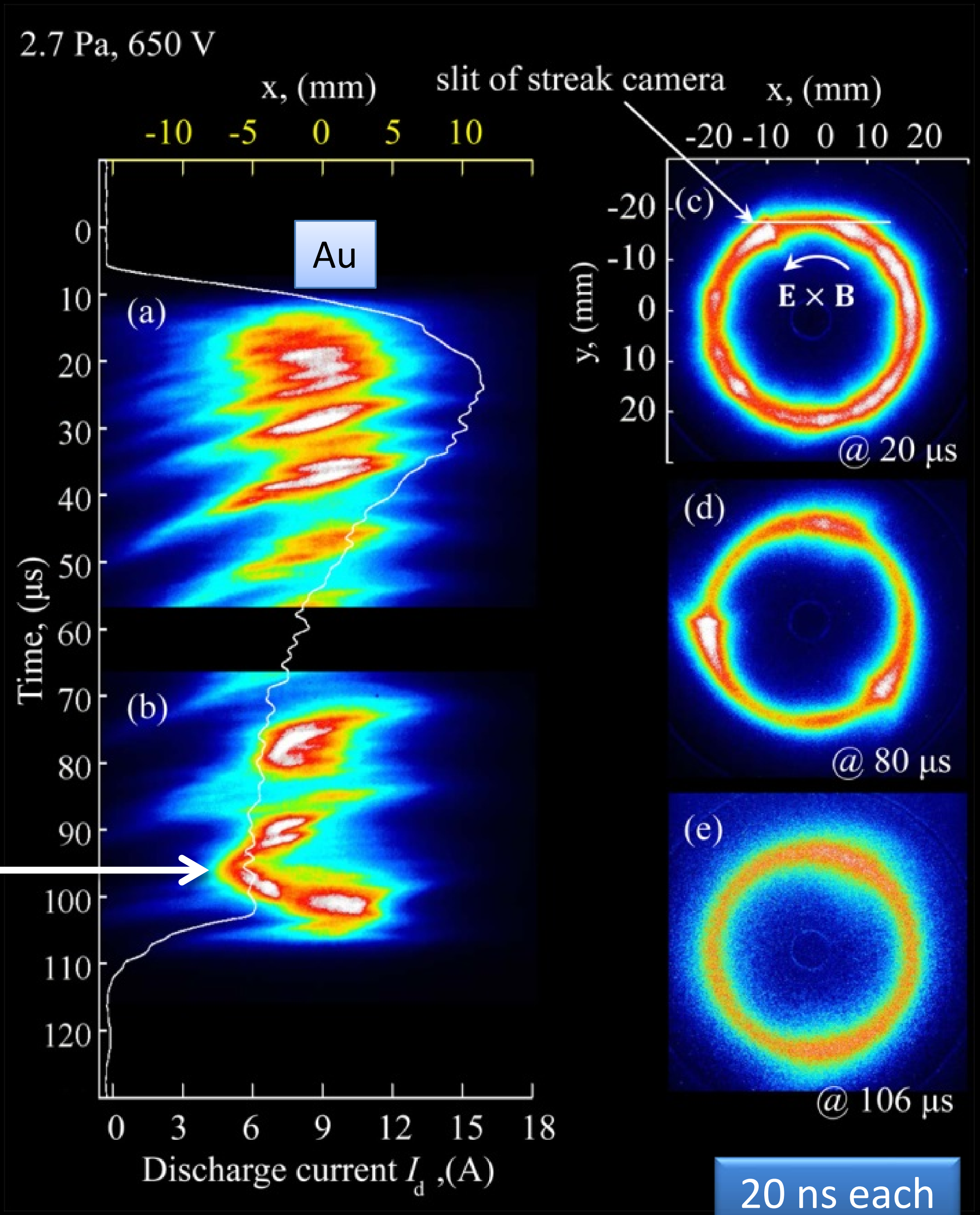

20 ns each

Y. Yang, *et al*., Appl. Phys. Lett. **105** (2014) 254101.

Plasma Potential from Emissive Probes

DC magnetron sputtering: conditions with exactly one spoke

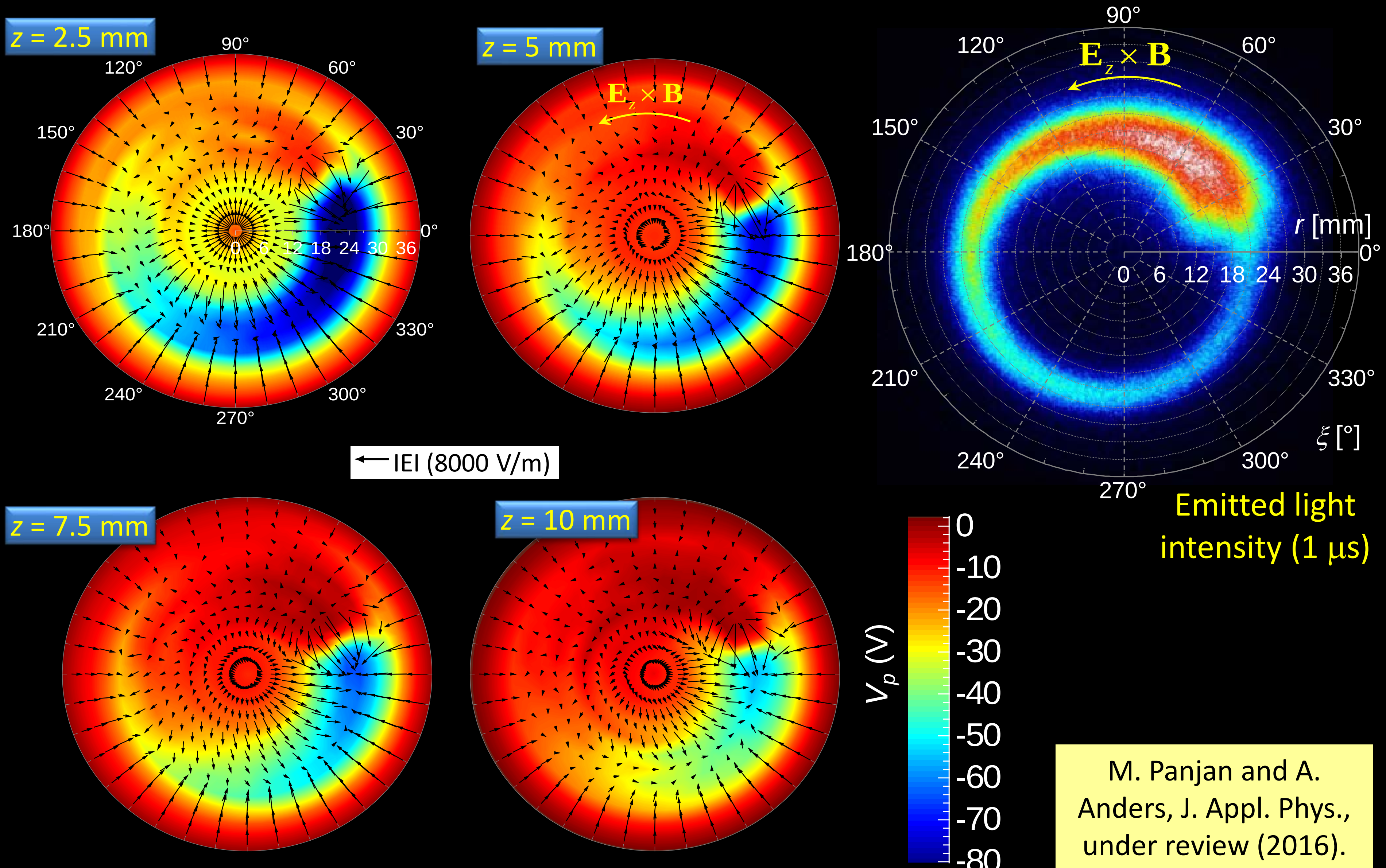

Emitted light intensity (1 µs)

M. Panjan and A. Anders, J. Appl. Phys., under review (2016).

Localized Energizing of Drifting Electrons

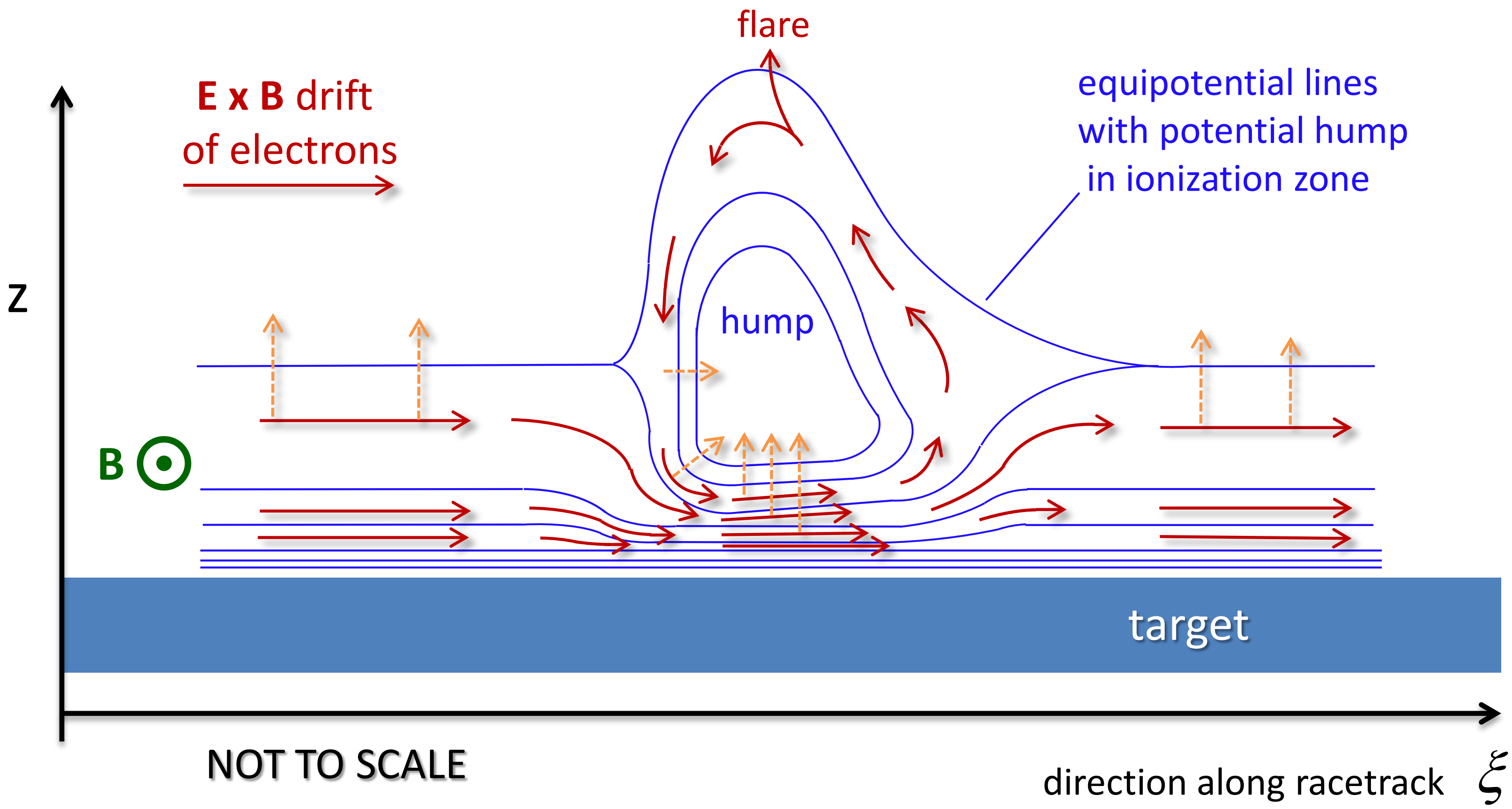

- electrons drift according to the local **E** and **B** fields
- ions are not magnetized, follow **E**-field

A. Anders, Appl. Phys. Lett. **105** (2014) 244104.

Reactive Sputtering
Target gets "poisoned"

- Reactive gas forms compound film not only on substrate but on target
- Several hystereses are observed
- Lot's of research how to make compound films on substrate while maintaining a metal surface on the target
    - Using optical emission or discharge current-voltage signals, for example, to control reactive gas flow, or power patterns

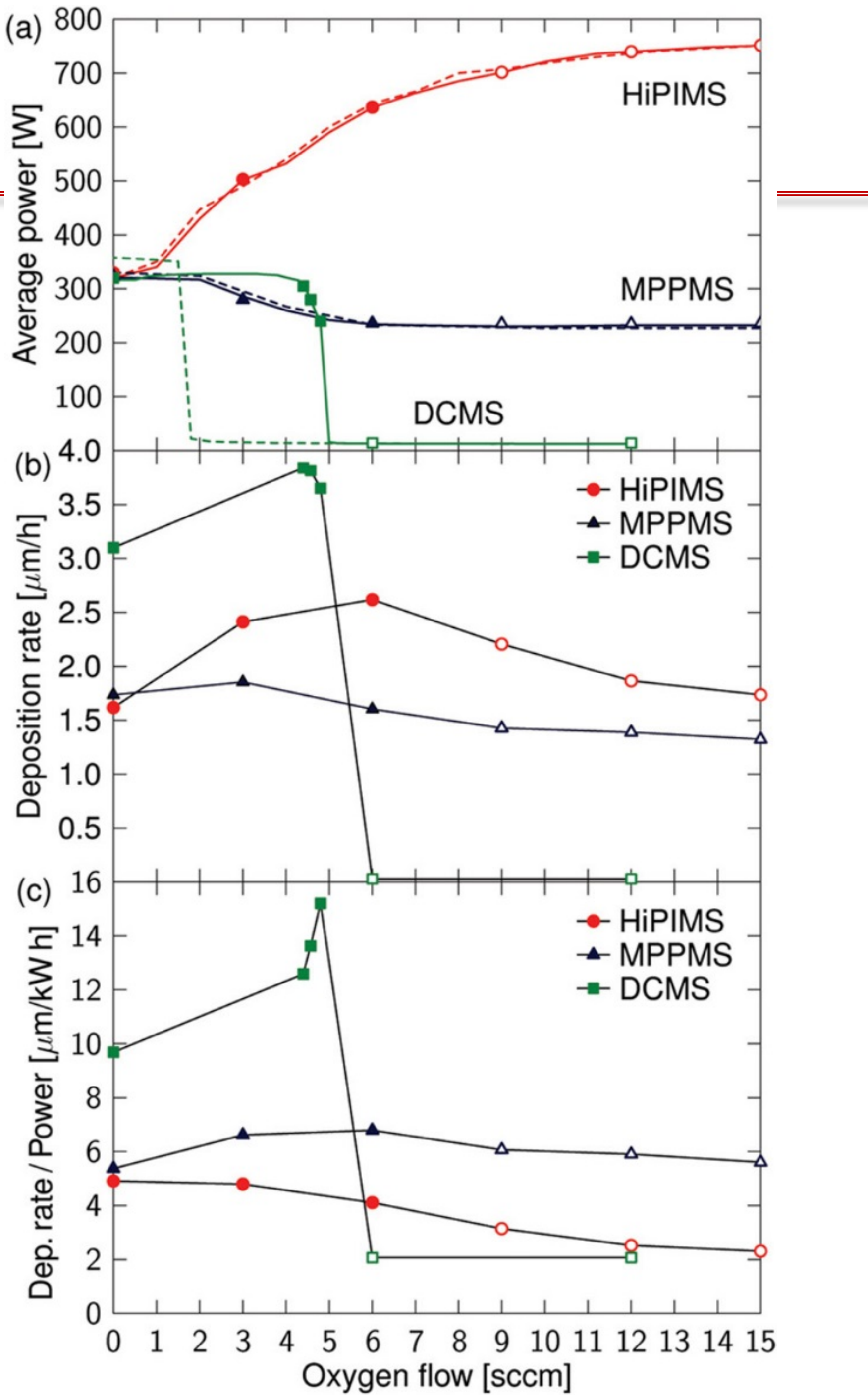

M. Hála, et al., J. Phys. D: Appl. Phys. 45 (2012) 055204.
See also tutorial: A. Anders, J. Appl. Phys. (2017), under review

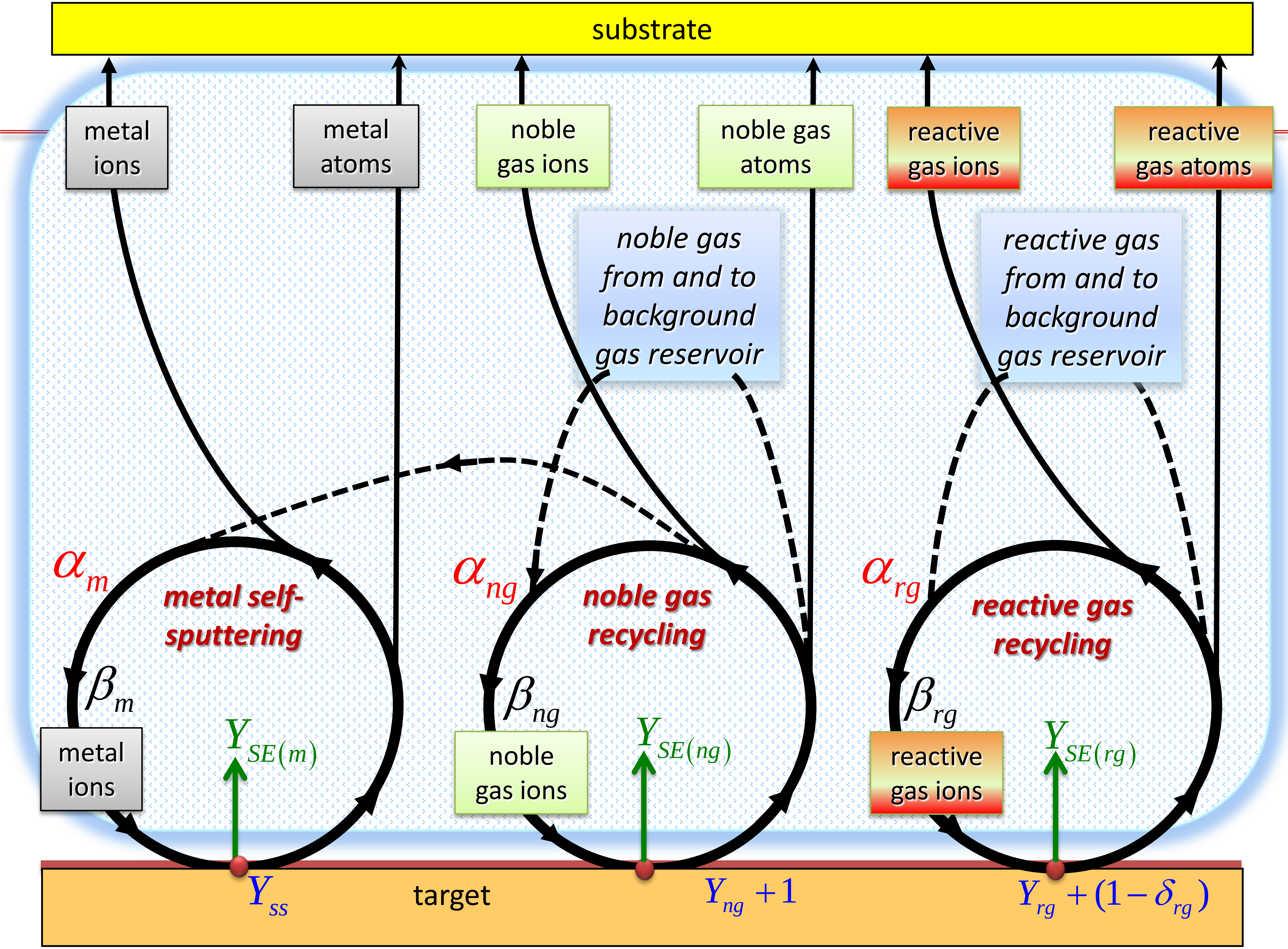
substrate
metal ions
metal atoms
noble gas ions
noble gas atoms
reactive gas ions
reactive gas atoms
noble gas from and to background gas reservoir
reactive gas from and to background gas reservoir
α_m
metal self-sputtering
β_m
metal ions
$Y_{SE(m)}$
α_{ng}
noble gas recycling
β_{ng}
noble gas ions
$Y_{SE(ng)}$
α_{rg}
reactive gas recycling
β_{rg}
reactive gas ions
$Y_{SE(rg)}$
Y_{ss}
target
$Y_{ng}+1$
$Y_{rg}+(1-\delta_{rg})$

Sputtering with a Plasma Lens

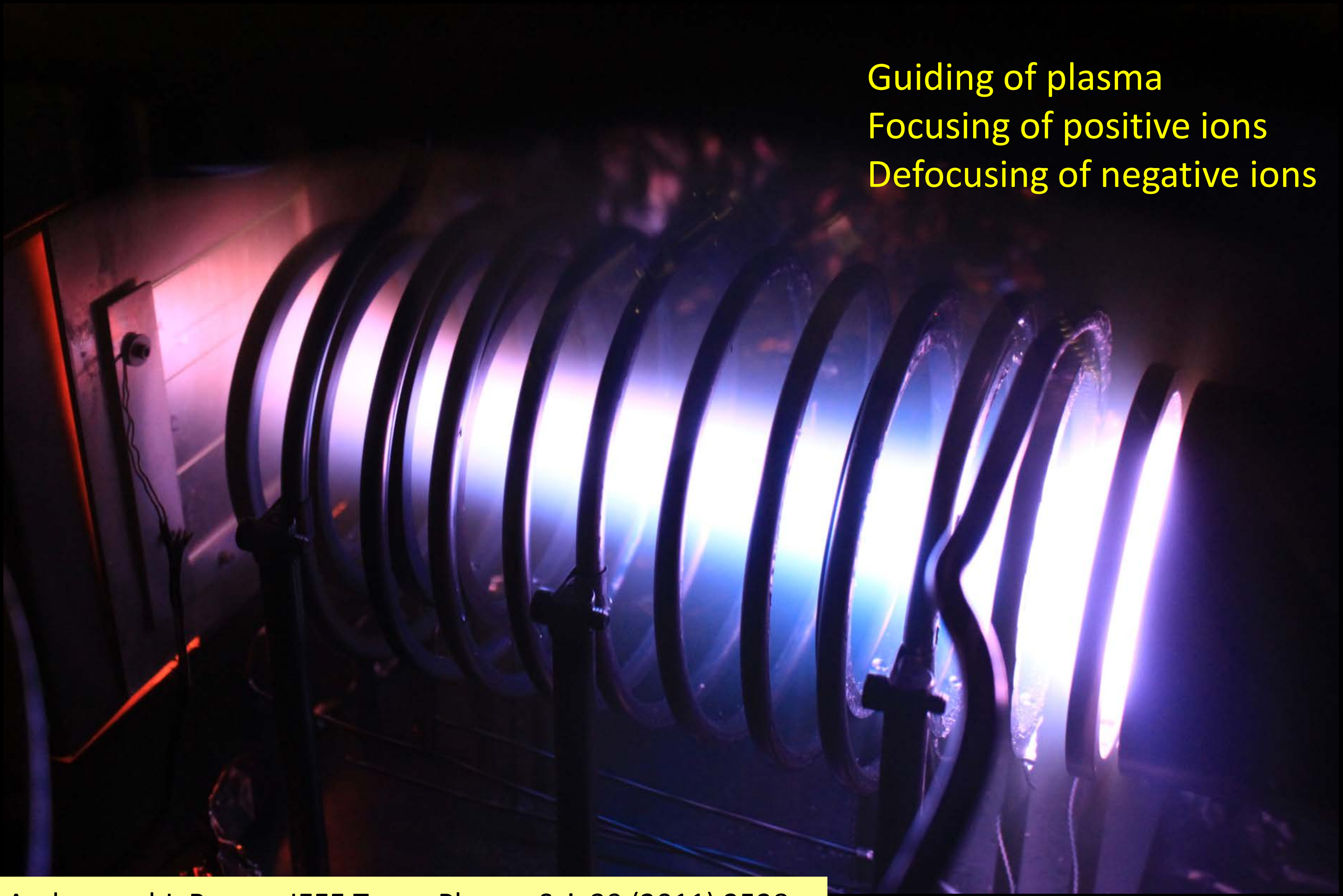

Guiding of plasma
Focusing of positive ions
Defocusing of negative ions

A. Anders and J. Brown, IEEE Trans. Plasma Sci. 39 (2011) 2528.

Mitigation of the Disappearing Anode Effect

- Dual Magnetron sputtering: 2 targets serve alternatingly as cathode and anode
- often medium frequency switching (~ 100 kHz)
- large targets → high pulsed power but not HiPIMS

Photo courtesy of VON ARDENNE

Dual Magnetron Sputtering in Cylindrical Geometry

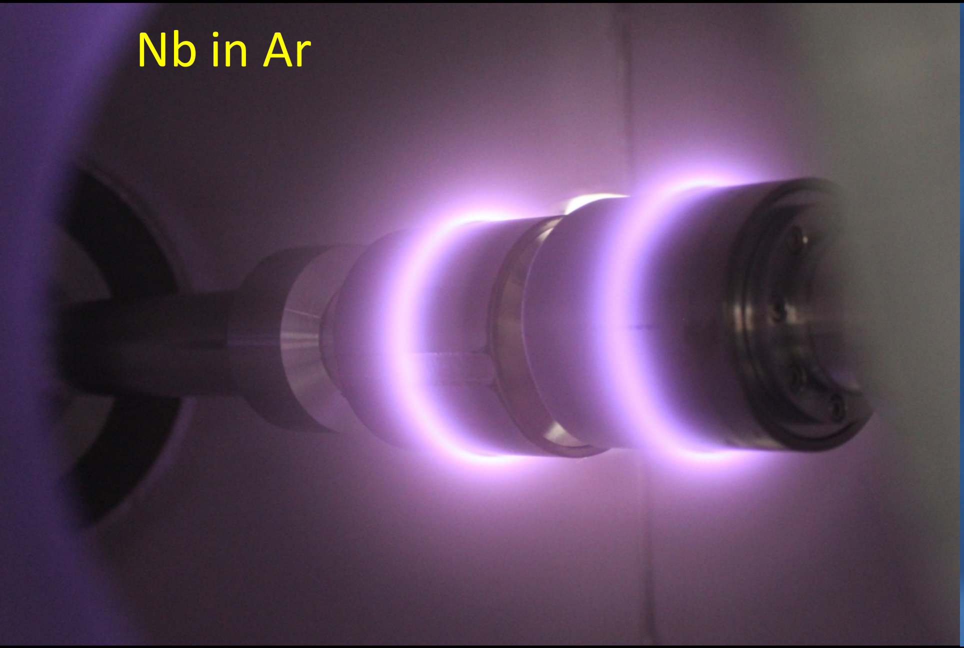

Low power →
gas plasma dominated

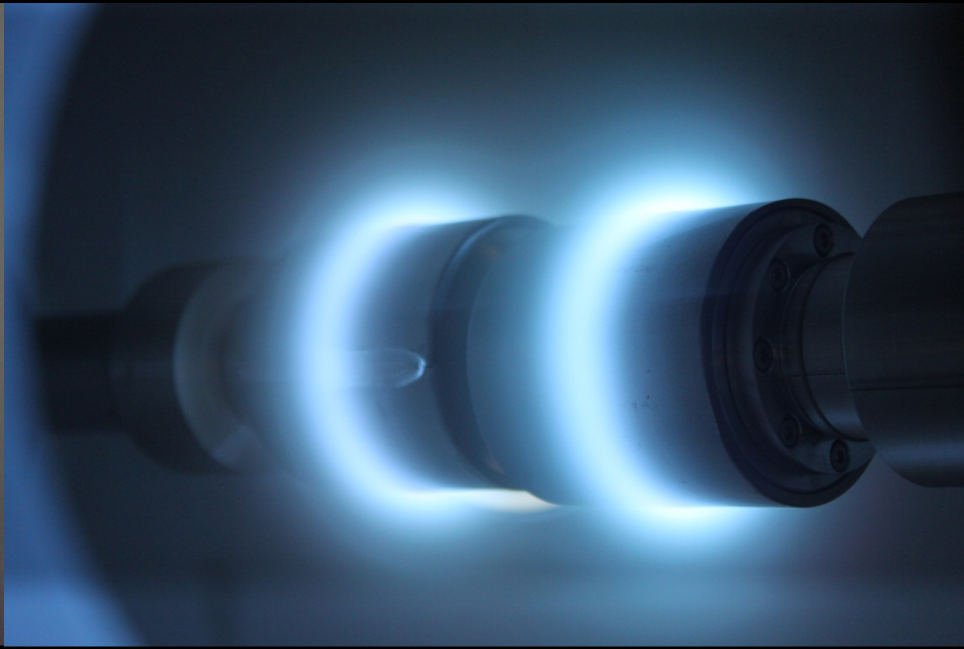

High power →
metal plasma dominated

A. Anders, *et al.*, 15th Int. Conf. RF Superconductivity, Chicago, Il, 2011.
http://accelconf.web.cern.ch/AccelConf/SRF2011/papers/tuioa06.pdf

Summary

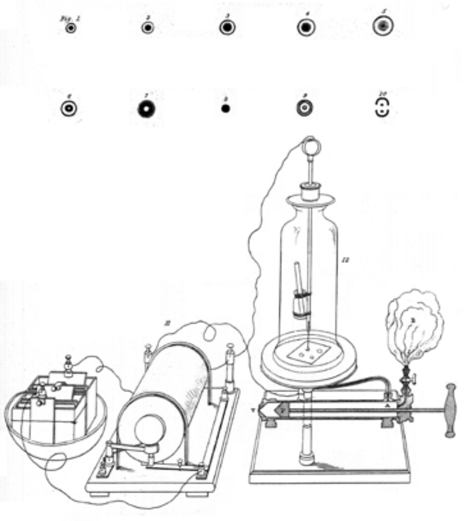

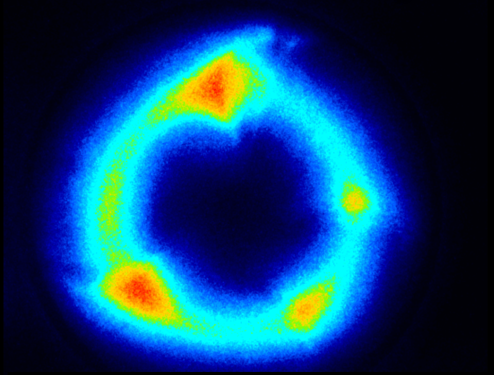

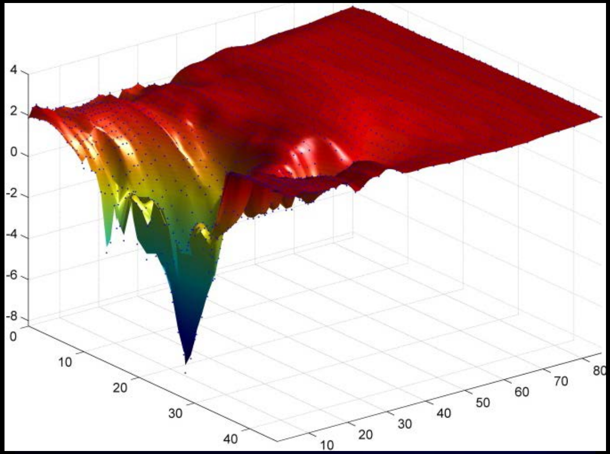
4
2
0
-2
-4
-6
-8
0
10
20
30
40
10
20
30
40
50
60
70
80

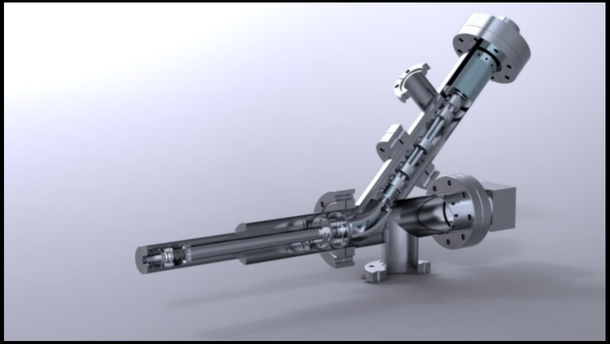

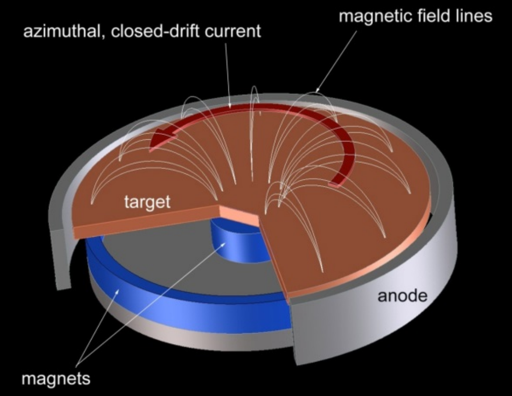
azimuthal, closed-drift current
magnetic field lines
target
anode
magnets

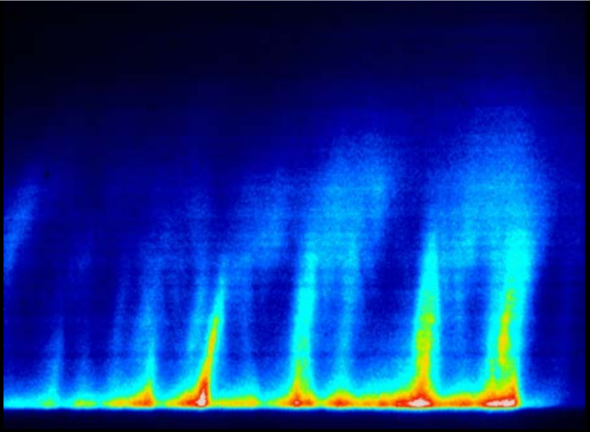

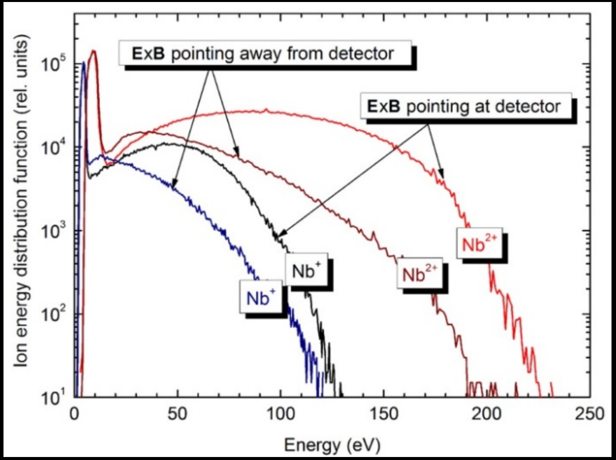
Ion energy distribution function (rel. units)
10^5
10^4
10^3
10^2
10^1
0
50
100
150
200
250
Energy (eV)
ExB pointing away from detector
ExB pointing at detector
Nb^+
Nb^+
Nb^{2+}
Nb^{2+}

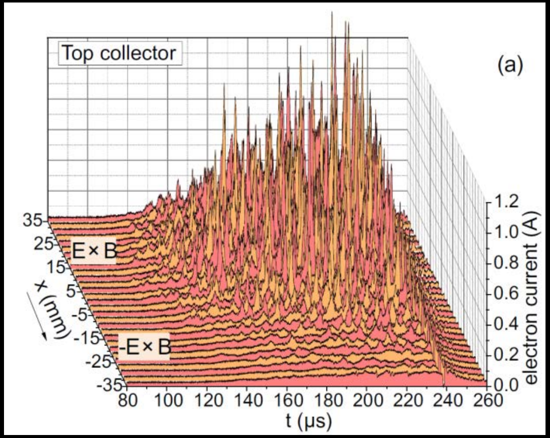
Top collector
(a)
E × B
-E × B
x (mm)
35
25
15
5
-5
-15
-25
-35
80
100
120
140
160
180
200
220
240
260
t (µs)
electron current (A)
1.2
1.0
0.8
0.6
0.4
0.2
0.0